In vivo imaging of the regulatory mechanisms in acute and chronic delayed type hypersensitivity reactions

Thesis submitted as requirement to fulfill the degree "Doctor of Philosophy" (Ph.D.)

at the

Faculty of Medicine

Eberhard Karls University

Tübingen

by

Dr. med. Johannes Walter Schwenck

2021

Dean:	Professor Dr. B. Pichler
1. Reviewer:	Professor Dr. B. Pichler
2. Reviewer:	Professor Dr. S. Wagner

Date of the oral examination: 03.08.2021

Content

1. Introduction

1.1 Background

The evolution led to the development of a complex immune system in the human body in order to defend itself against external pathogens, such as viruses or bacteria (1, 2). However, also chemical or physical stimuli can trigger inflammatory responses (3). The immune response is depending on a complex interplay in the inflamed tissue at a molecular and cellular level. Many diseases are caused by either an insufficient or an exaggerated immune response (2). Tissue damage by excessive immune responses can lead to a loss of function, which causes the symptoms of many autoimmune diseases like rheumatoid arthritis or multiple sclerosis (4). Therefore, an important task of the immune system is not only the elimination of the inflammatory trigger but also the complex regulation of the immune response especially in regards to excessive tissue damage (5). In contrary, insufficient immune responses are a major problem in infectious diseases but also in carcinogenesis and cancer immunotherapy (6, 7).

To reveal and understand the regulatory mechanisms of inflammation are of paramount importance to develop tailored therapies and enable treatment monitoring of various diseases. Despite enormous research efforts, to date only limited knowledge about the regulatory processes in inflamed tissue is available. Furthermore, only very few *in vivo* molecular imaging strategies have been developed to monitor non-invasively the time course of the

regulatory processes as well as therapeutic interventions in inflammatory diseases.

1.2 Delayed-type hypersensitivity reaction (DTHR)

The 2,4,6-trinitrochlorobenzene (TNCB) induced cutaneous DTHR, a well established inflammation model, provides profound insights into the emergence of acute and chronic T-cell driven inflammatory immune responses (8-11). The advantages of this model are the fast and reliable induction of the inflammation as well as the possibility for easy quantitative non invasive monitoring of clinical symptoms by assessing the ear swelling (8-10). To elicit a TNCB-specific T-cell dependent DTHR at the ear, sensitization with the hapten TNCB is indispensable, which is performed at the shaved abdomen of the experimental mice (8-11). Haptens are binding to proteins and modify them before they get presented as foreign antigens by dendritic cells (DC) (12). However, also other mechanisms are involved in the DC activation, as for example TNCB is also able to degrade hyaluronic acid, which activates DCs via Toll-like receptor (TLR)2 and TLR4 (13, 14). Furthermore, the release of extracellular adenosine triphosphate (ATP) from damaged cells is able to activate the NACHT, LRR and PYD domains-containing protein (NLRP) 3 inflammasome through the purine receptor P2X7 (15). This protein complex leads to the cleavage of the pro-Interleukin (IL)-1β and pro-IL-18 by caspase-1 and -5. These cytokines are crucial for the migration and antigen presentation by DCs as well as the activation, proliferation and immigration of T cells (16-19).

The migration of activated DCs to the draining lymph nodes (20) is depending on the activity of matrix metalloproteases (MMPs), which allows them to move through the tissue (21). In the draining lymph nodes the DCs present the processed antigens on major histocompatibility complex (MHC) II molecules tissue (22). Naive $CD4^+$ T lymphocytes (T helper cells; Th) bind with their T cell receptor to the antigen-loaded MHC II molecules of the antigen presenting cells (APC). Nevertheless, Bouloc et al. revealed that a TNCB specific DTHR is inducible in MHC II deficient mice, which is then induced by a MHC I dependent activation of $CD8^+$ T cells (23). If the T cell receptor of T cells recognizes its specific antigen in the presence of costimulatory signals (e.g. CD28 and CD80/CD86 interaction), the T cell will be activated and starts to differentiate, proliferate and migrate into the bloodstream (24, 25).

After successful sensitization, the second contact of the primed immune system to TNCB elicits a TNCB-specific adaptive immune response, which is performed in our experiments by application of 1% TNCB solution on the skin of the right ear. A striking feature of this model is that the opposite (left) ear serves as an internal control. While after the TNCB application at the right ear (challenge) an acute DTHR is induced, repeated applications of TNCB are causing a continuous development of a chronic cutaneous DTHR.

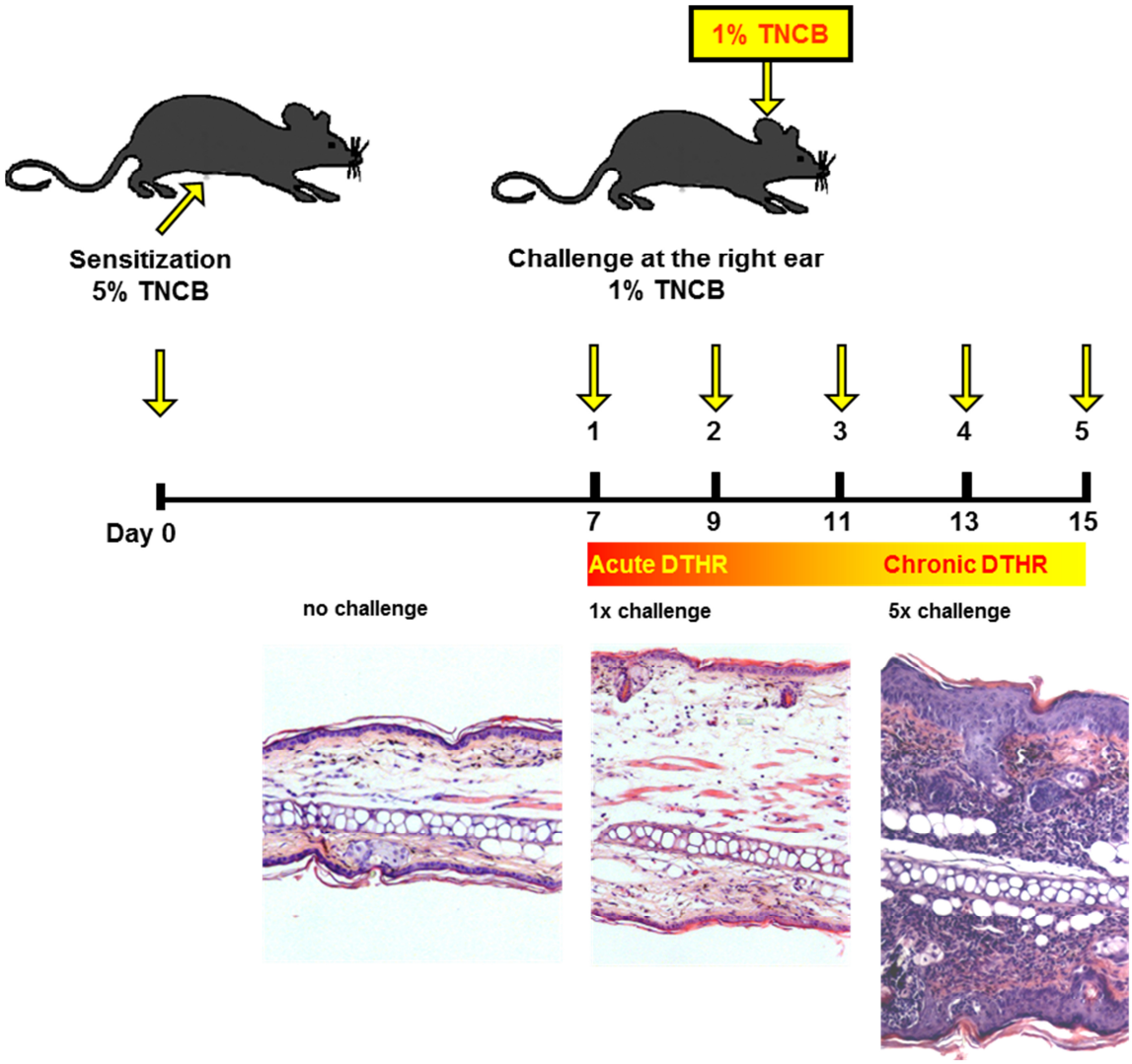

Figure 1: C57BL/6 mice were sensitized at the abdomen using a 5% TNCB solution. At day 7 the acute TNCB specific DTHR was elicited at the right ear by application of a 1% TNCB solution (challenge). Repetitive challenges up to five times induced a chronic DTHR. Ear tissue stained by Hematoxylin&Eosin (H&E) revealed a strong edema and leukocyte infiltration dominated by polymorphonuclear neutrophils in mice with acute DTHR 12 hours after the first challenge (center) compared naïve, non–TNCB-challenged ear tissue (left). Ear tissue derived after five challenges (chronic DTHR) displayed tissue remodeling characterized by acanthosis, hyperkeratosis, angiogenesis and a dense leukocyte infiltrate (right, 12 hours after challenge, magnification 100×). (Adapted from Schwenck et al. 2014 (8))

In the TNCB induced acute and chronic DTHR interferon-γ (IFN-γ) producing $CD4^+$ T cells (Th1) and $CD8^+$ cytotoxic T cells (Tc1) are dominating in comparison to other T-cell subsets (26). Interestingly, a contact allergic reaction can be elicited in the absence of MHC II and $CD4^+$ Th1 cells, which is then characterized by $CD8^+$ Tc1 cells (27). Furthermore, NK cells play an important role in the contact hypersensitivity and are able to elicit inflammatory responses independently of T and B cells (28). Chemokines and cytokines, like IL-8 (murine: macrophage inflammatory protein 2; MIP-2) and IL-1β, are promoting the immigration of neutrophilic granulocytes, mast cells and other effector cells by chemotaxis. Additionally, IL-17 is of particular importance for the migration of neutrophilic granulocytes (29). Furthermore, the immune infiltrate is heavily depending on the expression of adhesion molecules such as selectins and integrins on the cell surface and the vessel endothelia. In *in vivo* experiments, where adhesion molecules such as intercellular adhesion molecule (ICAM)-1, vascular cell adhesion molecule (VCAM)-1, α4β7 integrin, E-, L- or P-selectin are missing, a significantly reduced TNCB induced DTHR was observed (30-37).

The inflammatory infiltrate in the TNCB induced DTHR is dominated by neutrophilic granulocytes which form subepithelial abscesses. Activated neutrophilic granulocytes express tissue-destroying enzymes such as elastases and cathepsins but also myeloperoxidase which induces oxidative stress. Additionally, tumor necrosis factor (TNF), IL-8 (murine MIP-2), histamine and prostaglandins are released e.g. by activated mast cells (9, 38).

To avoid excessive tissue damage, the adaptive immune response is also triggering anti-inflammatory responses. For example, the inflamed tissue in TNCB induced DTHR is also infiltrated by regulatory T lymphocytes (Tregs). The Treg derived cytokine IL-10 reduces the immigration of circulating leukocytes (39, 40). Furthermore, the release of adenosine by Tregs leads to a reduced expression of the adhesion molecules E- and P-selectin on the vessel endothelia (41). Contact of Tregs with DCs suppresses the antigen presentation and thus, decreases T cell priming. Experimental studies revealed that the absence of Tregs significantly prolongs the inflammatory reaction (42).

1.3 Proteases in inflammation

Proteases fulfill diverse extra- and intracellular functions in healthy and diseased tissue. Proteases can be classified according to their catalytic residues in the active site, which also defines their specific cleavage sites. Catalytic residues comprise mostly amino acids, whereas the group of metalloproteases are using metal ions in their catalytic centers (43). An important group of metalloproteases are matrix metalloproteases (MMPs) which are containing a Zn^{2+} ion in the active site (44).

MMP activity has been explored in recent years in several experimental disease models, such as cardiovascular diseases (45, 46), chronic obstructive pulmonary disease (47), tumor progression and metastasis (48-51), as well as autoimmune diseases like rheumatoid arthritis (52). Recently we have investigated the increasing *in vivo* MMP activity during the time course of acute and chronic TNCB induced DTHR (8).

MMPs can be attached to the cellular membrane or released freely into the extracellular matrix (53, 54). Like other proteases, MMPs are expressed as inactive pro-forms and can be activated e.g. by cleavage through other proteases (55) or oxidation caused by reactive oxygen species (ROS) (56, 57).

In the inflamed tissue, neutrophilic granulocytes, macrophages, fibroblasts and mast cells secrete MMPs upon stimulation (57-61), which is dependent on NF-κB signaling (62-66). Also the activation of p38 mitogen-activated protein (MAP) kinases plays a decisive role in the expression of MMPs (67-70).

MMPs cleave components of the extracellular matrix such as collagen, fibronectin and laminin and are therefore crucial for tissue remodeling and immune cell migration (71, 72). Thus, MMPs are for example critically involved in the migration of activated DCs through the tissue (21). Moreover, MMPs facilitate angiogenesis by degrading the basal lamina and the extracellular matrix as well as untying the cell–cell contacts in the endothelium, which enables endothelial cells to migrate and proliferate (73). MMPs are also heavily contributing to the extracellular processing and activation of several important mediators and cytokines such as IL-1β, TNF, vascular endothelial growth factor (VEGF) as well as induction of E-selectin expression (74, 75). Mediators, which are bound to the extracellular matrix like e.g. the basic fibroblast growth factor (bFGF) or transforming growth factor (TGF), can be released by specific cleavage of binding motives via MMPs (53, 76-78).

Besides the MMPs, cysteine proteases like cathepsins are another important group of proteases, which were first discovered in lysosomes where they

degrade ingested proteins (79). Although cysteine-type cathepsins have been initially described as intracellular enzymes, complex intra- and extracellular interactions of cathepsins were discovered recently (80). Depending on the conditions, the half-life of cysteine cathepsins in cellular environment can account a few minutes up to multiple hours (81-83).

The ubiquitously expressed cysteine exopeptidase cathepsin B is critically involved in several steps during the activation of the innate and adaptive immune response (84). Consequently, elevated cathepsin B expression was described in many different diseases such as autoimmune diseases like rheumatoid arthritis (85) or multiple sclerosis (86), but also in pancreatitis (87), in the microenvironment of several tumor entities (88) as well as in neurodegeneration like Alzheimer´s disease (89). In the tumor microenvironment cathepsin B is one of the most abundantly expressed proteases of macrophages (90, 91).

Like other proteases cathepsin B is expressed as a proenzyme, which can be activated by cleavage of itself in the early endosome, a process called autocatalysis (84, 92). In the endolysome cathepsin B plays an important role in the processing of ingested antigens, which afterwards can be loaded on MHCII molecules and presented on the cellular surface to elicit an adaptive immune response. Interestingly, cathepsin B is highly active in MHC-dependent antigen processing within the lysosome but, unlike cathepsin S, the activity of cathepsin B is not obligatory (93-95).

Furthermore, cathepsin B is critically involved in TLR signaling (96), apoptosis (97) and TNF secretion (98). Regardless of the neutral pH in the extracellular

compartment, cathepsin B is an important factor in extracellular matrix remodeling and cell migration (99) as well as angiogenesis (100).

A variety of protease inhibitors have been developed in recent years. CA-074 is a irreversible inhibitor which specifically interacts with amino acids in the characteristic occluding loop next to the active site of intracellular cathepsin B *in vitro* (101, 102). Similarly, also inhibitor 17 is targeting the occluding loop next to the active site of cathepsin B (103).

1.4 Reactive oxygen species

Proteases are closely interacting with other molecular processes in the inflammatory tissue, e.g. reactive oxygen species (ROS) and reactive nitrogen species (RNS). ROS and RNS represent large groups of different oxidative molecules, which are on the one hand cellular stress factors occurring as byproducts of the cellular metabolism but on the other hand are acting as signaling and effector molecules e.g. generated by inflammatory cells like neutrophilic granulocytes or macrophages (104, 105).

neutrophilic granulocytes can be considered as a primary source of ROS/RNS in the TNCB-induced DTHR, because of their strong accumulation in both acute and chronic stage (8). Neutrophilic granulocytes elicit ROS/RNS during the so called „oxidative burst“, which is essential for the establishment of several autoimmune diseases like rheumatoid arthritis and psoriasis vulgaris (10).

ROS are generated within the cell via different biochemical mechanisms, leading to a large variety of chemically different ROS species with distinct half lifes in the intra- and extracellular environment. In the mitochondria oxygen is

converted by NADPH oxidase complexes (NOX) via oxidative phosphorylation into the primary radical superoxide anion (O_2^-), which can then quickly react to secondary ROS/RNS. The highly abundant ROS species hydrogen peroxide (H_2O_2) is generated by catalase or glutathione peroxidase and is able to diffuse through cellular membranes. Additionally, the enzyme MPO, which is heavily expressed by neutrophilic granulocytes but also by macrophages, generates a variety of ROS, like hypochlorous acid (HClO), hypothiocyanous acid (HOSCN) and others (106). A main source of RNS is the nitric oxide synthase (NOS) producing nitric oxide (NO), which reacts with O_2 to peroxynitrite ($ONOO^-$) (107).

Considering the important role of ROS/RNS in inflammatory immune responses, the establishment of antioxidative treatment approaches in inflammatory and autoimmune disease was a consequent aim. N-acetylcysteine (NAC) is the most often clinically applied antioxidant drug, which was shown to reduce ROS *in vitro* and *in vivo* in preclinical experiments (108-111). Cells are able to synthesize glutathione from NAC, but NAC seems to have much more effects independently of glutathione synthesis (112). For example, similar to NAC, the stereoisomer N-acetyl-D-cysteine, which can not be converted into glutathione, has antioxidative effects *in vivo* (110). In addition, NAC is able to contain T-cell activation *in vitro* mainly by inhibition of DCs (113).

In vivo, NAC reduced acute and chronic DTHR induced by TNCB and other allergens (8, 114, 115). Also, a suppressive effect on collagen-induced arthritis has also been reported (116). In human studies anti-inflammatory

effects in sepsis and cystic fibrosis have been observed (117-120), but unfortunately many clinical trials addressing ROS failed to improve the disease outcome significantly (121-125).

1.5 The NF-κB signaling pathway

The transcription factor NF-κB (nuclear factor 'kappa-light-chain-enhancer' of activated B-cells) is ubiquitously expressed in human as well as murine cells and is located in the cytoplasm when inactivated. After activation of membranous receptors such as TNF and TLR receptors, various pathways lead, to the activation of NF-κB. However, also other stimuli can trigger NF-κB activation, like for example ROS and RNS (126-128). Because premanufactured, preformed inactive NF-κB heterodimers are constitutively present in the cytoplasm, cells are able to respond to NF-κB-dependent signals very fast. The heterodimer NF-κB is formed by five different proteins in 15 possible combinations (129). Mainly, two major NF-κB signaling pathways are described inducing the transcription of specific genes. The heterodimer consisting of the proteins p50 and RelA (p65) mediates the canonical or classical NF-κB signaling pathway, while the heterodimer of p52 and RelB is eliciting the non-canonical or alternative NF-κB signaling pathway (126, 127, 130). The activation of the canonical signaling pathway is faster and associated with innate immune responses. A knockout of the canonical signaling pathway leads to a higher sensitivity for bacterial infections but to an increased resistance against viral infections (131). The slower, non-canonical pathway seems to be mainly involved in adaptive immune responses as well

as developmental processes e.g. during embryogenesis (132-135). Knockdown of the non-canonical pathway inhibits an adequate adaptive immune response against viruses (136). Both pathways are interacting with each other very closely, e.g. by cleavage of pro-forms or phosphorylation of kinases (129, 137-140).

Finally, both signaling pathways lead to the binding of NF-κB heterodimers to specific DNA promotors and the transcription of NF-κB dependent genes which are involved in many important processes such as cell proliferation and apoptosis (127, 141).

Regarding the regulation of the inflammatory response, NF-κB enables the transcription of important pro-inflammatory mediators such as IL-1β, IL-6 and TNF e.g. via activation of TNF-, TLR- or lymphotoxin receptors (63, 126, 133, 142). Therefore, the activation of DCs but also T and B lymphocytes is highly dependent on NF-κB (143-145). Beside its antioxidative effect, NAC inhibits also the activation of NF-κB by interaction with the IκBkinasen IKKα and IKKβ (146).

1.6 *In vivo* Optical Imaging

Molecular imaging has evolved a small, but growing portfolio of approaches to address regulatory mechanisms of inflammation. Optical imaging is an established molecular imaging method based on the *in vivo* detection of fluorescence, bioluminescence and chemiluminescence signals. The probes are injected intravenously (i.v.) or intraperitoneally (i.p.) into an experimental animal. The fluorescent dyes need to be excited by a light source with a

specific wavelength, while bioluminescence and chemiluminescence probes emitting photons which are occurring in biochemical reactions. The emitted fluorescence signal can be measured *in vivo* by a highly sensitive camera. An additionally recorded bright field image allows the signal to be assigned to the corresponding anatomical structures of the animal.

Through shielding of the scattered light using a light-proof "dark box" and cooling of the camera chip up to -70°C a highly specific and sensitive measurement of the emitted signal *in vivo* is possible. In case of fluorescence probes excitation and emission filters with the narrowest possible bandwidth decrease disturbing light sources like autofluorescence. The light absorption of water and hemoglobin in the used wavelength spectrum near of infrared (700-900 nm) is relatively low, which allows measurements in the tissue up to a depth of 2-3 cm (147, 148).

With optical imaging, molecular processes can be monitored *in vivo* without exposure to radioactive radiation. Further advantages over other methods of molecular *in vivo* imaging are the short acquisition time and the relatively low technical effort. However, absolute quantification and reliable three-dimensional reconstructions are not feasible with optical imaging.

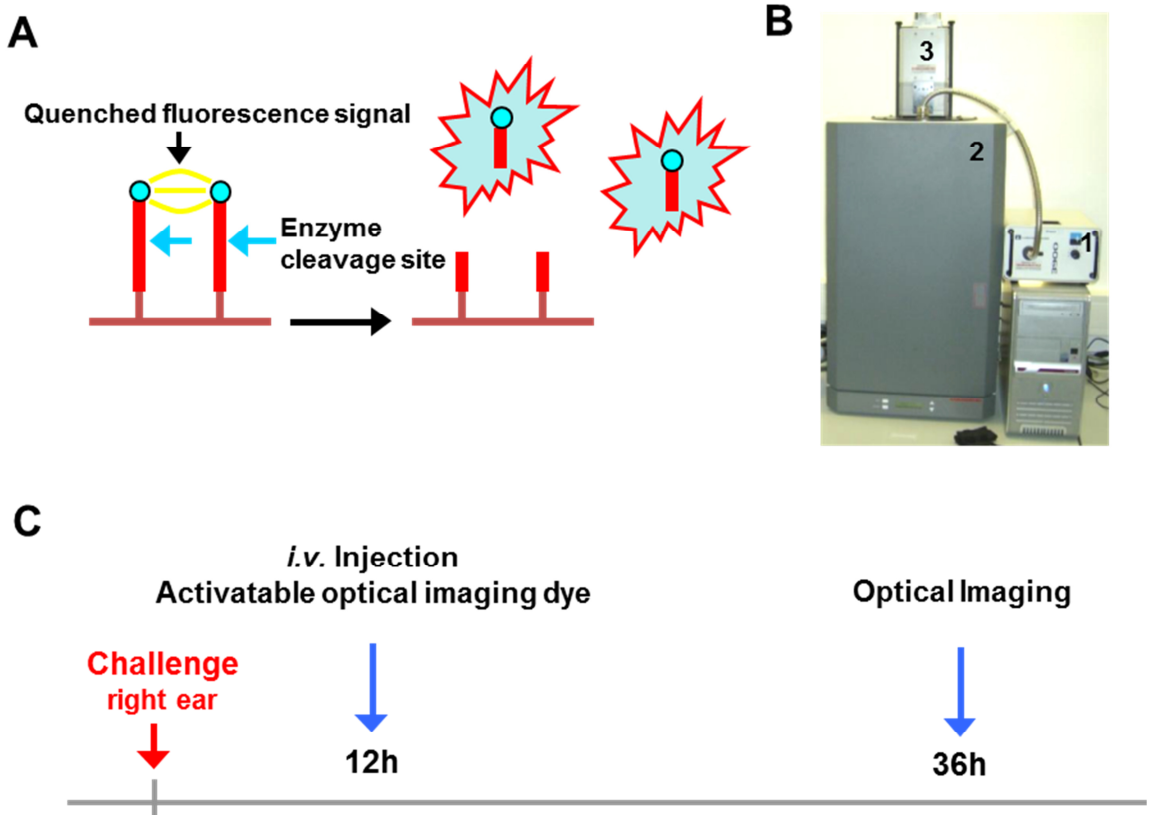

Figure 2: A Activatable optical imaging probes are designed in a way that without protease acitvity a peptide sequence is holding two fluorochromes closely together, which leads to a quenching of the fluorescence signal by fluorescent resonance energy transfer (FRET). Cleavage of the peptide sequence, which possesses a protease-specific cleavage site, activates the fluorescence and enables the measurement of a protease dependent signal by optical imaging. **B** The photograph shows an exemplary optical imaging setup which was typically used for the experiments in this thesis consisting of an excitation light source [1], a lightproof dark box [2] and a highly sensitive charge-coupled device (CCD) camera [3]. **C** In our experiments, the optical imaging probes were injected intravenously 12 hours after TNCB ear challenge when the peak of the inflammatory responses was reached in chronic DTHR. The *in vivo* optical imaging measurements were performed 24 hours later according to the manufacturer's recommendations and previous results (8, 149).

To assess the *in vivo* activity of cathepsins, protease activatable probes have been developed for noninvasive optical imaging (150, 151). These probes are possessing a peptide sequence which can be cleaved preferentially by specific proteases. If proteases, like cathepsin B, are cleaving this specific peptide sequence, the fluorescence signal is not quenched by fluorescence resonance energy transfer (FRET) anymore and a fluorescence signal depending on the specific protease activity can be measured using *in vivo* optical imaging (150, 151).

Recently, we investigated the *in vivo* MMP activity over the time course of acute and chronic cutaneous DTHR and monitored the anti-inflammatory treatment effect of NAC using a optical imaging probe, which is specifically activated by MMPs (8).

The *in vivo* detection of ROS in inflamed tissue is difficult, not only due to the short lifetime in the range of milliseconds up to minutes, but also due to the vast biochemical variety of the ROS/RNS species. So far, some approaches for non invasive *in vivo* ROS detection have been published, mostly based on the chemiluminescent probe luminol or derivatives like L-012 (152-159). The ROS species O_2^- oxidizes L-012, which is then emitting photons detectable by optical imaging (153, 160). Nevertheless, according to results from different groups also other ROS species are contributing to the measured L-012 chemiluminescent signal (152, 161, 162). Some investigators have also suggested that RNS lead to a pronounced L-012 signal (153, 161).

NF-κB-luciferase-reporter mice are enabling a non-invasive *in vivo* detection of NF-κB activation by bioluminescence optical imaging. The firefly luciferase

is expressed in these transgenic mice induced by three NF-κB response elements (163). These and similar imaging techniques to asses NF-κB activity by non invasive *in vivo* optical imaging in NF-κB-luciferase-reporter mice have been used already successfully in several experimental disease models such as bacterial infections (164), arthritis models (163, 165) and experimental tumor models (166, 167).

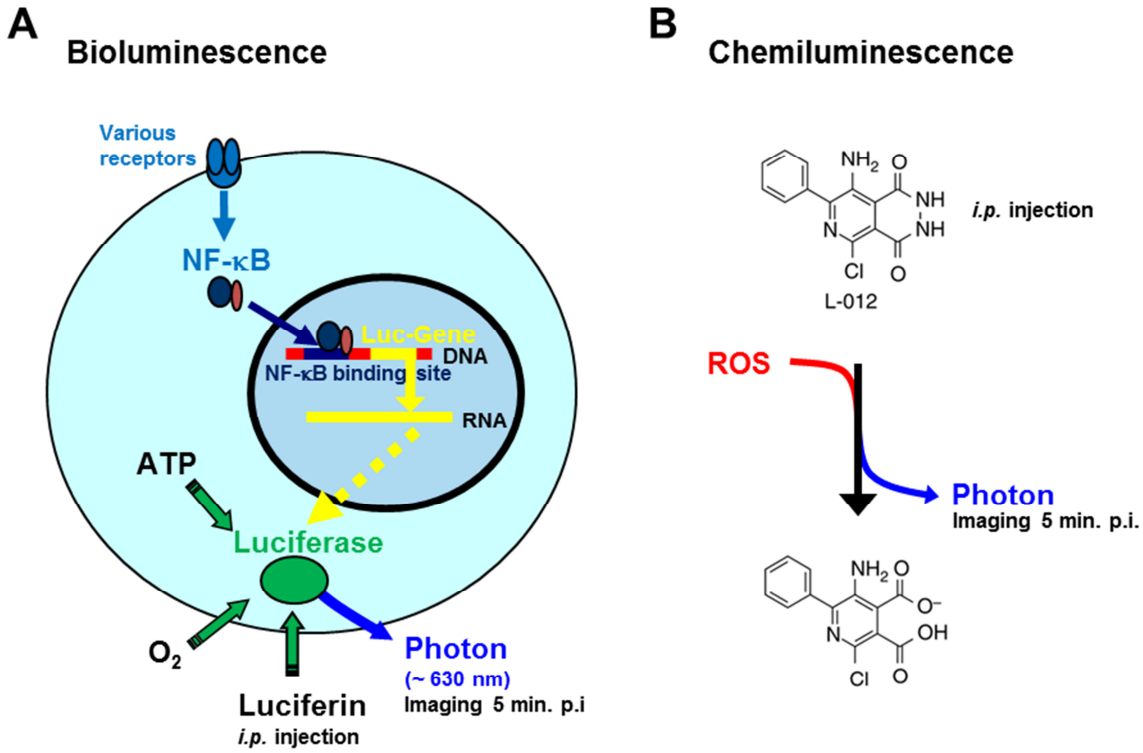

Figure 3: A The activation of the NF-κB pathway, e.g. by receptors on the cellular surface like TNF, leads to the NF-κB dependent expression of the enzyme luciferase. Luciferase is catalyzing the oxidation of luciferin using adenosine triphosphate (ATP) and oxygen (O_2) which results in the emissions of photons detectable by optical imaging. **B** The chemiluminescence agent L-012 reacts with ROS and forms intermediate products which are emitting measurable photons for optical imaging (adapted from Goiffon et al. 2015 (160)).

1.7 Aims

In this thesis optical imaging was employed to analyze the different molecular mechanisms involved in the regulation of inflammation, namely ROS/RNS production, the activation of the NF-κB pathway and the activity of cathepsin B. The T-cell driven acute and chronic TNCB induced DTHR served as a well established experimental model to study the dynamics of molecular events and their changes under targeted therapeutic interventions.

2. Results

This thesis consists of two original publications on the molecular processes in the inflamed tissue of acute and chronic TNCB-induced DTHR. The first publication focuses on the analysis of the temporal dynamics of ROS/RNS production and the activation of the inflammatory NF-κB pathway during acute and chronic inflammation (168). The second publication is delineating the *in vivo* cathepsin activity during the acute TNCB-specific DTHR. The cathepsin B-expressing inflammatory cells at the sites of inflammation and draining lymph nodes were identified and the effects of cathepsin B deficiency as well as specific therapeutic interventions were investigated (169).

2.1 Temporal Dynamics of Reactive Oxygen and Nitrogen Species and NF-κB Activation during Acute and Chronic T Cell-Driven Inflammation (168)

The article included in this chapter was published in

Molecular Imaging and Biology 2020 Jun;22(3):504-514.

”Temporal Dynamics of Reactive Oxygen and Nitrogen Species and NF-κB Activation During Acute and Chronic T Cell–Driven Inflammation”

Johannes Schwenck, Roman Mehling, Wolfgang M. Thaiss, Daniela Kramer, Irene Gonzalez Menendez, Hasan Halit Öz, Dominik Hartl, Klaus Schulze-Osthoff, Stephan Hailfinger, Kamran Ghoreschi, Leticia Quintanilla-Martinez, Harald Carlsen, Martin Röcken, Bernd J. Pichler, Manfred Kneilling.

MOLECULAR IMAGING AND BIOLOGY

Mol Imaging Biol (2019)
DOI: 10.1007/s11307-019-01412-8

WMIS World Molecular Imaging Society
esmi European Society for Molecular Imaging

RESEARCH ARTICLE

Temporal Dynamics of Reactive Oxygen and Nitrogen Species and NF-κB Activation During Acute and Chronic T Cell–Driven Inflammation

Johannes Schwenck,[1,2] Roman Mehling,[1] Wolfgang M. Thaiss,[1,3] Daniela Kramer,[4] Irene Gonzalez Menendez,[5] Hasan Halit Öz,[6] Dominik Hartl,[6] Klaus Schulze-Osthoff,[4,7] Stephan Hailfinger,[4] Kamran Ghoreschi,[8] Leticia Quintanilla-Martinez,[5] Harald Carlsen,[9] Martin Röcken,[7,10] Bernd J. Pichler,[1,7] Manfred Kneilling[1,10]

[1]*Werner Siemens Imaging Center, Department of Preclinical Imaging and Radiopharmacy, Eberhard Karls University, 72076, Tübingen, Germany*
[2]*Department of Nuclear Medicine, Eberhard Karls University, 72076, Tübingen, Germany*
[3]*Department of Diagnostic and Interventional Radiology, Eberhard Karls University, 72076, Tübingen, Germany*
[4]*Interfaculty Institute of Biochemistry, Eberhard Karls University of Tübingen, Tübingen, Germany*
[5]*Department of Pathology, Eberhard Karls University, 72076, Tübingen, Germany*
[6]*Department of Pediatrics I, Eberhard Karls University, 72076, Tübingen, Germany*
[7]*German Cancer Consortium (DKTK) and German Cancer Research Center, 69120, Heidelberg, Germany*
[8]*Department of Dermatology, Venereology and Allergology, Charité – Universitätsmedizin Berlin, 10117, Berlin, Germany*
[9]*Department of Chemistry, Biotechnology and Food Science, Norwegian University of Life Sciences, 1432, Ås, Norway*
[10]*Department of Dermatology, Eberhard Karls University, 72076, Tübingen, Germany*

Abstract

Purpose: Reactive oxygen and nitrogen species (ROS/RNS) production and the NF-κB activation are critically involved in inflammatory responses, but knowledge about the temporal dynamics during acute and chronic inflammation is limited. Here, we present a comparative longitudinal *in vivo* study of both parameters in an experimental model of acute and chronic T cell–driven delayed-type hypersensitivity reaction (DTHR) using noninvasive optical imaging.

Procedures: Trinitrochlorobenzene (TNCB)-sensitized NF-κB-luciferase-reporter and wild-type mice were TNCB challenged on the right ear to elicit acute DTHR and then repetitively challenged (up to five times) to induce chronic DTHR. Mice were treated with the ROS-scavenging and NF-κB inhibiting molecule N-acetylcysteine (NAC) or underwent sham treatment. ROS/RNS production was noninvasively analyzed *in vivo* using the ROS-/RNS-sensitive chemiluminescent probe L-012, and NF-κB activation was measured using NF-κB-luciferase-reporter mice. H&E staining, CD3 and myeloperoxidase (MPO) immunohistochemistry (IHC), and quantitative PCR (qPCR) analyses were employed to investigate immune cell

Electronic supplementary material The online version of this article (https://doi.org/10.1007/s11307-019-01412-8) contains supplementary material, which is available to authorized users.

Correspondence to: Manfred Kneilling; *e-mail:* manfred.kneilling@med.uni-tuebingen.de

Published online: 03 September 2019

infiltration and expression of NF-κB- and ROS-/RNS-driven genes.
Results: In acute DTHR, we found strongly elevated ROS/RNS production and NF-κB activation 12 h after the 1st TNCB ear challenge, peaking at 24 h after the challenge. In chronic DTHR, ROS production peaked as early as 4 h after the 5th TNCB challenge, whereas NF-κB activity peaked after 12 h. The increase in ROS/RNS production in acute DTHR was higher than the increase in NF-κB activity but the relationship was inverse in chronic DTHR. Treatment with the ROS scavenger NAC had differential effects on ROS/RNS production and NF-κB activation during acute and chronic DTHR. *Ex vivo* cross-validation by histopathology and qPCR analysis correlated closely with the *in vivo* imaging results.
Conclusions: Noninvasive *in vivo* imaging is capable of assessing the temporal dynamics of ROS/RNS production and NF-κB activation during progression from acute to chronic DTHR and enables monitoring of anti-inflammatory treatment responses.

Key Words: Optical imaging, Delayed-type hypersensitivity reaction, Contact allergy, N-acetylcysteine, Contact hypersensitivity reaction, Inflammation, Anti-inflammatory effect, L-012, NF-κB

Introduction

Reactive oxygen species (ROS) and reactive nitrogen species (RNS), a heterogeneous group of oxidative molecules, are common stress factors for cells. ROS/RNS appear in both physiological, e.g., as byproducts of cellular metabolism or as signaling molecules, and pathological conditions, such as when ROS/RNS are generated by inflammatory cells, including polymorphonuclear neutrophils (PMNs) or macrophages [1, 2].

In particular, oxidative phosphorylation in mitochondria and NADPH oxidase complexes (NOX) convert oxygen into the primary radical superoxide anion (O_2^-), which is rapidly converted into secondary ROS/RNS. Membrane-permeable hydrogen peroxide (H_2O_2) is generated by catalase or glutathione peroxidase. Myeloperoxidase (MPO) generates various other ROS, such as hypochlorous acid (HClO), hypothiocyanous acid (HOSCN), and other radicals, by oxidation of organic and inorganic substrates [3]. Further, RNS such as peroxynitrite are formed by a reaction between O_2^- and nitric oxide (NO), which is produced by nitric oxide synthases (NOS) [4]. Since ROS/RNS participate in multiple biochemical interactions, the roles of ROS/RNS in inflammation have more than one dimension: both pro- and anti-inflammatory roles have been described, which lead to either tissue-destructive or tissue-protective effects [5].

Therefore, maintenance of a regulated balance between ROS/RNS and antioxidants is necessary for the control of immune responses. The multiple effects of ROS become evident in patients with chronic granulomatous disease (CGD), which is caused by an inherited deficiency of NOX2 activity. CGD patients suffer from both persistent bacterial and fungal infections as well as autoimmune diseases such as arthritis [6].

The immunomodulatory effects of ROS/RNS on inflammatory immune responses are caused by a variety of mechanisms, including interactions with signaling pathways such as nuclear factor (erythroid-derived 2)-like 2 (NRF2) or p38 mitogen-activated protein (MAP) kinases [7], but they also influence the mechanisms of antigen presentation and T cell receptor signaling as well as aerobic glycolysis in activated $CD4^+$ T cells [3]. A major ROS-sensitive regulator of inflammatory immune responses is the NF-κB pathway [8]. The NF-κB protein family consists of five proteins that can form multiple heterodimeric NF-κB protein complex and induce the transcription of many genes, including pro-inflammatory mediators such as IL-1β, IL-6, and TNF as well as other pro- and antioxidative target genes [9].

So far, little is known about the temporal dynamics of ROS/RNS production and their interactions with inflammatory pathways, such as NF-κB. Due to the short lifetime, ranging from milliseconds to minutes, and the chemical variety of different ROS, measurement of ROS/RNS remains challenging. A few detection strategies have been described to noninvasively study ROS production *in vivo* [10–17].

L-012 is a luminol-based chemiluminescent (CL) probe, which was evaluated for preclinical *in vivo* optical imaging (OI) experiments by Kielland et al. [10]. The oxidized form of L-012 reacts with O_2^- to form an excited-state intermediate, which emits detectable photons by chemiluminescence [11]. Some investigators have suggested that RNS lead to a pronounced L-012 chemiluminescent signal, while the contribution of H_2O_2 to the luminescent signal is relatively small [11, 18].

In this study, we focused on the temporal dynamics of ROS/RNS production and their influence on NF-κB signaling by noninvasive *in vivo* OI in acute and chronic TNCB-induced cutaneous contact hypersensitivity, a well-characterized and established experimental model for T cell–driven DTHR [19–21]. DTHRs are orchestrated mainly by interferon-γ-producing $CD4^+$ (Th1) and $CD8^+$ (Tc1) T cells [22, 23] and characterized by accumulations of PMNs. PMNs elicit ROS/RNS during oxidative burst, which is critically involved in the pathogenesis of several

autoimmune diseases, such as rheumatoid arthritis and psoriasis vulgaris [24].

To our knowledge, this is the first noninvasive *in vivo* study investigating the temporal dynamics of ROS/RNS production and NF-κB activation in parallel during different stages of inflammation, employing L-012 and NF-κB-luciferase-reporter mice combined with *ex vivo* cross-validation employing H&E staining, CD3- and MPO-IHC, and qPCR analysis of NF-κB- and ROS-driven genes. In addition, we studied the influence of NAC treatment on ROS/RNS production and NF-κB activation dynamics using these two imaging tools.

Materials and Methods

Animal Experiments

We used 8- to 12-week-old female C57BL/6 mice from Charles River Laboratories (Sulzfeld, Germany) and NF-κB-luciferase-reporter mice provided by Harald Carlsen (Norwegian University of Life Sciences, Ås, Norway) [25]. Animal experiments were approved by the Regierungspräsidium Tübingen. The details on the animal experiments are provided in the electronic supplementary material (ESM).

Treatment Approach

Two days prior to the first TNCB ear challenge, we started to add NAC continuously to the drinking water until the experiments were finished (5 mg/ml; Sigma-Aldrich, Steinheim, Germany) [20]. Sham-treated mice received normal drinking water.

Optical Imaging

To measure *in vivo* NF-κB activation, we injected luciferin (150 mg/kg body weight) i.p. into NF-κB-luciferase-reporter mice 5 min before OI ($n = 10$). For *in vivo* ROS detection, we injected wild-type mice with ROS-sensitive L-012 (25 mg/kg body weight; i.p.) 5 min before OI ($n = 8$). L-012 (Wako Chemical, Neuss, Germany) was dissolved in ultrapure H_2O at a concentration of 5 mg/ml. To assess L-012 chemiluminescence and NF-κB-luciferase bioluminescence signals *in vivo*, we used the IVIS Spectrum OI System (PerkinElmer, Rodgau-Jügesheim, Germany). For details, see ESM.

RNA Extraction and Gene Expression Analysis, Histopathology, and Statistical Analysis

Details are described in the ESM.

Results

Time Course of ROS Production and NF-κB Activity in Acute and Chronic Cutaneous DTHR

First, we evaluated the time course of ROS/RNS production and NF-κB activity in acute DTHR at baseline, 4 h, 12 h, and 24 h after the 1st challenge. At baseline, we recorded only very faint L-012 signal in ears of wild-type mice (Fig. 1a). Additionally, a faint luciferase-mediated signal was recorded in inflamed ears of NF-κB reporter mice (Fig. 1b). As early as 4 h after the 1st TNCB challenge, ear thickness had increased, but we found no enhancement of ROS/RNS production or NF-κB activation (Fig. 1a and b). However, 12 h after the 1st TNCB challenge, both ROS/RNS production and NF-κB activity in inflamed ears increased dramatically (ROS/RNS: 60-fold; NF-κB activity: 18-fold) when compared with baseline and it further increased at 24 h.

We next compared the signal intensities from L-012 chemiluminescence and bioluminescence from inflamed ears of NF-κB-reporter mice at baseline with the signal intensities at 4 h, 12 h, and 24 h post-TNCB challenge. The increase in ROS-/RNS-mediated L-012 signal intensity in inflamed ears was significantly higher than the measured increase in NF-κB activity 12 h after the first TNCB challenge (Fig. 1c).

As repeated TNCB challenges lead to chronic cutaneous DTHR [20], we investigated the time course of ROS/RNS and NF-κB activity after the 3rd and 5th TNCB ear challenges. During early chronic DTHR, we determined clear enhancement of ROS/RNS production and NF-κB activity in inflamed ears by 4 h after the 3rd TNCB ear challenge (Fig. 2a and b). The peak in ROS/RNS production and NF-κB activity shifted from 24 h after the 1st TNCB ear challenge to 12 h after the 3rd TNCB ear challenge. In contrast, the ear thickness indicated no significant change between 12 h and 24 h after the 3rd TNCB ear challenge. ROS/RNS production was already present as early as 4 h after the 5th TNCB ear challenge, whereas the NF-κB activity did not peak until 12 h after the 5th challenge (Fig. 2a and b).

When comparing the relative change in ROS/RNS production and NF-κB activity in the inflamed ears with early chronic and chronic cutaneous DTHR to the baseline at 0 h before the 1st TNCB ear challenge, we determined before (0 h) the 3rd and 5th TNCB ear challenge slightly elevated NF-κB activity values. ROS/RNS production values were remarkably elevated most probably due to the PNMs infiltrating the chronically inflamed ears after the previous TNCB challenges (Figs. 2c, 3b). The relative increase in NF-κB activity at 12 h and 24 h after the 3rd and 4 h, 12 h, and 24 h after the 5th TNCB ear challenge was more pronounced than the increase in ROS/RNS production (Fig. 2c). Interestingly, when calculating the relative change in signal intensity within the course of the 3rd or 5th TNCB ear challenge, using the 0 - h timepoint of the 3rd or 5th challenge as baseline, the relative increase in NF-κB activity 12 h and 48 h after the 3rd TNCB ear

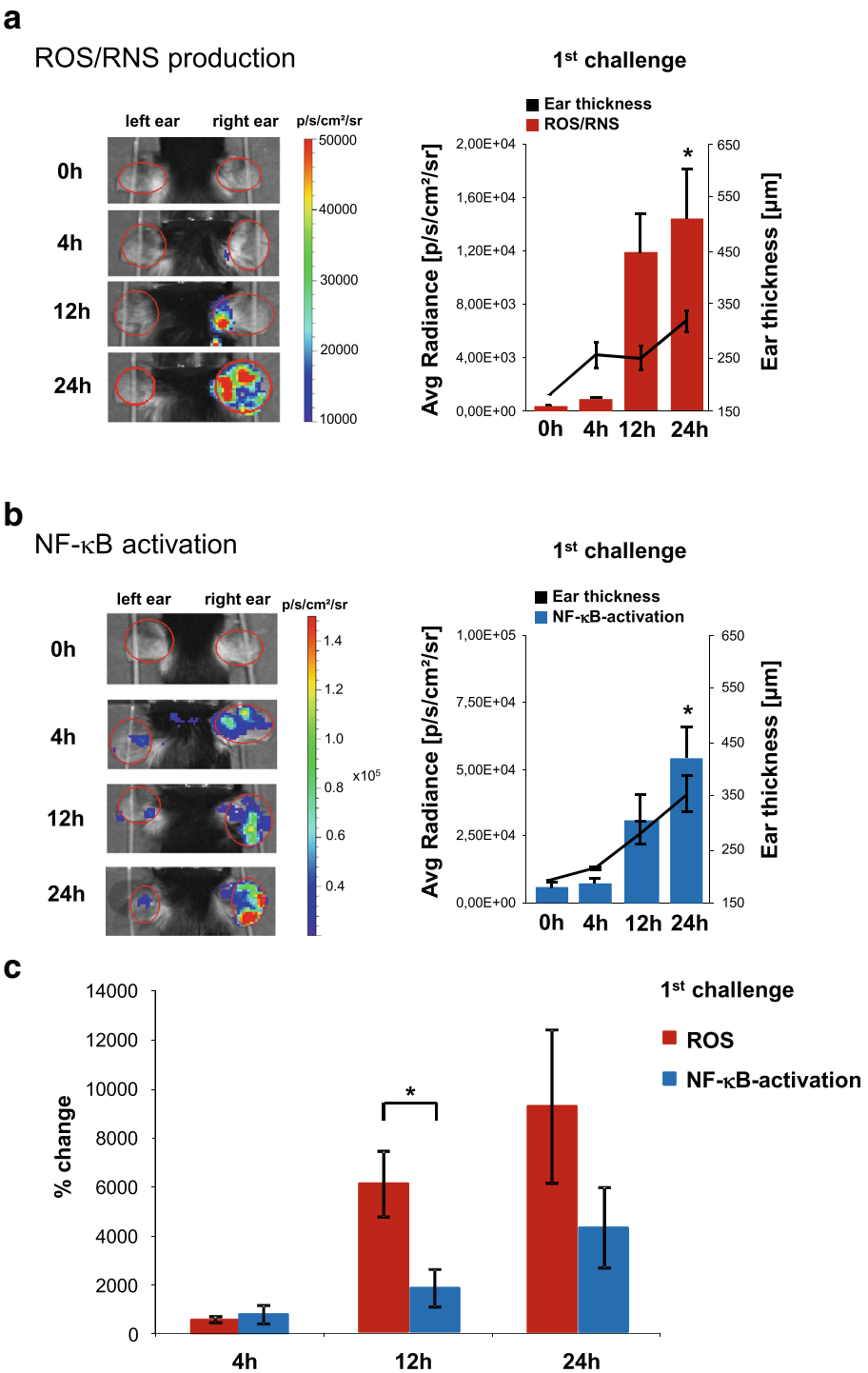

Fig. 1 ROS/RNS production and NF-κB activity in C57BL/6 wild-type mice and C57BL/6 NF-B-luciferase-reporter mice with acute cutaneous DTHR; L-012: $n = 8$; NF-κB-luciferase-reporter mice: $n = 10$. (A) Temporal dynamics of ROS/RNS production (L-012 optical imaging). The peak of the signal intensity (24 h) and the baseline signal intensity was compared using a paired, two tailed Student's *t* test. (B) Temporal dynamics of NF-κB activity. (NF-κB-luciferase-reporter mice) the peak of the signal intensity (24 h) and the baseline signal intensity was compared using a paired, two tailed Student's *t* test. (C) To compare the increase in ROS/RNS production with the increase in NF-κB activation, we calculated the relative change compared with baseline (not inflamed healthy ear) at 0 h, initially before the 1st TNCB ear challenge. Relative enhancement of ROS/RNS production was significantly stronger than relative activation of NF-κB 12 h after the 1st TNCB challenge (unpaired, two-tailed Student's *t* test). Data are presented as the mean ± SEM.

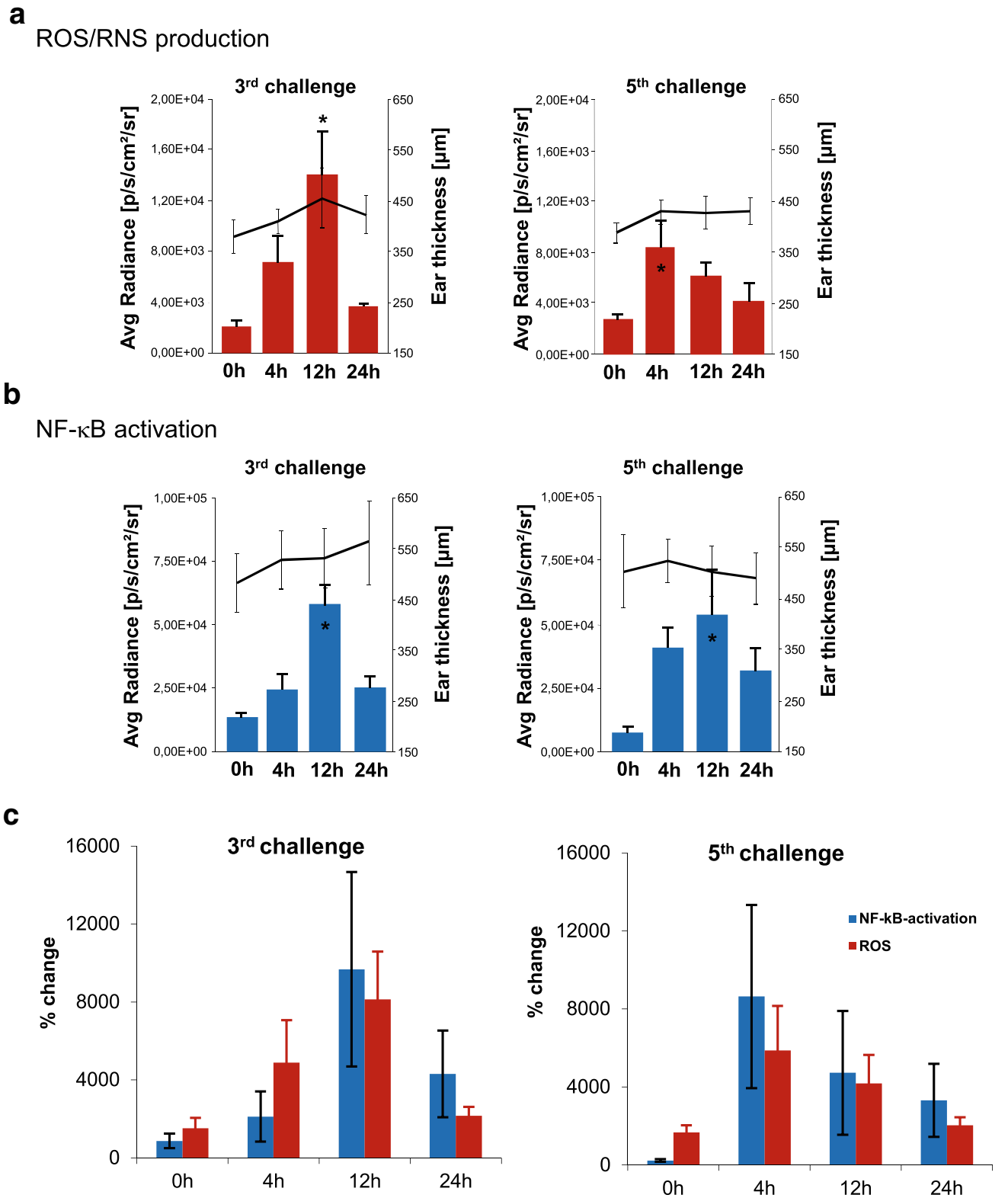

Fig. 2 ROS/RNS production and NF-κB activity in C57BL/6 wild-type mice and C57BL/6 NF-κB-luciferase-reporter mice with early chronic and cutaneous chronic DTHR; L-012: $n = 8$; NF-κB-luciferase-reporter mice: $n = 10$. (A) Temporal dynamics of ROS/RNS production (L-012 optical imaging). The peak of the signal intensity (24 h) and the baseline signal intensity was compared using a paired, two tailed Student's *t* test. (B) Temporal dynamics of NF-κB activity (NF-κB-luciferase-reporter mice). The peak of the signal intensity (24 h) and the baseline signal intensity was compared using a paired, two tailed Student's *t* test. (C) To compare the increase in ROS/RNS production with the increase in NF-B activation, we calculated the relative change compared with baseline in healthy not inflamed ears initially before (0 h) the 1st TNCB ear challenge. Data are presented as the mean ± SEM.

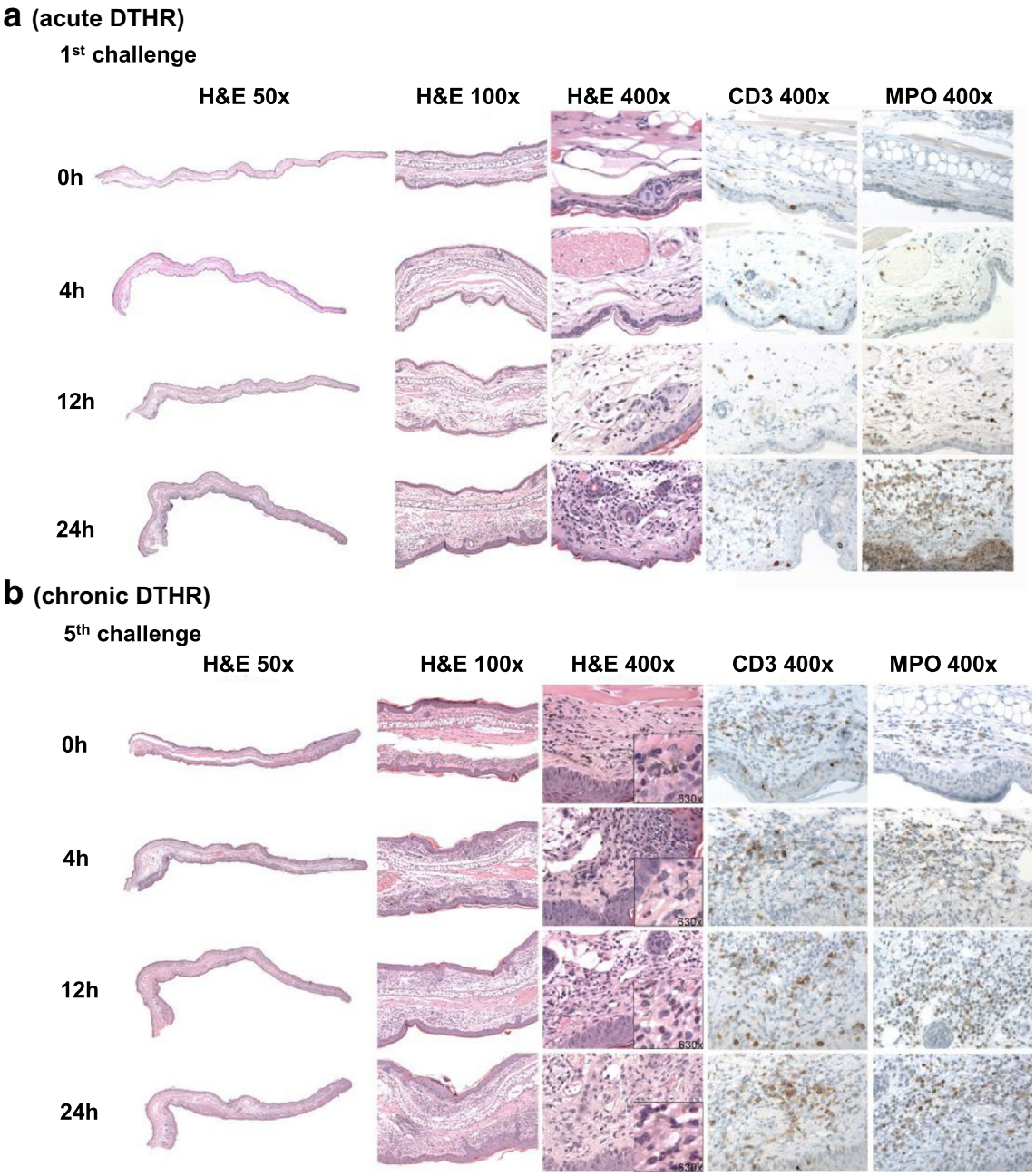

Fig. 3 Standard H&E histopathology as well as CD3 and MPO IHC from (a) naïve mice (0 h), inflamed ears with (a) acute cutaneous DTHR 4 h, 12 h, and 24 h after the 1st TNCB ear challenge and (b) chronic cutaneous DTHR before (48 h after the 4th TNCB ear challenge) 4 h, 12 h, and 24 h after the 5th TNCB ear challenge ($n = 4$; only 12 h after the 5th TNCB ear challenge: $n = 3$).

challenge and especially 4 h, 12 h, and 24 h after the 5th TNCB ear challenge rose up to 80-fold while the relative increase in ROS/RNS production was moderate (Suppl. Fig. 1, see ESM).

Ex vivo Analysis of Inflamed Ears with Acute and Chronic Cutaneous DTHR

For *ex vivo* cross-validation of our *in vivo* imaging results on ROS/RNS production and NF-κB activity, we performed H&E staining and CD3- and MPO-IHC as well as qPCR analysis focusing on NF-κB and ROS-/RNS-driven genes in inflamed ears with acute and chronic cutaneous DTHR.

Standard H&E histopathology as well as CD3- and MPO-IHC revealed in inflamed ears with acute cutaneous DTHR (4 h after the 1st TNCB ear challenge) edema with dilated blood vessels and the presence of MPO^+ PMNs within the blood vessels, but not in the surrounding tissue. Only scarce $CD3^+$ T cells were found in the dermis. At 12 h after the 1st TNCB ear challenge, the edema was more evident, with large dilated blood vessels and extravasation of PMNs,

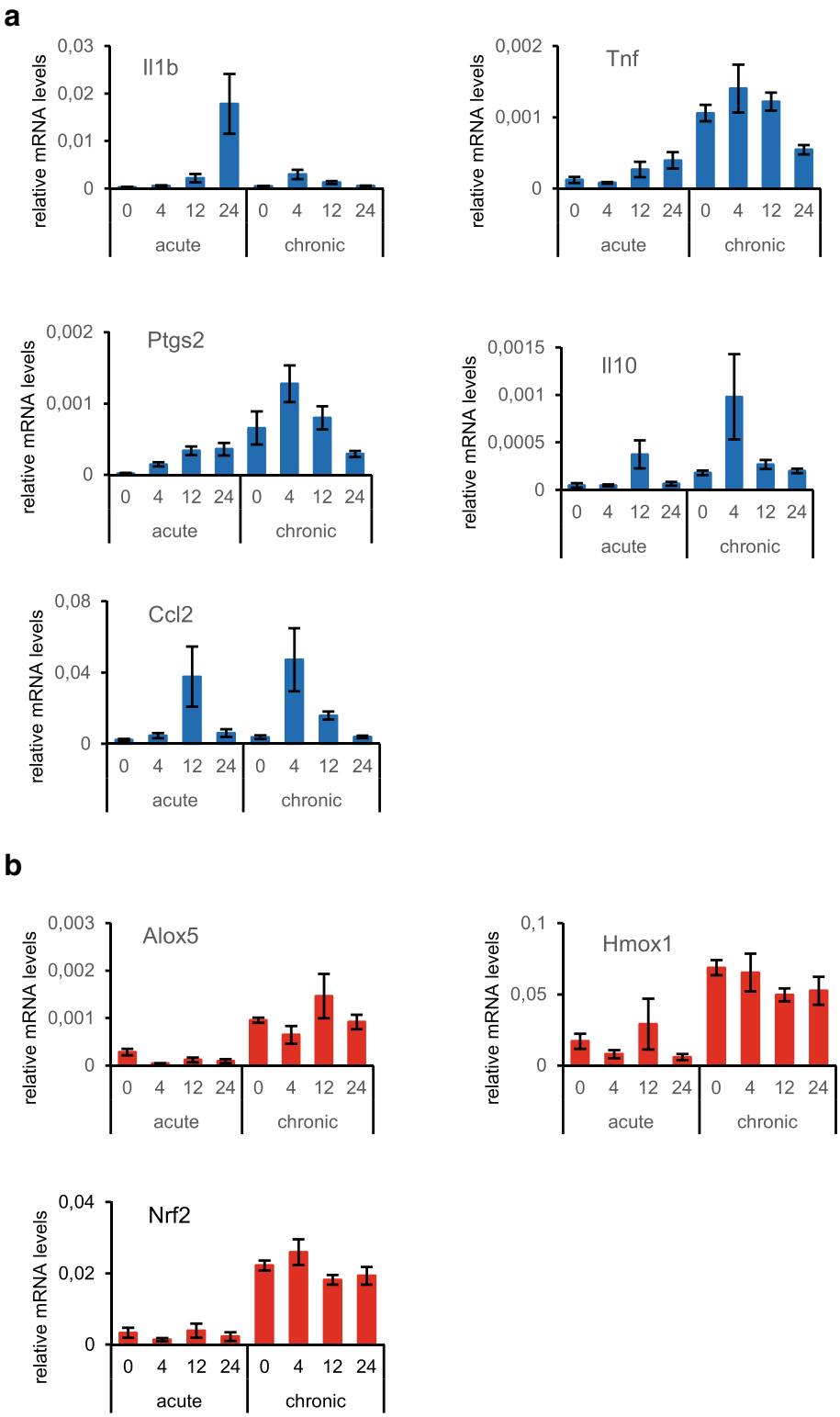

Fig. 4 qPCR analysis of NF-κB- and ROS-/RNS-driven genes of ((a) naïve mice (0 h), inflamed ears with (a) acute cutaneous DTHR 4 h, 12 h, and 24 h after the 1st TNCB ear challenge and (b) chronic cutaneous DTHR before (48 h after the 4th TNCB ear challenge) 4 h, 12 h, and 24 h after the 5th TNCB ear challenge ($n = 4$). Data are represented as mean +/- SEM.

which were also found in large clusters in the dermis. Scarce $CD3^+$ T cells and macrophages were present within the epidermis and in the dermis, while PMNs were significantly increased in the dermis. Strikingly, 24 h after the 1st TNCB ear challenge, a massive infiltration of PMNs within the dermis accompanied with abscesses and small crusts was

observed together with a mild increase of $CD3^+$ T cells and macrophages within the dermis (Fig. 3a; Suppl. Table 2; Suppl. Fig. 2—see ESM).

Before the 5th TNCB ear challenge, 48 h after the 4th TNCB ear challenge, we observed thickening of the epidermis as a consequence of the chronic inflammation. The dermis showed a mild edema accompanied with dilated blood vessels and an infiltrate of $CD3^+$ T cells and macrophages but only a few MPO^+ PMNs. After 4 h, 12 h, and 24 h, a similar thickened epidermis with few small crusts and abscesses were identified together with an increased infiltrate of $CD3^+$ T cells and MPO^+ PMNs within the dermis (Fig. 3b; Suppl. Table 2; Suppl. Fig. 2—see ESM). In summary, the histopathological evaluation of the degree of inflammation and the homing dynamics of MPO^+ PMNs during acute and chronic cutaneous DTHR fit well with our *in vivo* ROS/RNS production and NF-κB activity imaging results. The increase in RNS/ROS production was accompanied with a pronounced PMN recruitment within the inflamed ears (Fig. 3a, b).

Next, we focused on the gene expression patterns in healthy and inflamed ears with acute and chronic cutaneous DTHR. A remarkable increase in the expression of NF-κB-driven genes encoding Il1b, TNF, and Ptgs2 (COX-2) became evident 12 h after the 1st TNCB ear challenge. In line with the NF-κB imaging results, induction of pro-inflammatory gene expression peaked after 24 h. Ccl2 and Il10 mRNA expression reached a maximum as early as 12 h after the 1st TNCB ear challenge (Fig. 4a). In chronic DTHR, all investigated NF-κB-driven genes peaked already 4 h after 5th TNCB ear challenge (Fig. 4a), which coincided with the strongly enhanced NF-κB signal in the inflamed ears of the luciferase-reporter mice peaking at 12 h (Fig. 2b). The mRNA expression levels of ROS-inducible genes did not follow the *in vivo* dynamics of ROS production during acute and chronic DTHR (Fig. 4b). Nevertheless, an increase in mRNA expression of ROS-regulated proteins (Nrf2, Hmox1 (HO-1), and Alox5 (LOX-5)) was evident in chronic cutaneous DTHR when compared with the acute phase (Fig. 4b).

Impact of NAC Treatment on ROS Production and NF-κB Activity

Next, we analyzed the differential effects of NAC treatment on ROS/RNS production expression and NF-κB activity during acute and chronic DTHR. In agreement with our recent experiments [20], NAC treatment significantly suppressed TNCB-induced ear-swelling responses during acute and chronic DTHR when compared with those of sham-treated mice.

Despite the reported significant anti-inflammatory effect of NAC (Fig. 5a), its impact on ROS/RNS production and NF-κB activity was heterogeneous. Maximum ROS/RNS production in inflamed ears was reached at 12 h after the 1st challenge in sham-treated mice and at 24 h in NAC-treated mice, whereas NF-κB expression peaked at 24 h in sham-treated mice and at 12 h in NAC-treated mice (Fig. 5b and c). Intriguingly, ROS production was higher in NAC-treated mice at 24 h following the 1st TNCB ear challenge than in sham-treated mice.

After the 3rd TNCB ear challenge, which corresponded to early chronic DTHR, ROS/RNS production in inflamed ears of NAC-treated mice was normal at 4 h and 12 h post challenge, but it was 3-fold higher at 24 h post challenge compared with that of sham-treated mice. In contrast, NF-κB activity in inflamed ears of NAC-treated mice was completely unchanged 4–24 h after TNCB ear challenge when compared with that of sham-treated mice (Fig. 5b and c).

After the 5th challenge, during chronic cutaneous DTHR, we observed almost no reduction in ROS production in inflamed ears of NAC-treated mice when compared with that of inflamed ears of sham-treated mice (Fig. 5b). In contrast, NF-κB activity was strongly reduced 4 h after the 5th TNCB ear challenge as a consequence of NAC treatment and was marginally elevated after 12 h and 24 h in comparison with that of sham-treated mice (Fig. 5c).

Histological analysis of inflamed ears 24 h after the 5th TNCB ear challenge, a time point when the ear-swelling response in NAC-treatment mice was only moderately reduced compared with the sham-treatment (Fig. 5a), revealed acanthosis with the presence of intra-epidermal PMNs and focal hyperkeratosis as well as edema and dilated blood and lymphatic vessels in the dermis in both experimental groups (Fig. 5c; Suppl. Fig. 3—see ESM). The inflammatory infiltrate was focal and mild in the H&E staining, while CD3 and MPO IHC did not reveal significant differences between the two experimental groups (Fig. 5d), correlating well to our *in vivo* L-012 imaging results (Fig. 5c).

Discussion

In this study, we noninvasively evaluated the temporal dynamics of ROS/RNS production and NF-κB activation during acute and chronic cutaneous DTHR *in vivo*. During acute cutaneous DTHR, both ROS/RNS production and NF-κB activation were strongly increased 12 h after the first TNCB challenge and reached a maximum after 24 h. During early chronic cutaneous DTHR, ROS/RNS production and NF-κB activation peaked simultaneously 12 h after the third repetitive TNCB ear challenge. While in chronic cutaneous DTHR, after five repetitive TNCB ear challenge, we were able to measure strongly elevated ROS/RNS production and NF-κB activation as early as 4 h (Fig. 2a and b).

Both ROS/RNS production and NF-κB have been extensively investigated *in vitro* but have hardly been investigated *in vivo*. Sustained ROS stress *in vitro* causes proteasome inactivation by 50–80 % and therefore less degradation of the inhibitory I-κBα protein, resulting in suppressed NF-κB activation [26].

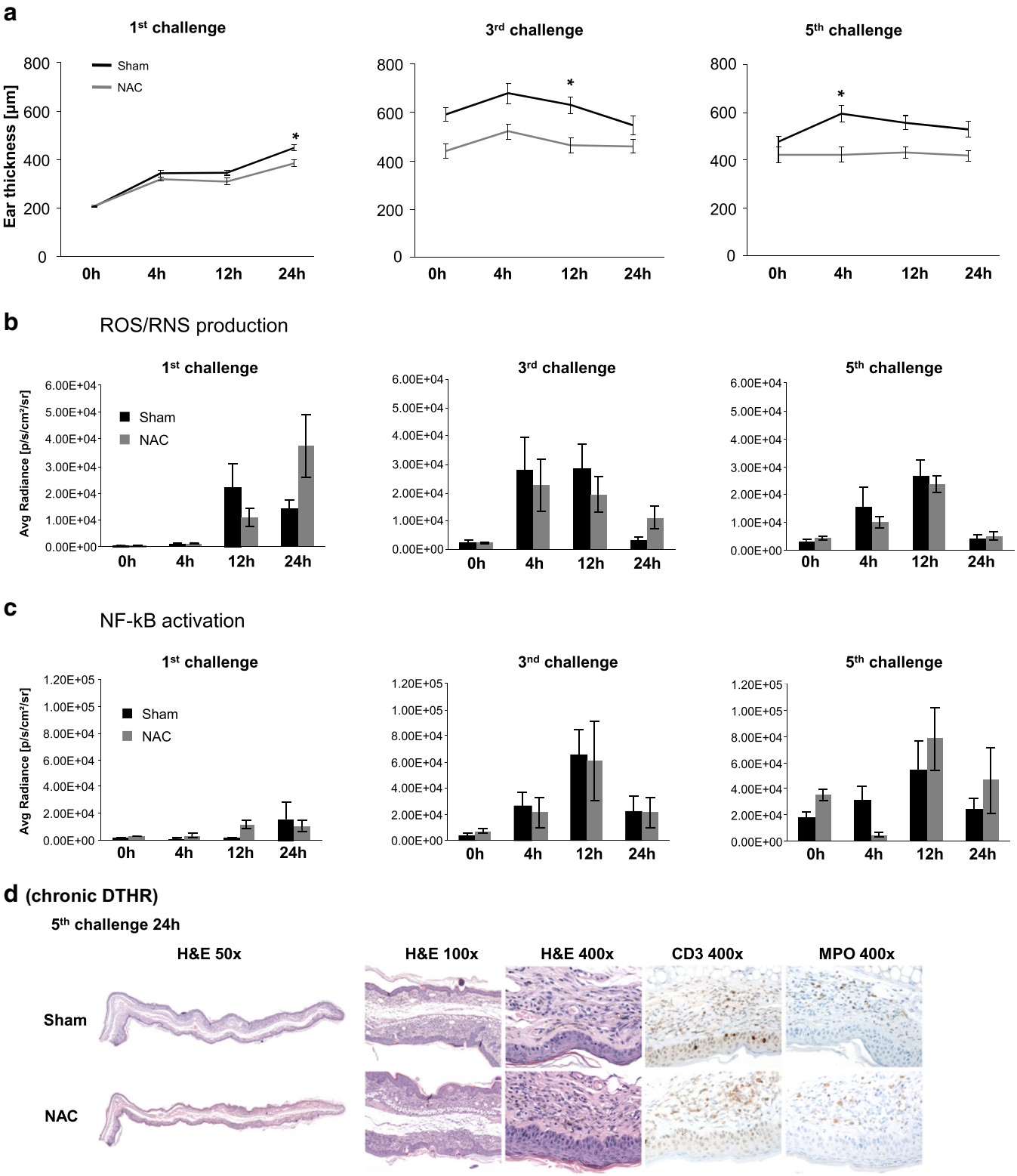

Fig. 5 Impact of NAC-treatment on ROS/RNS production and NF-κB activity (NF-κB-luciferase-reporter mice: NAC treatment $n = 5$, sham treatment $n = 4$; L-012: NAC treatment $n = 5$, sham treatment $n = 5$). (A) Time course of the ear thickness 0–24 h after the 1st, 3rd, and 5th TNCB ear challenges. (B) Temporal dynamics of ROS/RNS production in inflamed ears of NAC-treated or sham-treated mice with acute, early chronic, and chronic cutaneous DTHR. (C) Temporal dynamics of NF-κB activation in inflamed ears of NAC-treated or sham-treated mice with acute, early chronic, and chronic cutaneous DTHR. Data are presented as mean ± SEM. (D) H&E histology and MPO and CD3 IHC 24 h after the 5th TNCB ear challenge (chronic cutaneous DTHR; $n = 4$).

A characteristic feature of the NF-κB signaling pathway is that immediate responses to various stimuli are feasible, as the transcription factors are stored in an inactive state in the cytoplasm. In general, two distinct NF-κB signaling pathways that result in two different NF-κB-dependent gene expression patterns have been described (See Suppl. 1 Discussion in ESM).

Among the NF-κB-driven genes are multiple antioxidant and ROS-/RNS-promoting gene targets, but NF-κB itself also heavily influences ROS/RNS expression [27]. ROS/RNS measurements are especially challenging *in vivo*. In our study, we confirmed the feasibility of noninvasively determining ROS/RNS production *in vivo* and longitudinally monitoring the changes in ROS/RNS production during progression from acute to chronic cutaneous DTHR. We employed the chemiluminescent probe L-012, which has been extensively used in several *in vitro* studies, but the use of L-012 in *in vivo* studies is rare. Kielland et al. used L-012 for *in vivo* studies in experimental LPS-induced acute systemic inflammation, PMA-induced inflammation of the ear, and collagen-induced arthritis [10].

Another established chemiluminescent probe is lucigenin. Tseng et al. demonstrated that the lucigenin chemiluminescent signal is independent of MPO but requires NADPH oxidase (Phox) activity in macrophages, while the luminol chemiluminescent signal largely depends on MPO expression by PMNs [28].

In our experiments, the measured L-012 signal intensity in inflamed ears with acute cutaneous DTHR closely followed the infiltration of MPO^+ PMNs, both peaking 24 h after the 1st TNCB ear challenge (Figs. 1a,3a). In chronic DTHR, a slightly elevated L-012 signal intensity was detectable before the 5th TNCB ear challenge (0 h), 48 h after the 4th TNCB ear challenge, as a consequence of the already established skin inflammation and the presence of MPO^+ PMNs (Figs. 2a, 3b). The L-012 signal peaked already after 4 h, coinciding with an increased number of MPO^+ PMNs in the dermis. Thereafter, the L-012 signal decreased until 24 h after the 5th TNCB ear challenge, while the number of MPO^+ PMNs remained constant (Figs. 2a, 3b). Interestingly, the ROS/RNS production values in chronic cutaneous DTHR were lower than in the acute phase of inflammation (Figs. 1a, 2a). Analysis of the genomic expression of ROS-/RNS-driven antioxidative proteins revealed elevated expression patterns in chronic cutaneous DTHR when compared with the acute phase (Fig. 4b). This might explain why the ROS/RNS production values, determined by L-012 optical imaging, were lower in chronic when compared with acute cutaneous DTHR as antioxidative proteins need time to be produced and expressed [29–31]. The mRNA expression of ROS-/RNS-inducible genes is a part of the cellular response to oxidative stress, the regulation of which is slower and maybe more complex than the response to NF-κB activation which reached similarly high signal intensity levels in NF-κB-reporter mice with acute and chronic cutaneous DTHR (Fig. 1b, Fig. 2b). In addition, it has to be taken in account that the immune cell infiltrate in acute and chronic cutaneous DTHR differs significantly (Fig. 3a and b). Thus, the NF-κB activity in acute DTHR might be mainly related to the affected keratinocytes and the infiltration of PMNs, whereas in the chronic phase, the immune cell infiltrate is more heterogeneous and composed of PMNs, T cells, B cells, and macrophages. For instance, the strongly enhanced Il1b mRNA expression in acute DTHR most likely originates from keratinocytes, whereas the immune cell infiltrate might be mainly responsible for the elevated TNF expression (Fig. 4a and b).

We used two different noninvasive *in vivo* tools to measure ROS/RNS production and NF-κB activation and to longitudinally monitor the antioxidative and NF-κB signaling inhibiting properties of NAC during different stages of cutaneous DTHR. In accordance with our previously published data [20], NAC was highly efficient in suppressing ear-swelling responses during acute and chronic cutaneous DTHR due to its antioxidative and NF-κB-inhibiting effects (Fig. 5a).

Surprisingly, we were not able to identify a clear trend when comparing the measured *in vivo* ROS/RNS production and NF-κB activity in inflamed ears of NAC- and sham-treated mice (Fig. 5b and c). At the later time points, especially 24 h after the 1st (acute DTHR) and 3rd (early chronic DTHR) TNCB ear challenges, we observed enhanced ROS/RNS production in inflamed ears of NAC-treated mice, but at the earlier time points, we saw a rather reduced ROS/RNS production when compared with that of the sham-treatment (Fig. 5b). Thus, NAC treatment might mainly change the temporal dynamics of ROS/RNS production. Despite the indisputable therapeutic effect of NAC (Fig. 5a, right graph), we measured almost no NAC treatment-induced effect on ROS/RNS production in inflamed ears with chronic cutaneous DTHR 24 h after the 5th TNCB ear challenge (Fig. 5b, right graph). NAC treatment was effective during acute, and early chronic and chronic cutaneous DTHR. We observed an elevated baseline (0 h) NF-κB activity level, strongly reduced levels at 4 h after the 5th TNCB ear challenge, and rather enhanced activity after 12 h and 24 h (Fig. 5c).

Despite its widespread use, e.g., as a mucolytic agent or antidote for acetaminophen intoxication, many of the complex and controversial effects induced by NAC are still under debate (See Suppl. 2 Discussion in ESM).

Conclusions

The temporal dynamics of ROS/RNS production and NF-κB activity during the progression from acute to chronic T cell–driven cutaneous DTHR, and during a ROS/RNS and NF-κB activity targeting treatment approach, can be noninvasively monitored *in vivo*. Our study revealed that ROS/RNS production and also NF-κB activity are highly dynamic and are part of a complex interplay between immune cell migration and gene expression. Determination of the temporal dynamics of ROS/RNS production and NF-κB activity may open a new avenue to understand, characterize, and noninvasively monitor inflammatory responses *in vivo*;

therefore, it might enable the improvement of therapeutic interventions. This knowledge could be a prerequisite for the identification of the therapeutic windows for innovative treatment approaches in other types of DTHR, such as psoriasis or rheumatoid arthritis.

Acknowledgments. This work was supported by the German Research Foundation (SFB TRR156, TP C03 to M.K. & B.P., TP B03 to M.R. & A.Y., and TP B09 to D.K. & S.H.), the Medical Faculty of the Eberhard Karls University Tübingen ("PATE"), and the Werner Siemens-Foundation. The authors thank Daniel Bukala, Funda Cay, Maren Harant, and Natalie Mucha for their excellent technical support, as well as Gregory Bowden for providing language editing.

Compliance with Ethical Standards

Conflict of Interest

The authors declare that they have no conflicts of interest.

References

1. Ray PD, Huang BW, Tsuji Y (2012) Reactive oxygen species (ROS) homeostasis and redox regulation in cellular signaling. Cell Signal 24:981–990
2. Winterbourn CC, Kettle AJ, Hampton MB (2016) Reactive oxygen species and neutrophil function. Annu Rev Biochem 85:765–792
3. Forrester SJ, Kikuchi DS, Hernandes MS, Xu Q, Griendling KK (2018) Reactive oxygen species in metabolic and inflammatory signaling. Circ Res 122:877–902
4. Adams L, Franco MC, Estevez AG (2015) Reactive nitrogen species in cellular signaling. Exp Biol Med (Maywood) 240:711–717
5. Hultqvist M, Olsson LM, Gelderman KA, Holmdahl R (2009) The protective role of ROS in autoimmune disease. Trends Immunol 30:201–208
6. Magnani A, Brosselin P, Beaute J et al (2014) Inflammatory manifestations in a single-center cohort of patients with chronic granulomatous disease. J Allergy Clin Immunol 134:655–662 e658
7. D'Autreaux B, Toledano MB (2007) ROS as signalling molecules: mechanisms that generate specificity in ROS homeostasis. Nat Rev Mol Cell Biol 8:813–824
8. Bonizzi G, Karin M (2004) The two NF-kappaB activation pathways and their role in innate and adaptive immunity. Trends Immunol 25:280–288
9. Pahl HL (1999) Activators and target genes of Rel/NF-kappaB transcription factors. Oncogene 18:6853–6866
10. Kielland A, Blom T, Nandakumar KS, Holmdahl R, Blomhoff R, Carlsen H (2009) In vivo imaging of reactive oxygen and nitrogen species in inflammation using the luminescent probe L-012. Free Radic Biol Med 47:760–766
11. Zielonka J, Lambeth JD, Kalyanaraman B (2013) On the use of L-012, a luminol-based chemiluminescent probe, for detecting superoxide and identifying inhibitors of NADPH oxidase: a reevaluation. Free Radic Biol Med 65:1310–1314
12. Boutagy NE, Wu J, Cai Z, Zhang W, Booth CJ, Kyriakides TC, Pfau D, Mulnix T, Liu Z, Miller EJ, Young LH, Carson RE, Huang Y, Liu C, Sinusas AJ (2018) In vivo reactive oxygen species detection with a novel positron emission tomography tracer, (18)F-DHMT, allows for early detection of anthracycline-induced cardiotoxicity in rodents. JACC Basic Transl Sci 3:378–390
13. Carroll V, Michel BW, Blecha J, VanBrocklin H, Keshari K, Wilson D, Chang CJ (2014) A boronate-caged [(1)(8)F]FLT probe for hydrogen peroxide detection using positron emission tomography. J Am Chem Soc 136:14742–14745
14. Carroll VN, Truillet C, Shen B, Flavell RR, Shao X, Evans MJ, VanBrocklin HF, Scott PJH, Chin FT, Wilson DM (2016) [(11)C]Ascorbic and [(11)C]dehydroascorbic acid, an endogenous redox pair for sensing reactive oxygen species using positron emission tomography. Chem Commun (Camb) 52:4888–4890
15. Chu W, Chepetan A, Zhou D, Shoghi KI, Xu J, Dugan LL, Gropler RJ, Mintun MA, Mach RH (2014) Development of a PET radiotracer for non-invasive imaging of the reactive oxygen species, superoxide, in vivo. Org Biomol Chem 12:4421–4431
16. Okamura T, Okada M, Kikuchi T, Wakizaka H, Zhang MR (2015) A (1)(1)C-labeled 1,4-dihydroquinoline derivative as a potential PET tracer for imaging of redox status in mouse brain. J Cereb Blood Flow Metab 35:1930–1936
17. Zhang W, Cai Z, Li L, Ropchan J, Lim K, Boutagy N, Wu J, Stendahl J, Chu W, Gropler R, Sinusas A, Liu C, Huang Y (2016) Optimized and automated radiosynthesis of [(18)F]DHMT for translational imaging of reactive oxygen species with positron emission tomography. Molecules 21
18. Daiber A, Oelze M, August M, Wendt M, Sydow K, Wieboldt H, Kleschyov AL, Munzel T (2004) Detection of superoxide and peroxynitrite in model systems and mitochondria by the luminol analogue L-012. Free Radic Res 38:259–269
19. Kneilling M, Mailhammer R, Hultner L, Schonberger T, Fuchs K, Schaller M, Bukala D, Massberg S, Sander CA, Braumuller H, Eichner M, Maier KL, Hallmann R, Pichler BJ, Haubner R, Gawaz M, Pfeffer K, Biedermann T, Rocken M (2009) Direct crosstalk between mast cell-TNF and TNFR1-expressing endothelia mediates local tissue inflammation. Blood 114:1696–1706
20. Schwenck J, Griessinger CM, Fuchs K et al (2014) In vivo optical imaging of matrix metalloproteinase activity detects acute and chronic contact hypersensitivity reactions and enables monitoring of the antiinflammatory effects of N-acetylcysteine. Mol Imaging 13
21. Schwenck J, Maier FC, Kneilling M, Wiehr S, Fuchs K (2017) Non-invasive in vivo fluorescence optical imaging of inflammatory MMP activity using an activatable fluorescent imaging agent. J Vis Exp
22. Feldmann M, Brennan FM, Maini RN (1996) Role of cytokines in rheumatoid arthritis. Annu Rev Immunol 14:397–440
23. Veale DJ, Ritchlin C, FitzGerald O (2005) Immunopathology of psoriasis and psoriatic arthritis. Ann Rheum Dis 64(Suppl 2):ii26–ii29
24. Biedermann T, Kneilling M, Mailhammer R, Maier K, Sander CA, Kollias G, Kunkel SL, Hültner L, Röcken M (2000) Mast cells control neutrophil recruitment during T cell-mediated delayed-type hypersensitivity reactions through tumor necrosis factor and macrophage inflammatory protein 2. J Exp Med 192:1441–1452
25. Carlsen H, Moskaug JO, Fromm SH, Blomhoff R (2002) In vivo imaging of NF-kappa B activity. J Immunol 168:1441–1446
26. Wu M, Bian Q, Liu Y et al (2009) Sustained oxidative stress inhibits NF-kappaB activation partially via inactivating the proteasome. Free Radic Biol Med 46:62–69
27. Morgan MJ, Liu ZG (2011) Crosstalk of reactive oxygen species and NF-kappaB signaling. Cell Res 21:103–115
28. Tseng JC, Kung AL (2012) In vivo imaging of inflammatory phagocytes. Chem Biol 19:1199–1209
29. Hanschmann EM, Godoy JR, Berndt C, Hudemann C, Lillig CH (2013) Thioredoxins, glutaredoxins, and peroxiredoxins–molecular mechanisms and health significance: from cofactors to antioxidants to redox signaling. Antioxid Redox Signal 19:1539–1605
30. Poprac P, Jomova K, Simunkova M, Kollar V, Rhodes CJ, Valko M (2017) Targeting free radicals in oxidative stress-related human diseases. Trends Pharmacol Sci 38:592–607
31. Sies H, Berndt C, Jones DP (2017) Oxidative stress. Annu Rev Biochem 86:715–748

Electronic Supplementary Material

Differential Temporal Dynamics of Reactive Oxygen and Nitrogen Species and NF-κB Activation during Acute and Chronic T Cell-Driven Inflammation

Journal: Molecular Imaging and Biology

Johannes Schwenck[1,2], Roman Mehling[1], Wolfgang M. Thaiss[1,3], Daniela Kramer[4], Irene Gonzalez Menendez[5], Hasan Halit Öz[6], Dominik Hartl[6], Klaus Schulze-Osthoff[4,7], Stephan Hailfinger[4], Kamran Ghoreschi[8], Leticia Quintanilla-Martinez[5], Harald Carlsen[9], Martin Röcken[7,10], Bernd J. Pichler[1,7], Manfred Kneilling[1,10*]

[1]Werner Siemens Imaging Center, Department of Preclinical Imaging and Radiopharmacy, Eberhard Karls University, 72076 Tübingen, Germany

[2]Department of Nuclear Medicine, Eberhard Karls University, 72076 Tübingen, Germany

[3]Department of Diagnostic and Interventional Radiology, Eberhard Karls University, 72076 Tübingen, Germany

[4]Interfaculty Institute of Biochemistry, Eberhard Karls University of Tübingen, Germany

[5]Department of Pathology, Eberhard Karls University, 72076 Tübingen, Germany

[6]Department of Pediatrics I, Eberhard Karls University, 72076 Tübingen, Germany

[7]German Cancer Consortium (DKTK) and German Cancer Research Center, 69120 Heidelberg, Germany

[8]Department of Dermatology, Venereology and Allergology, Charité – Universitätsmedizin Berlin, 10117 Berlin, Germany

[9]Department of Chemistry, Biotechnology and Food Science, Norwegian University of Life Sciences, 1432, Ås, Norway

[10]Department of Dermatology, Eberhard Karls University, 72076 Tübingen, Germany

* Corresponding author email: manfred.kneilling@med.uni-tuebingen.de

telephone: +49-7071-29-86870

fax: +49-7071-29-4451

Short title: *In vivo* imaging of ROS production and NF-κB activation in inflammation

Materials and Methods

Animal experiments

Mice were sensitized by topical application of TNCB (5% TNCB; 80 µl dissolved in a 4:1 mixture of acetone/Miglyol 812; Sasol, Witten, Germany) to the abdomen and challenged on the right ear at day 7 (1% TNCB; 20 µl dissolved in a 9:1 mixture of acetone/Miglyol 812) to elicit acute DTHR. To induce chronic DTHR, mice were challenged every 48 h, for up to 5 times. Ear swelling was quantified by measuring the ear thickness with a micrometer (Kroeplin, Schlüchtern, Germany) before TNCB ear challenge and 4 h to 24 h afterwards. All measurements of the challenged right ears were compared to the nonchallenged left ears of the mice.

Optical imaging

OI measurements were performed 5 min after injection of 100 µl L-012 solution (5 mg/ml) (170). During optical imaging, mice were anesthetized by inhalation of isoflurane-O_2 (1.5% Forane, Abbott GmbH, Wiesbaden, Germany) and placed on a heating pad to maintain body temperature between 36°C and 37°C. To measure the whole upper surface area of the mouse ears, the ears were carefully fixed on a flat black plate by a nylon thread. Regions of interest (ROIs) were drawn on the right and left ears, enabling a semiquantitative analysis of the detected bioluminescence and chemiluminescence average radiance [p/s/cm^2/sr] as previously described (8, 170). Image analysis was performed using Living Image Software (Perkin Elmer).

RNA extraction and gene expression analysis

Ear samples of the treated mice were sheared in Qiazol (79306, Qiagen) and total RNA was isolated in accordance with the manufacture`s protocol. Genomic DNA was removed by DNAse I digestion (EN0523, Thermo Fisher), followed by cDNA synthesis using oligo(dT) primer (SO132, Thermo Fisher) and Revert Aid reverse transcriptase (EP0441, Thermo Fisher). The expression of the indicated genes was quantified using the Green Master mix (M3023, Genaxxon) and self-designed primers (Suppl Table 1). PCR conditions were as follows: Initial denaturation 15 min at 95°C, followed by 45 cycles of 95°C for 15 s and 60°C for 45 s. Relative mRNA levels were calculated by normalization to the reference gene *Actin* using the $2^{-\Delta\Delta CT}$ method.

Histopathology

Tissue samples were fixed in 4% formalin and subsequently paraffin embedded. For histology 3-5 µm-thick sections were cut and stained with haematoxylin and eosin (H&E). Immunohistochemistry was performed on an automated immunostainer (Ventana Medical Systems, Inc.) according to the company's protocols for open procedures with slight modifications. The slides were stained with the antibodies CD3 (Clone SP7, DCS Innovative Diagnostik-Systeme GmbH u. Co. KG, Hamburg, Germany) and MPO (Anti-Myeoloperoxidase Ab-1, Lab Vision UK, Ltd., Newmarket, Suffolk). Appropriate positive and negative controls were used to confirm the adequacy of the staining. Photomicrographic images were acquired with an Axioskop 2

plus Zeiss microscope equipped with a Jenoptik (Laser Optik System, Jena, Germany) ProgRes C10 plus camera and software. The epidermal inflammation score was based on the presence and number of epidermal abscesses and crusts per section (0 = no damage, 1 = presence of abscesses, 2 = between 1 and 5 crusts, 3 = between 6 and 10 crusts, 4 = more than 11 crusts). A semiquantative analysis of dermal inflammation was also performed ("-" = no inflammatory infiltrate, "+" = minimal inflammatory cells, "++" = mild inflammation, "+++" = moderate inflammation, "++++" = severe presence of inflammatory cells).

Statistical analysis

A paired, two tailed Student's t test was used to compare the peak of the optical imaging signal and the baseline signal **(**Fig. 1a and b; Fig. 2a and b**)**. Unpaired, two-tailed Student's t test was utilized to compare the relative changes of ROS production and NF-κB activation after the first TNCB challenge as well as after the third and the fifth TNCB challenge (Fig. 1c and 2c). Differences in ear thickness, L-012 signal intensities or NF-κB activation signal intensities (NF-κB reporter mice) between NAC- and sham-treated mice were examined by unpaired, two-tailed Student's t test (Fig. 3a - c). P values below 0.05 were considered statistically significant. Quantitative data are reported as the mean and standard error of the mean (± 1 SEM).

Suppl. Discussion 1

The heterodimer of the proteins p50 and RelA (p65) form the canonical NF-κB signaling pathway, whereas p52 and RelB are driving the alternative (non-canonical) NF-κB signaling pathway (130, 171, 172). While the canonical NF-κB signaling pathway is faster and more involved in unspecific innate immune responses, the slower alternative pathway is associated with adaptive immune responses and developmental processes (173-176). Knockout experiments revealed that mice deficient in alternative NF-κB signaling are unable to develop an adequate adaptive immune response against viral infections (177). However, mice deficient in classical NF-κB signaling are more sensitive to bacterial infections (131). Together both, the canonical and alternative NF-κB signaling pathway, represent an interdependent, highly complex regulation system that are influencing each other by expression of NF-κB-monomers, phosphorylation or cleavage of pro-forms (139, 178-181). Both NF-κB signaling pathways are interacting with hundreds of gene loci due to a distinct palindromic DNA sequence (182). Physiologically NF-κB signaling is involved in embryonal development as well as in immune reactions. The relevance of functional NF-κB signaling is underlined by multiple diseases directly caused by genetic malfunctions of NF-κB proteins leading mostly to immune defects or developmental disorders (182). Beyond that, the onsets of a broad range of diseases are caused by cellular responses transmitted by NF-κB signaling, including cancer or neurodegeneration (183, 184).

ROS species interfere with both the canonical as well as the noncanonical NF-κB signaling pathways and are believed to be major regulators of NF-κB-mediated cell responses (185-189). How ROS/RNS interact with NF-κB pathways has not yet been fully elucidated. *In vitro* experiments show that cysteines of NF-κB signaling molecules can be oxidized by ROS/RNS, resulting in inactivation of NF-κB signaling molecules. This inactivation can in turn lead to activation or inactivation of the NF-κB signaling pathway depending on the negative or positive regulatory function of the oxidized NF-κB signaling molecule. The oxidation can be reversed by antioxidative glutathione (186). Furthermore, the oxidation of a specific cysteine within the p50 molecule can lead to the inhibition of its DNA binding and therefore to reduced NF-κB signaling. In contrast, mitochondrial ROS are able to enhance NF-κB signaling (190). Modulatory signaling pathways upstream of NF-κB (e.g., TNF signaling by ROS) are another mode of interaction (186, 191).

Suppl. Discussion 2

It has been demonstrated that NAC can increase the ability of the NF-κB transcription factor subunit p65 to bind to DNA (192). Previously, we reported a suppressive effect of NAC treatment on matrix metalloproteinase activity and angiogenesis (8). The p38 MAP kinase pathway represents another major ROS-sensitive signaling pathway that is involved in establishing and maintaining inflammatory responses (193-197). NAC effectively inhibits p38 MAP kinase signaling in T cells and dendritic cells (198, 199). In our experiments, we observed a nonuniform effect of NAC treatment on *in vivo*

ROS/RNS production and NF-κB activity despite the clear anti-inflammatory effect demonstrated by the reduced ear swelling responses, possibly due to interactions with other pathways.

Supplementary References

1. Fuchs K, Kuehn A, Mahling M, et al. (2017) In Vivo Hypoxia PET Imaging Quantifies the Severity of Arthritic Joint Inflammation in Line with Overexpression of Hypoxia-Inducible Factor and Enhanced Reactive Oxygen Species Generation. J Nucl Med 58:853-860.
2. Schwenck J, Griessinger CM, Fuchs K, et al. (2014) In vivo optical imaging of matrix metalloproteinase activity detects acute and chronic contact hypersensitivity reactions and enables monitoring of the antiinflammatory effects of N-acetylcysteine. Mol Imaging 13.
3. Perkins ND (2007) Integrating cell-signalling pathways with NF-kappaB and IKK function. Nat Rev Mol Cell Biol 8:49-62.
4. Hayden MS, Ghosh S (2004) Signaling to NF-kappaB. Genes Dev 18:2195-2224.
5. Hayden MS, Ghosh S (2008) Shared principles in NF-kappaB signaling. Cell 132:344-362.
6. Bonizzi G, Karin M (2004) The two NF-kappaB activation pathways and their role in innate and adaptive immunity. Trends Immunol 25:280-288.
7. Brown KD, Claudio E, Siebenlist U (2008) The roles of the classical and alternative nuclear factor-kappaB pathways: potential implications for autoimmunity and rheumatoid arthritis. Arthritis Res Ther 10:212.
8. Sun SC (2011) Non-canonical NF-kappaB signaling pathway. Cell Res 21:71-85.
9. Luftig M, Yasui T, Soni V, et al. (2004) Epstein-Barr virus latent infection membrane protein 1 TRAF-binding site induces NIK/IKK alpha-dependent noncanonical NF-kappaB activation. Proc Natl Acad Sci U S A 101:141-146.
10. Droebner K, Klein B, Paxian S, Schmid R, Stitz L, Planz O (2010) The alternative NF-kappaB signalling pathway is a prerequisite for an appropriate immune response against lymphocytic choriomeningitis virus infection. Viral Immunol 23:295-308.
11. Sha WC, Liou HC, Tuomanen EI, Baltimore D (1995) Targeted disruption of the p50 subunit of NF-kappa B leads to multifocal defects in immune responses. Cell 80:321-330.
12. O'Dea E, Hoffmann A (2010) The regulatory logic of the NF-kappaB signaling system. Cold Spring Harb Perspect Biol 2:a000216.
13. Shih VF, Tsui R, Caldwell A, Hoffmann A (2011) A single NFkappaB system for both canonical and non-canonical signaling. Cell Res 21:86-102.
14. Basak S, Shih VF, Hoffmann A (2008) Generation and activation of multiple dimeric transcription factors within the NF-kappaB signaling system. Mol Cell Biol 28:3139-3150.
15. Rao P, Hayden MS, Long M, et al. (2010) IkappaBbeta acts to inhibit and activate gene expression during the inflammatory response. Nature 466:1115-1119.
16. Madge LA, May MJ (2010) Classical NF-kappaB activation negatively regulates noncanonical NF-kappaB-dependent CXCL12 expression. J Biol Chem 285:38069-38077.

17. Zhang Q, Lenardo MJ, Baltimore D (2017) 30 Years of NF-kappaB: A Blossoming of Relevance to Human Pathobiology. Cell 168:37-57.
18. Karin M (2009) NF-kappaB as a critical link between inflammation and cancer. Cold Spring Harb Perspect Biol 1:a000141.
19. Mincheva-Tasheva S, Soler RM (2013) NF-kappaB signaling pathways: role in nervous system physiology and pathology. Neuroscientist 19:175-194.
20. D'Autreaux B, Toledano MB (2007) ROS as signalling molecules: mechanisms that generate specificity in ROS homeostasis. Nat Rev Mol Cell Biol 8:813-824.
21. Morgan MJ, Liu ZG (2011) Crosstalk of reactive oxygen species and NF-kappaB signaling. Cell Res 21:103-115.
22. Dolado I, Swat A, Ajenjo N, De Vita G, Cuadrado A, Nebreda AR (2007) p38alpha MAP kinase as a sensor of reactive oxygen species in tumorigenesis. Cancer Cell 11:191-205.
23. Torres M, Forman HJ (2003) Redox signaling and the MAP kinase pathways. Biofactors 17:287-296.
24. Michiels C, Minet E, Mottet D, Raes M (2002) Regulation of gene expression by oxygen: NF-kappaB and HIF-1, two extremes. Free Radic Biol Med 33:1231-1242.
25. Hughes G, Murphy MP, Ledgerwood EC (2005) Mitochondrial reactive oxygen species regulate the temporal activation of nuclear factor kappaB to modulate tumour necrosis factor-induced apoptosis: evidence from mitochondria-targeted antioxidants. Biochem J 389:83-89.
26. Lingappan K (2018) NF-kappaB in Oxidative Stress. Curr Opin Toxicol 7:81-86.
27. Liu J, Yoshida Y, Yamashita U (2008) DNA-binding activity of NF-kappaB and phosphorylation of p65 are induced by N-acetylcysteine through phosphatidylinositol (PI) 3-kinase. Mol Immunol 45:3984-3989.
28. Kamata H, Manabe T, Kakuta J, Oka S, Hirata H (2002) Multiple redox regulation of the cellular signaling system linked to AP-1 and NFkappaB: effects of N-acetylcysteine and H2O2 on the receptor tyrosine kinases, the MAP kinase cascade, and IkappaB kinases. Ann N Y Acad Sci 973:419-422.
29. Wuyts WA, Vanaudenaerde BM, Dupont LJ, Demedts MG, Verleden GM (2003) N-acetylcysteine reduces chemokine release via inhibition of p38 MAPK in human airway smooth muscle cells. Eur Respir J 22:43-49.
30. Hashimoto S, Gon Y, Matsumoto K, Takeshita I, Horie T (2001) N-acetylcysteine attenuates TNF-alpha-induced p38 MAP kinase activation and p38 MAP kinase-mediated IL-8 production by human pulmonary vascular endothelial cells. Br J Pharmacol 132:270-276.
31. Dong C, Davis RJ, Flavell RA (2002) MAP kinases in the immune response. Annu Rev Immunol 20:55-72.
32. Ashwell JD (2006) The many paths to p38 mitogen-activated protein kinase activation in the immune system. Nat Rev Immunol 6:532-540.
33. Verhasselt V, Vanden Berghe W, Vanderheyde N, Willems F, Haegeman G, Goldman M (1999) N-acetyl-L-cysteine inhibits primary human T cell responses at the dendritic cell level: association with NF-kappaB inhibition. J Immunol 162:2569-2574.

34. Bruchhausen S, Zahn S, Valk E, Knop J, Becker D (2003) Thiol antioxidants block the activation of antigen-presenting cells by contact sensitizers. J Invest Dermatol 121:1039-1044.

Suppl. Table 1

gene	forward primer	reverse primer
Actin	AGGAGTACGATGAGTCCGGC	GGTGTAAAACGCAGCTCAGTA
Alox5	TGTACACACCAGTTCCTGGC	GTTTGGTTGAGCTGGATGGC
Ccl2	CTGGAGCATCCACGTGTTGG	CCCATTCCTTCTTGGGGTCAG
Hmox1	TGACACCTGAGGTCAAGCAC	AAGTGACGCCATCTGTGAGG
Il10	GCATTTGAATTCCCTGGGTGAG	CATGGCCTTGTAGACACCTTGG
Il1b	AGCTGAAAGCTCTCCACCTC	GCTTGGGATCCACACTCTCC
Nrf2	TAGTTCTCCGCTGCTCGGAC	TGTCTTGCCTCCAAAGGATGTC
Ptgs2	AGCAGATGACTGCCCAACTC	GGAAGCTCCTTATTTCCCTTCAC
Tnf	AAGTTCCCAAATGGCCTCCC	TTGCTACGACGTGGGCTAC

Suppl. Table 2

1st challenge

	score	MPO	CD3
naive	0	-	-
naive	0	-	-
naive	0	-	-
naive	0	-	-
4 h	0	-	-
4 h	0	-	-
4 h	0	+	+
4 h	0	+	+
12 h	0	+	+
12 h	0	++	+
12 h	0	++	+
12 h	0	+++	+
24 h	1	+	+
24 h	2	++++	+
24 h	2	++++	++
24 h	3	++++	+

5th challenge

	score	MPO	CD3
0 h	0	+++	+
0 h	1	+	++
0 h	2	++	+
0 h	2	+	++
4 h	2	++	+
4 h	2	+	+
4 h	0	+++	++
4 h	2	+++	+++
12 h	2	+++	+++
12 h	2	++	++
12 h	2	++	+++
24 h	2	+++	+++
24 h	2	+++	+++
24 h	1	++	+++
24 h	2	++	++

Results of the histological scoring: Epidermal inflammation score was based on the presence and number of epidermal abscesses and crusts per section (0 = no damage, 1 = presence of abscesses, 2 = between 1 and 5 crusts, 3 = between 6 and 10 crusts, 4 = more than 11 crusts). IHC was analysed by a semiquantative analysis of dermal inflammation ("-" = no inflammatory infiltrate, "+" = minimal inflammatory cells, "++" = mild inflammation, "+++" = moderate inflammation, "++++" = severe presence of inflammatory cells). (n = 4; only 12 h after the 5th TNCB ear challenge: n = 3).

Suppl. Fig. 1

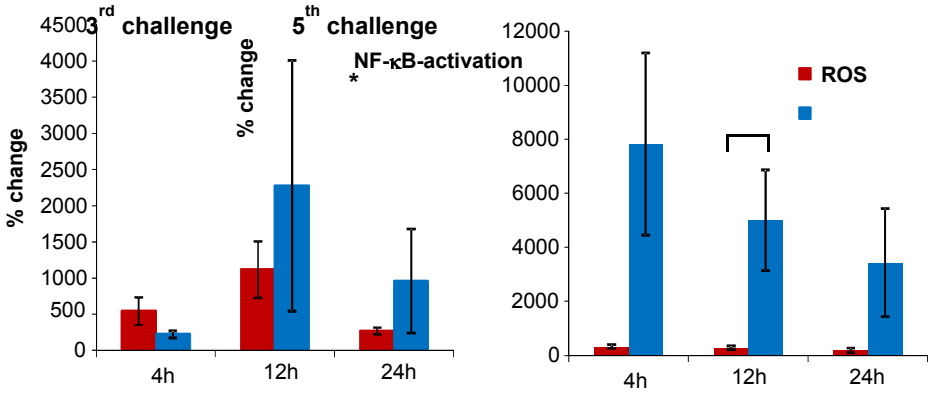

When calculating the relative change in signal intensity within the course of the 3rd or 5th TNCB ear challenge, using 0 h of the 3rd or 5th challenge as baseline, the relative increase in NF-κB activity 12 h and 48 h after the 3rd TNCB ear challenge and especially 4 h, 12 h and 24 h after the 5th TNCB ear challenge was impressively higher whereas the relative increase in ROS/RNS production was moderate. 12 h after the 5th TNCB challenge the relative change in NF-κB activation was significantly higher compared to the relative change in ROS/RNS production (unpaired, two-tailed Student's *t*-test). Data are presented as the mean ± SEM.

Suppl. Fig. 2

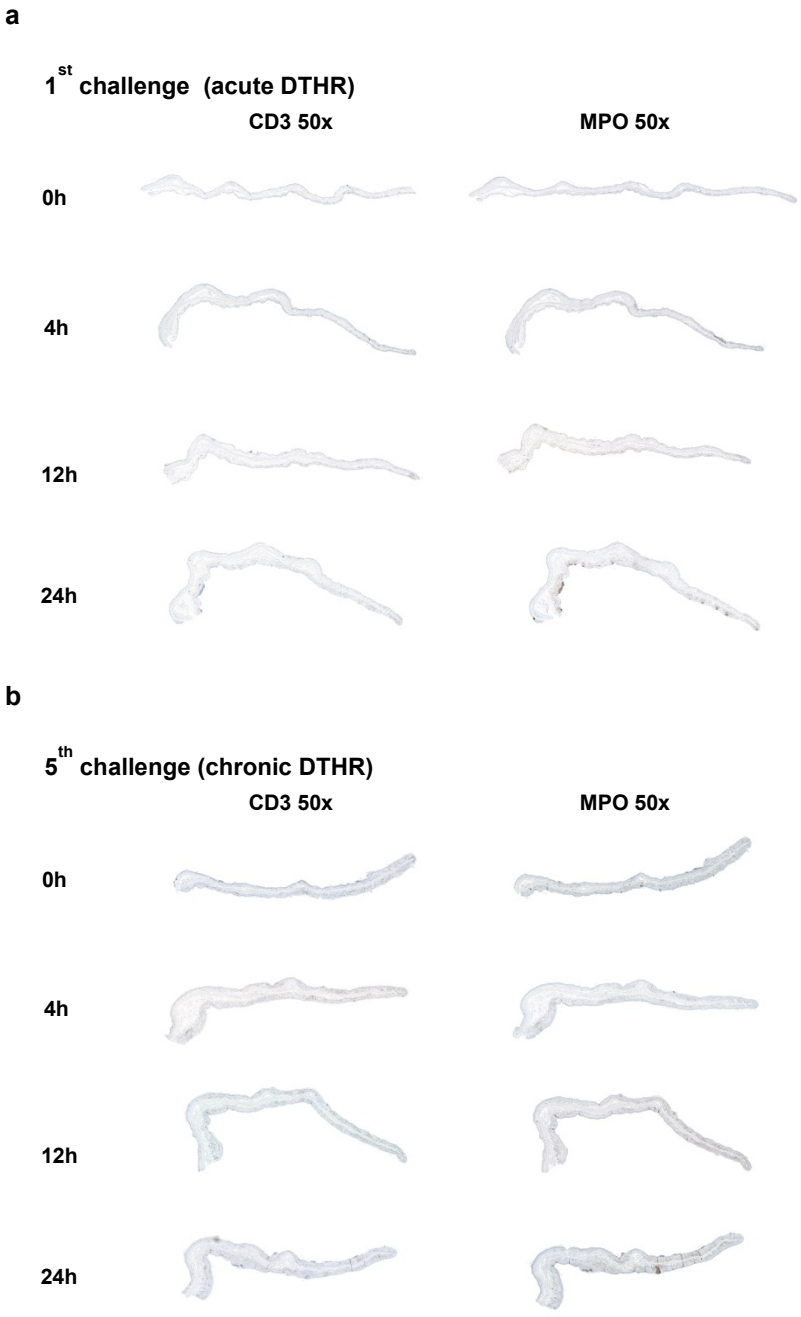

Corresponding images with 50x magnification of the CD3 and MPO IHC from **(a)** naïve mice (0 h), inflamed ears with **(a)** acute cutaneous DTHR 4 h, 12h and 24 h after the 1st TNCB ear challenge and **(b)** chronic cutaneous DTHR

before (48 h after the 4th TNCB ear challenge) 4 h, 12h and 24 h after the 5th TNCB ear challenge (n = 4; only 12 h after the 1st TNCB ear challenge: n = 3).

Suppl. Fig. 3

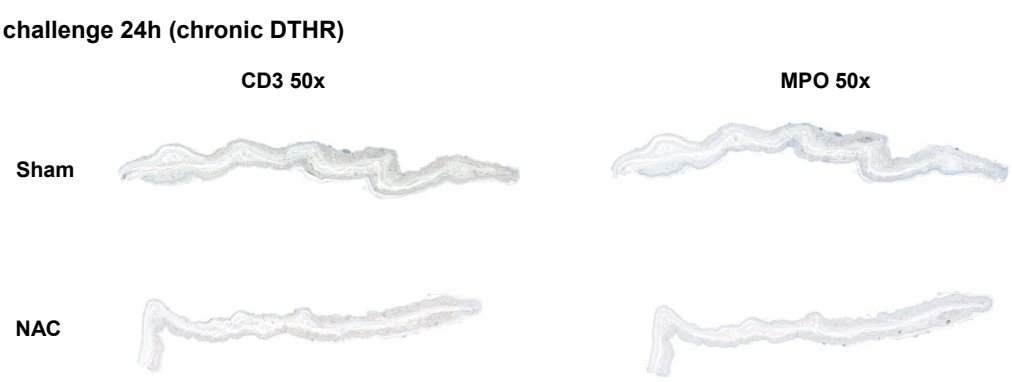

Corresponding images with 50x magnification of the CD3 and MPO IHC of NAC- and sham treated mice 24 h after the last TNCB ear challenge. CD3 and MPO IHC did not reveal significant differences between the two experimental groups.

2.2 Cysteine-type Cathepsins Promote the Effector Phase of Acute Cutaneous Delayed-Type Hypersensitivity Reactions (169)

The article included in this chapter was published in

Theranostics 2019 May 31;9(13):3903-3917.

”Cysteine-type cathepsins promote the effector phase of acute cutaneous delayed-type hypersensitivity reactions”

Johannes Schwenck, Andreas Maurer, Birgit Fehrenbacher, Roman Mehling, Philipp Knopf, Natalie Mucha, Dennis Haupt, Kerstin Fuchs, Christoph M. Gries-singer, Daniel Bukala, Julia Holstein, Martin Schaller, Irene Gonzalez Menendez, Kamran Ghoreschi, Leticia Quintanilla-Martinez, Michael Gütschow, Stefan Laufer, Thomas Reinheckel, Martin Röcken, Hubert Kalbacher, Bernd J Pichler, Manfred Kneilling.

IVYSPRING INTERNATIONAL PUBLISHER

Theranostics

2019; 9(13): 3903-3917. doi: 10.7150/thno.31037

Research Paper

Cysteine-type cathepsins promote the effector phase of acute cutaneous delayed-type hypersensitivity reactions

Johannes Schwenck[1,2], Andreas Maurer[1,3], Birgit Fehrenbacher[4], Roman Mehling[1], Philipp Knopf[1], Natalie Mucha[1], Dennis Haupt[1], Kerstin Fuchs[1], Christoph M. Griessinger[1], Daniel Bukala[1], Julia Holstein[4], Martin Schaller[4], Irene Gonzalez Menendez[5], Kamran Ghoreschi[4,5], Leticia Quintanilla-Martinez[6], Michael Gütschow[7], Stefan Laufer[8], Thomas Reinheckel[9,10], Martin Röcken[4], Hubert Kalbacher[3], Bernd J Pichler[1,11], Manfred Kneilling[1,4]✉

1. Werner Siemens Imaging Center, Department of Preclinical Imaging and Radiopharmacy Eberhard Karls University, 72076 Tübingen, Germany
2. Department of Nuclear Medicine and Clinical Molecular Imaging, Eberhard Karls University, 72076 Tübingen, Germany
3. Interfaculty Institute of Biochemistry, Eberhard Karls University, 72076 Tübingen, Germany
4. Department of Dermatology, Eberhard Karls University, 72076 Tübingen, Germany
5. Department of Dermatology, Venereology and Allergology, Charité – Universitätsmedizin Berlin, 10117 Berlin, Germany
6. Department of Pathology, Eberhard Karls University, 72076 Tübingen, Germany
7. Pharmaceutical Institute, Pharmaceutical Chemistry I, University of Bonn, 53121 Bonn, Germany
8. Department of Pharmaceutical and Medicinal Chemistry, Institute of Pharmacy, Eberhard Karls University, 72076 Tübingen, Germany
9. Institute of Molecular Medicine and Cell Research, Medical Faculty, Albert-Ludwigs University, 79085 Freiburg, Germany
10. German Cancer Consortium (DKTK), partner site Freiburg and German Cancer Research Center (DKFZ), Heidelberg, Germany
11. German Cancer Consortium (DKTK), partner site Tübingen and German Cancer Research Center (DKFZ), Heidelberg, Germany

✉ Corresponding author: email: manfred.kneilling@med.uni-tuebingen.de; telephone: +49-7071-29-83427; fax: +49-7071-29-4451

Received: 2018.10.28; Accepted: 2019.03.28; Published: 2019.05.31

Abstract

Cysteine-type cathepsins such as cathepsin B are involved in various steps of inflammatory processes such as antigen processing and angiogenesis. Here, we uncovered the role of cysteine-type cathepsins in the effector phase of T cell-driven cutaneous delayed-type hypersensitivity reactions (DTHR) and the implication of this role on therapeutic cathepsin B-specific inhibition.

Methods: Wild-type, cathepsin B-deficient (Ctsb$^{-/-}$) and cathepsin Z-deficient (Ctsz$^{-/-}$) mice were sensitized with 2,4,6-trinitrochlorobenzene (TNCB) on the abdomen and challenged with TNCB on the right ear to induce acute and chronic cutaneous DTHR. The severity of cutaneous DTHR was assessed by evaluating ear swelling responses and histopathology. We performed fluorescence microscopy on tissue from inflamed ears and lymph nodes of wild-type mice, as well as on biopsies from psoriasis patients, focusing on cathepsin B expression by T cells, B cells, macrophages, dendritic cells and NK cells. Cathepsin activity was determined noninvasively by optical imaging employing protease-activated substrate-like probes. Cathepsin expression and activity were validated *ex vivo* by covalent active site labeling of proteases and Western blotting.

Results: Noninvasive *in vivo* optical imaging revealed strong cysteine-type cathepsin activity in inflamed ears and draining lymph nodes in acute and chronic cutaneous DTHR. In inflamed ears and draining lymph nodes, cathepsin B was expressed by neutrophils, dendritic cells, macrophages, B, T and natural killer (NK) cells. Similar expression patterns were found in psoriatic plaques of patients. The biochemical methods confirmed active cathepsin B in tissues of mice with cutaneous DTHR. Topically applied cathepsin B inhibitors significantly reduced ear swelling in acute but not chronic DTHR. Compared with wild-type mice, Ctsb$^{-/-}$ mice exhibited an enhanced ear swelling response during acute DTHR despite a lack of cathepsin B expression. Cathepsin Z, a protease closely related to cathepsin B, revealed compensatory expression in inflamed ears of Ctsb$^{-/-}$ mice, while cathepsin B expression was reciprocally elevated in Ctsz$^{-/-}$ mice.

Conclusion: Cathepsin B is actively involved in the effector phase of acute cutaneous DTHR. Thus, topically applied cathepsin B inhibitors might effectively limit DTHR such as contact dermatitis or

psoriasis. However, the cathepsin B and Z knockout mouse experiments suggested a complementary role for these two cysteine-type proteases.

Key words: inflammation, proteases, cathepsin B, optical imaging, delayed-type hypersensitivity

Introduction

Proteases are known for their diverse extra- and intracellular functions under both physiological and pathological conditions. Cysteine-type cathepsins, a large family of proteases, were first found in lysosomes and have been considered strict intracellular enzymes that degrade ingested proteins [1]. However, in recent years, complex intra- and extracellular interactions of cathepsins have been discovered [2].

In this study, we focused on cathepsin B, a ubiquitously expressed cysteine exopeptidase [3]. Cathepsin B is expressed as a proenzyme, which is activated in early endosomes by autocatalytic cleavage [3, 4]. In the acidic pH of the endolysosomal cell compartment, cathepsin B is involved in the antigen processing crucial for adaptive immunity. Indeed, the contribution of cathepsin B to Toll-like receptor (TLR) signaling [5], apoptosis [6] and tumor necrosis factor (TNF) secretion [7] is critical for the innate immune response. Although cathepsin B is unstable at neutral pH, several experiments have shown that cathepsin B is involved in extracellular processes such as angiogenesis [8], extracellular matrix remodeling and cell migration [9]. Thus, a wide variety of diseases, such as rheumatoid arthritis [10], multiple sclerosis [11], pancreatitis [12], cancer [13] and Alzheimer´s disease [14], are associated with enhanced cathepsin B expression.

Noninvasive optical imaging using protease-activatable probes is a well-established tool to determine the activity of cathepsins *in vivo* [15, 16]. The protease-activatable probe features a peptide sequence preferentially cleaved by the corresponding protease. Cleavage at this site by proteases such as cathepsin B, Z, L or S abolishes the fluorescence resonance energy transfer (FRET)-mediated quenching of the fluorescence signal, enabling the measurement of cathepsin activity by *in vivo* optical imaging [15, 16].

Contact hypersensitivity reactions are cutaneous delayed-type hypersensitivity reactions (DTHR) mediated by interferon (IFN)-γ-producing $CD8^+$ (cytotoxic T (Tc)1) and $CD4^+$ (T helper (Th)1) cells. Our group extensively studied the role of mast cell TNF secretion [17], matrix metalloproteinase (MMP) activity [18], $\alpha_V\beta_3$ integrin expression and angiogenesis [19] in acute and chronic experimental 2,4,6-trinitrochlorobenzene (TNCB)-induced cutaneous DTHR. Because TNF secretion [7] and angiogenesis [8] are considered cathepsin B-dependent, this protease seems to be a further candidate target molecule for therapeutic approaches for cutaneous DTHR. To date, no *in vivo* data exist regarding the efficacy of specific topically applied cathepsin B inhibitors in inflammatory processes such as T cell-driven, TNCB-induced cutaneous DTHR. The irreversible cathepsin B inhibitor CA-074 was developed from the broad-spectrum cathepsin inhibitor E-64 [20] and highly selectively inhibits intracellular cathepsin B *in vitro* [21]. To attain enhanced selectivity, CA-074 interacts with amino acids in the characteristic structural feature of cathepsin B, the occluding loop, as does the recently designed inhibitor 17 [22].

In this study, we focused on the *in vivo* sites of cathepsin activity and the identification of cathepsin B-expressing inflammatory cells at the inflammation sites and draining lymph nodes. To our knowledge, the topical application of cathepsin B inhibitors has not yet been tested. Here, we investigated the efficacy of the topical, highly specific cathepsin B inhibitors CA-074 and inhibitor 17 to suppress ear swelling responses in TNCB-induced experimental cutaneous DTHR.

Materials and Methods

Animals

In this study, we used 8- to 12-week-old female C57BL/6 mice (Charles River Laboratories, Sulzfeld, Germany). Cathepsin B-deficient ($Ctsb^{-/-}$) and cathepsin Z-deficient ($Ctsz^{-/-}$) mice were backcrossed to the C57BL/6 genetic background for 10 generations [23, 24]. All animal experiments and methods were approved by the Regierungspräsidium Tübingen and were performed in accordance with relevant guidelines and regulations.

In vivo experiments

We sensitized mice on the shaved abdomen (size, approximately 2 cm × 2 cm) by applying 80 µL of 5% TNCB dissolved in a 4:1 mixture of acetone/Miglyol 812 (SASOL, Witten, Germany). To elicit acute cutaneous DTHR, the animals were challenged with 20 µL of 1% TNCB (dissolved in a 1:9 mixture of acetone/Miglyol 812) on both sides of the right ear seven days later. The TNCB ear challenge was repeated every 2-3 days on the right ear, up to five times, to induce chronic cutaneous DTHR. As a

control, naïve (nonsensitized) mice were challenged with 1% TNCB on the right ear (irritant-toxic reaction). We measured the ear thickness with a micrometer (Kroeplin, Schlüchtern, Germany) and quantified ear swelling by subtracting the ear thickness before ear challenge from the ear thickness 12 h to 24 h after ear challenge.

Treatment approach

The cathepsin B inhibitor CA-074 (PeptaNova, Sandhausen, Germany) and a newly developed cathepsin B inhibitor, called inhibitor 17 [25], were dissolved in a 1:9 mixture of acetone/Miglyol 812 (SASOL), and 20 µL of the 0.1 mM CA-074 or 0.1 mM inhibitor 17 solution was applied topically to the right ear every 24 h starting three days prior to the first TNCB ear challenge. As the sham-treatment, we used a 9:1 mixture of acetone/Miglyol 812 (SASOL).

Histology

We sacrificed mice 24 h after TNCB ear challenge and fixed the ear tissue in 4% buffered formalin. We embedded the tissue in paraffin, cut 5-µm sections using a microtome (Leica, Wetzlar, Germany) and performed hematoxylin and eosin (H&E)-staining according to standard procedures [26].

Optical imaging

In vivo cathepsin activity was measured by optical imaging using a ProSense activatable fluorescent probe, the corresponding noncleavable control probe and CatB680 (PerkinElmer, Waltham, USA). We injected the probes intravenously 12 h after TNCB ear challenge and performed *in vivo* optical imaging measurements 24 h later according to the recommendation of the manufacturer. For optical imaging, a Hamamatsu Aequoria Dark Box and a C4880 Hamamatsu dual mode cooled CCD camera (Hamamatsu Photonics Deutschland GmbH, Herrsching, Germany) were used. During the measurement, mice were anesthetized by the inhalation of isoflurane-O_2 (1.5%; Forane, Abbott GmbH, Wiesbaden, Germany) and heated to maintain the body temperature between 36 °C and 37 °C.

For the appropriate determination of signal intensity (SI) by optical imaging, we carefully fixed the ears planar on a flat black plate using a nylon thread [18]. Regions of interest (ROI) were drawn on the images of the TNCB-challenged right ear and the untreated left ear (internal control) and analyzed semiquantitatively using Wasabi imaging software (Hamamatsu).

Fluorescence microscopy

Mouse ears and (cervical) draining lymph nodes were collected 24 h after the first TNCB ear challenge, placed in RPMI (Biochrom, Berlin, Germany) and immediately frozen in liquid nitrogen. Skin biopsies were taken from patients with plaque psoriasis. The biomaterial collection study was approved by the ethics committee of Eberhard Karls University (protocol 545/2014BO2), and patients provided written informed consent. Frozen sections were fixed with periodate-lysine-paraformaldehyde (0.1 M L-lysine-HCl; 2% paraformaldehyde; and 0.01 M sodium metaperiodate, pH 7.4). Sections were blocked using donkey serum and were then incubated with the following primary antibodies (Ab): rabbit anti-cathepsin B (1:20, antibodies-online GmbH, Aachen, Germany), goat anti-CD20 (1:50, Santa Cruz Biotechnology, Dallas, USA), mouse anti-CD20 (1:100, Agilent, Santa Clara, USA), goat anti-CD3-ε (1:50, Santa Cruz Biotechnology), hamster anti-49b-Alexa Fluor 647 (Biolegend, San Diego, USA), rabbit anti-CD56 (1:100, Cell Marque, Rocklin, USA), rat anti-F4/80 (1:100, Abcam, Cambridge, UK), mouse anti-CD163 (1:100, DCS, Hamburg, Germany), Armenian hamster anti-CD11c-Alexa Fluor 647 (BioLegend) and rabbit anti-Factor XIIIa (1:100, DCS, Hamburg, Germany). Bound antibodies were visualized using Dylight 549- and Dylight 649-conjugated donkey anti-rabbit IgG (Dianova, Hamburg, Germany), Cy3-conjugated donkey anti-rabbit IgG (Dianova), Cy5-conjugated donkey anti-goat IgG (Dianova), Cy5-conjugated donkey anti-mouse IgG, (Dianova), Dylight 549-conjugated donkey anti-rat IgG (Dianova), Cy3-conjugated donkey anti-goat IgG (Dianova) and Alexa 647-conjugated donkey anti-rabbit IgG (Dianova) antibodies. For nuclear staining, we used Yopro (1:2000, Invitrogen, Carlsbad, USA) and mounted the slides using Mowiol (Hoechst, Frankfurt, Germany). Sections were analyzed using an LSM 800 (Zeiss, Oberkochen, Germany) or a Leica TCS-SP/Leica DM RB confocal laser scanning microscope (Leica Microsystems, Wetzlar, Germany) and an HCX PL APO 63×/1.132-0.6 oil CS objective lens. Images were processed with Leica Confocal Software (LCS, version 2.61). The original magnification was ×63. Cells double positive for cathepsin B and the specific cell surface antigen were counted in representative areas, and the means are displayed as a percentage of the mean of all cells expressing the specific cell surface antigen.

Active site labeling

Mouse ears and draining lymph nodes were collected 24 h after the first TNCB ear challenge and homogenized in lysis buffer (100 mM citrate/phosphate; 2 mM EDTA; 1% NP40, pH 5) using an Ultra-Turrax disperser (IKA-Werke, Staufen,

Germany). Lysates were cleared by centrifugation (20800 g, 10 min) and stored at -80 °C. Active site labeling of cysteine proteases was performed as previously described [27]. Briefly, 10 µg of cellular protein was preincubated for 15 minutes with 12.5 µM E-64d or solvent control (dimethylsulfoxide; DMSO) in the presence of 50 mM dithiothreitol, followed by the addition of 12.5 µM DCG-04 and incubation at room temperature for 30 minutes. Samples were then subjected to reducing SDS-PAGE on minigels containing 15% polyacrylamide, followed by Western blotting. The biotinylated probe was detected on PVDF membranes using either streptavidin-conjugated peroxidase, Amersham ECL Prime substrate and Amersham Hyperfilm ECL photosensitive film (Amersham, GE Healthcare) or IRDye 680LT streptavidin and an Odyssey Sa imaging system (LI-COR Biotechnology, Bad Homburg, Germany; samples from $Ctsb^{-/-}$/$Ctsz^{-/-}$/wild-type mice are shown in Figure 4B). To validate the specificity of the cathepsin B bands, which were identified at 27-30 kDa by active site labeling, we used an anti-cathepsin B antibody (goat anti-cathepsin B, 1:2222; R&D Systems, Minneapolis, USA) and an anti-cathepsin Z antibody (goat anti-cathepsin Z, 1:2222; R&D Systems, Minneapolis, USA) visualized by a donkey anti-goat IgG antibody (LI-COR, Lincoln, USA), as shown in Figure S5. The original blots are shown in Figures S7-S13.

Flow cytometry

Spleens and lymph nodes were passed through a 70 µm cell strainer to achieve a single-cell suspension, which was then washed in phosphate-buffered saline (PBS) supplemented with 1% fetal bovine serum. Spleens were subjected to an additional erythrocyte lysis step with ACK lysing buffer (BioWhittaker, Basel, Switzerland). Cells were counted with a C-Chip disposable counting chamber (NanoEnTek, Seoul, Korea), and $4.5x10^6$ cells per sample were used for staining. For the T cell panel, flow cytometry staining was performed using monoclonal antibodies (mAbs) against the following proteins and conjugated to the indicated fluorophores: V450-CD3, V500-CD45.2, FITC-CD8, PE-CD4, APC-Cy7-CD62L, Fc-Block (all from BD Biosciences, Franklin Lakes, USA), PE-Cy7-CD69 (eBioscience, Santa Clara, USA), and APC-NK1.1 (Miltenyi Biotec, Bergisch Gladbach, Germany). For the myeloid cell panel, PE-F4/80 (BioLegend, San Diego, USA), V500-CD45.2, APC-CD11c, PE-Cy7-CD11b, Fc-Block (all from BD Biosciences), V450-Gr1, FITC-MHC-II, and APC-Cy7-CD19 (all from eBioscience) were used. Single-cell suspensions were input to a BD LSR Fortessa (BD Biosciences), and analysis was performed using FlowJo software (Ashland, USA).

For intracellular flow cytometry (Figure S1) ears and draining cervical lymph nodes were collected 24 h after the first TNCB ear challenge. The ears were cut into very small pieces and incubated in a digestion mix containing collagenase IV (Worthington, Lakewood, USA) and DNase I (Sigma, St. Louis, USA) in RPMI (Biochrom, Berlin, Germany). After tissue digestion, the ears and lymph nodes were passed through a 70 µm cell strainer to achieve a single-cell suspension, which was then washed with FACS buffer (phosphate-buffered saline supplemented with 2 % fetal bovine serum and 5 mM EDTA). Non-specific bindings were blocked using Fc-Block (BioLegend, San Diego, USA) and donkey serum (Millipore, Burlington, USA). Surface and viability staining was performed using following antibodies and dyes: Pacific Blue™-CD3, PE-CD19, PE-Cy7-NK1.1 (all from BioLegend, San Diego, USA), Fixable Viability Dye eFluor™ 520 (eBioscience, Santa Clara, USA). For intracellular staining, cells were fixed with 2 % Formaldehyde and cell membrane was permeabilized by incubation with 90 % Methanol followed by washing with FACS buffer containing 0.5 % Saponin. Cells were then incubated with goat-anti-cathepsin B antibody 1:1000 (R&D Systems, Minneapolis, USA) and donkey anti-goat-Alexa Fluor 647 1:800 (Dianova, Hamburg, Germany) was used as secondary antibody. For negative control, cells were incubated only with the secondary antibody. The expression of cell surface antigens and cathepsin B was analyzed by LSRII flow cytometer (BD Biosciences, Heidelberg, Germany) and FlowJo software (Ashland, USA).

Statistical analysis

An unpaired, two-tailed Student's t-test was used to compare the optical imaging signal intensities (Figure 1B right/left ear; Figure S2B/D, CA-074/sham-treatment; Figure S5A, $Ctsb^{-/-}$/wild-type mice).

To analyze the differences in the optical imaging signal intensities between the inflamed right ears of mice with irritative-toxic reactions and cutaneous DTHR after 1, 3 and 5 challenges, we used one-way analysis of variance (ANOVA; Figure 1D). Differences in the ear swelling responses were compared by an unpaired, two-tailed Student's t-test (Figure 4A). According to Bonferroni correction for multiple comparisons, the significance level was adjusted to $p< 0.0125$.

Differences in the ear swelling responses between the sham- and CA-074-treated groups with chronic cuteaneous DTHR were compared by Dunnett's test (Figure S2A). We analyzed the ear swelling responses between $Ctsb^{-/-}$ and wild-type

mice with acute cutaneous DTHR using an unpaired, two-tailed Student's t-test with Bonferroni correction of the significance level ($p < 0.025$) due to multiple comparisons (Figure 5A; Figure S3A). Ctsz$^{-/-}$ mice were compared only qualitatively due to the small sample size (Figure 5A).

Quantitative data are reported as the means ± standard errors of the mean (SEMs).

Results

In vivo protease activity in acute and chronic TNCB-induced cutaneous DTHR

To measure protease activity in chronic cutaneous DTHR induced in mice by five TNCB challenges, we employed noninvasive imaging of ears using a substrate-like protease-activated probe (ProSense). This probe can be cleaved by several proteases and subsequently detected by fluorescence-based optical imaging [28]. ProSense or the noncleavable control probe was injected 12 h after the fifth challenge, and optical imaging was performed 24 h later. We found a 4-fold increase in protease activity in the inflamed right ear compared with that in the untreated left ear. In contrast, the noncleavable control probe produced only a very faint background signal, indicating that only the cleavable probe emits a signal of reasonable intensity (Figure 1A/B).

Considering that proteases are significantly activated during chronic cutaneous DTHR, we focused on the specific participation of cathepsins using an optical imaging probe preferentially cleaved by cathepsin B (CatB680) but cleavable to a lesser extent, by other cathepsins, such as cathepsin S [29]. The ear tissue of an untreated naïve control mouse yielded a faint fluorescence signal corresponding to low cathepsin activity in healthy tissue (Figure 1C/D). In the ear with acute cutaneous DTHR elicited by one TNCB challenge one week after sensitization, the

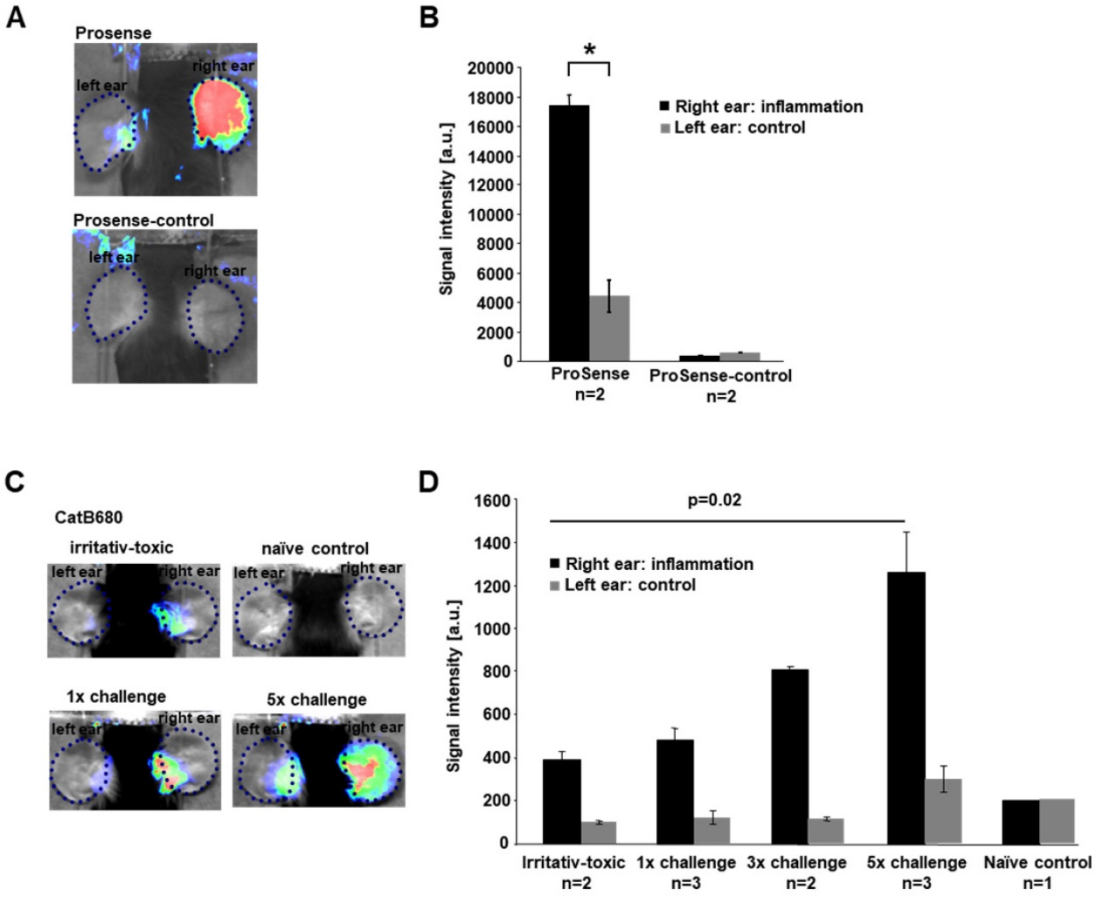

Figure 1: *In vivo* imaging of proteases in cutaneous DTHR. Mice were sensitized with 5% TNCB on the abdomen and, after one week, were challenged with 1% TNCB on the right ear to induce acute cutaneous DTHR. As a control, nonsensitized mice were challenged with 1% TNCB on the right ear (irritative-toxic reaction). To induce chronic cutaneous DTHR, mice were repetitively challenged every two days, up to five times. **A:** ProSense, a probe activatable by several proteases, and ProSense-control, a nonactivatable probe, were injected 12 h after the fifth challenge, and *in vivo* optical imaging was performed 24 h later. **B:** The ProSense signal intensity was 4-fold higher in the inflamed right ears than in the control left ears. The nonactivatable control probe displayed almost no signal (n=2; unpaired, two-tailed Student's t-test; mean±SEM). **C/D:** The signal intensity of CatB680, a probe preferentially activated by cathepsin B, was measured after the first, third and fifth TNCB challenges. After the first challenge, the signal intensity was 4-fold higher than that in untreated control ears. After the third and fifth challenges, the signal intensity increased to 400% and 620% of the control signal intensity (one-way ANOVA; mean±SEM). Unsensitized mice, which developed an irritative-toxic reaction after a single challenge, showed a slightly lower signal than sensitized mice. Untreated naïve mice showed signal intensities similar to those in the untreated left ears.

CatB680 signal was 4-fold higher than that in the healthy ear. However, this signal was only slightly higher than that in the ears of nonsensitized naïve mice after a single TNCB challenge (nonspecific irritative-toxic control; Figure 1C/D). Ongoing accelerated chronic cutaneous DTHR was associated with an almost linear increase in the CatB680 signal intensity. After five TNCB ear challenges, the signal intensity in chronically inflamed right ears was 2.6-fold higher than that in ears with acute cutaneous DTHR. Importantly, in this context, the signal intensity in the control ears of mice challenged with TNCB five times on the contralateral ears was slightly increased as a consequence of some degree of TNCB spread caused by the cleaning behavior of the experimental mice (Figure 1C/D).

Cellular sources of cathepsin B in acute cutaneous DTHR

To determine the cellular sources of cathepsin B in acute cutaneous DTHR, we conducted immunofluorescence microscopy analyses of ears and draining lymph nodes obtained 24 h after a single TNCB ear challenge. Based on cell surface marker expression, we focused on cathepsin B expression in dendritic cells (DCs; CD11c), B cells (CD20), T cells (CD3), macrophages (F4/80), and NK cells (CD49b). For quantification, we assessed the percentage of cathepsin B-positive CD11c-, CD20-, CD3-, F4/80- and CD49b-expressing cells (Figure 2A). In the healthy ears of naïve mice, which exhibited neither histopathological signs of inflammation nor a leukocytic infiltrate, we could identify almost no cathepsin B-expressing resident cells. However, in ears with acute TNCB-induced cutaneous DTHR, we found strong edema, as well as extensive infiltration of inflammatory cells, as reported by Schwenck et al. [18]. In the present study, cathepsin B expression was detected in 36% of CD11c-positive cells (mainly dendritic cells), 27% of CD20-positive B cells, 26% of CD3-positive T cells, 25% of F4/80-positive macrophages and 15% of CD49b-positive NK cells in ear tissue with acute TNCB-induced cutaneous DTHR (Figure 2A/B). Interestingly, acute cutaneous DTHR was associated with an impressively higher percentage of cathepsin B-positive inflammatory cells in draining lymph nodes than in inflamed ear tissue (Figure 2C). Specifically, in lymph nodes, we detected cathepsin B expression in 73% of dendritic cells, 64% of B cells, 63% of T cells, 80% of macrophages and 64% of NK cells (Figure 2C). Even in lymph nodes of naïve healthy mice, 11% of dendritic cells, 27% of B cells, 38% of T cells, 6% of macrophages and 53% of NK cells stained positive for cathepsin B (Figure 2D). Importantly, in this context, cathepsin B was found within the cell cytoplasm as well as in the extracellular space. Intracellular cathepsin B flow cytometry analysis revealed a strong cathepsin B expression in the leucocytes with high granularity (most probably neutrophils) isolated from the inflamed ears with acute cutaneous DTHR (Figure S1).

To determine whether our results are applicable to human disease, we analyzed skin tissue from a patient suffering from psoriasis. Like experimental cutaneous DTHR in mice, psoriatic lesions were dominated by neutrophils (Figure 3A). Immunofluorescence microscopy revealed notable cathepsin B expression in B cells, dendritic cells, T cells and NK cells, in accordance with our murine data (Figure 3B).

Specific cathepsin inhibition suppresses acute but not chronic cutaneous DTHR

To address the role of cathepsin B expression and the therapeutic potential of cathepsin B inhibition in acute and chronic cutaneous DTHR, we topically treated TNCB-sensitized mice with the cathepsin B inhibitor CA-074 twice daily. This compound irreversibly inactivates its target, cathepsin B, selectively at nanomolar concentrations but tends to inhibit multiple cysteine-type cathepsins at higher concentrations. We started topical CA-074 treatment four days after sensitization and three days prior to the first TNCB ear challenge to ensure no impairment of the sensitization phase and to achieve a sufficient degree of cathepsin B inhibition. Topically administered CA-074 significantly reduced the ear swelling responses 12 h and 24 h after the first TNCB challenge (Figure 4A) but displayed no significant therapeutic effect on chronic cutaneous DTHR (Figure S2A). In contrast, histological H&E staining of CA-074-treated ears with acute cutaneous DTHR revealed strong reductions in ear thickness, edema, hyperkeratosis, acanthosis and inflammatory cell infiltration of compared with these features in sham-treated ears (Figure 4B). Interestingly, noninvasive *in vivo* optical imaging of CA-074-treated mice using the CatB680 probe showed that the signal intensity in the inflamed ears was not significantly reduced compared to that in the ears of wild-type mice (Figure S2B), suggesting that other proteases may be involved in the activation of the CatB680 optical imaging probe (see discussion). *Ex vivo* optical imaging of draining lymph nodes revealed a tendency towards decreased CatB680 signal intensity, while the contralateral cervical, axillary, inguinal and mesenteric lymph nodes and the thymus, including the perithymic lymph nodes, remained unaffected (Figure S2C/D).

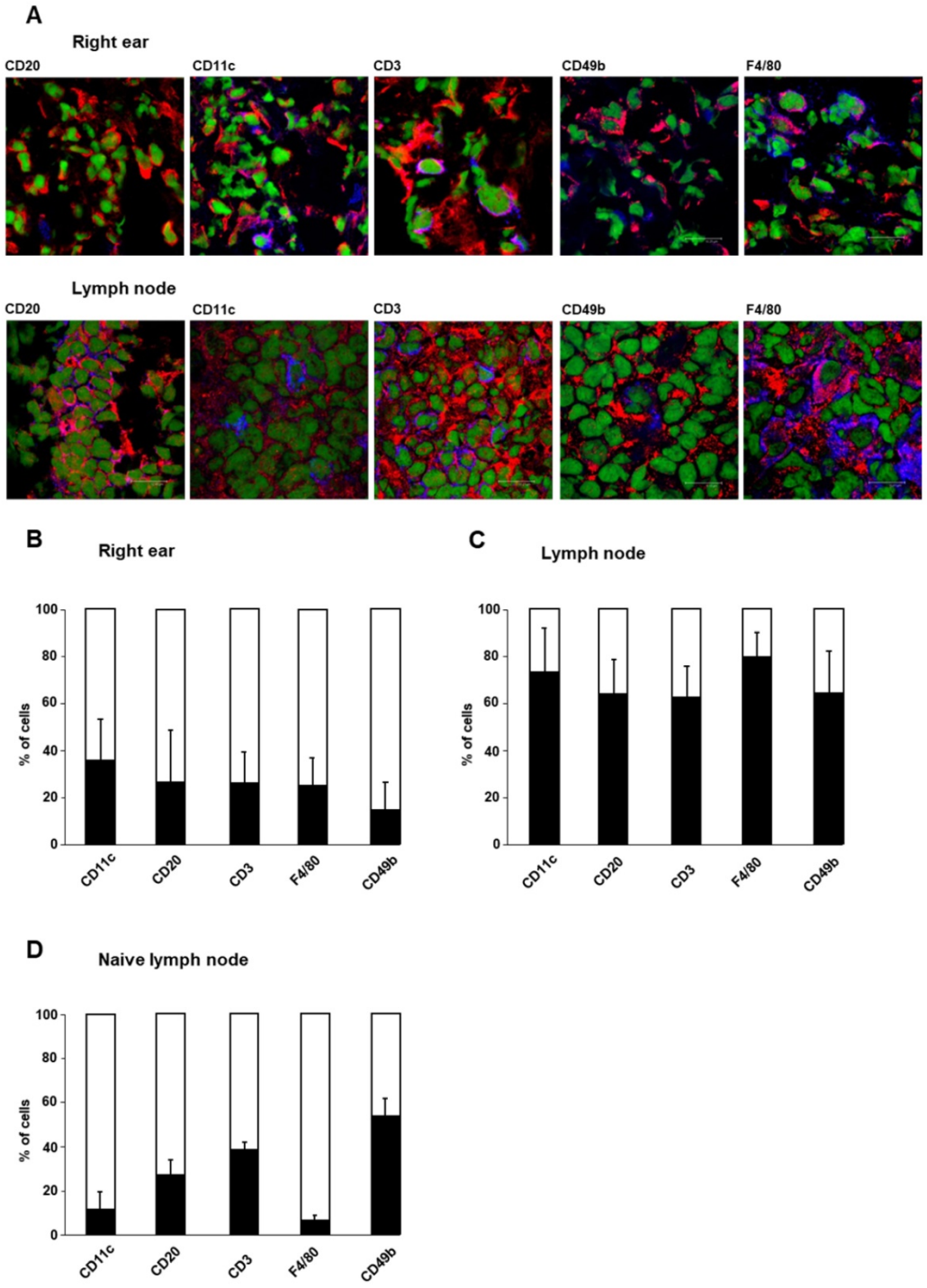

Figure 2: Cellular sources of cathepsin B. Cellular sources of cathepsin B were analyzed by immunofluorescence microscopy using staining with a cathepsin B-specific antibody. The cell types of cathepsin B-expressing cells were determined by antibodies against specific surface antigens. **A:** Immunofluorescence staining of cathepsin B (red) and specific cell surface antigens (blue) in tissue from the right ear and draining lymph nodes of sensitized mice 24 h after TNCB challenge allowed the identification of cathepsin B-expressing immune cells (green represents nuclei). Cells with both antibodies bound appear purple. **B:** Cells onto which both anti-cathepsin B- and anti-cell surface antigen antibodies bound (purple), were counted. The results are shown as the percentage of all cells expressing the specific cell surface antigen (blue+purple). At the site of inflammation (the right ear) in sensitized mice 24 h after TNCB challenge, CD11c-positive dendritic cells exhibited the highest percentage of cells expressing cathepsin B, while CD49b-positive NK cells expressed cathepsin B most rarely among the immune cell populations (n=4; mean±SEM). **C:** In draining lymph nodes of sensitized mice 24 h after TNCB challenge, the percentage of cells expressing cathepsin B was higher than that in inflamed ear tissue. Almost 80% of the F4/80-positive macrophages expressed cathepsin B, while only a few cells in the other populations produced cathepsin B (n=4; mean±SEM). **D:** In cervical lymph nodes of naïve mice, 53% of the CD49b-positive NK cells expressed cathepsin B, while the expression of cathepsin B in F4/80-positive macrophages and CD11c-positive dendritic cells was comparatively low (n=2 mean±SEM).

To exclude potential off-target effects of CA-074, we tested the anti-inflammatory potential of a second cathepsin B inhibitor. We selected the recently developed inhibitor 17, which strongly differs from CA-074 in its chemical characteristics and exhibited potent inhibitory effects on cathepsin B *in vitro* [22]. Inhibitor 17 reduced ear swelling in acute cutaneous DTHR most effectively at 24 h after the TCNB

challenge (Figure S3A). At this time point, H&E histology of the ears derived from sham- or inhibitor 17-treated mice confirmed reduced edema and leukocyte infiltration as a consequence of inhibitor 17 treatment (Figure S3B).

Active site labeling confirms the therapeutic inhibition of cathepsin B

We chose to use *ex vivo* active site labeling of cysteine-type cathepsins to demonstrate sufficient specific cathepsin B inhibition by CA-074 during acute cutaneous DTHR. Thus, we labeled protease active sites using the activity-based probe DCG-04 [30], which was developed from the broad-spectrum cathepsin inhibitor E-64d. First, we labeled lysates of inflamed ear tissue obtained from mice 24 h after a single TNCB challenge. Competitive labeling with E-64d, which does not produce a signal in this assay, revealed signal suppression by E-64d in several bands, thereby indicating the positions of active cathepsins on the gels (Figure 4C). Treatment of mice with the covalently binding cathepsin B inhibitor CA-074 abolished DCG-04 labeling of a single band, thereby identifying cathepsin B and proving selective inhibition of this protease *in vivo*. Hence, active cathepsin B was present at the site of the inflammatory process, i.e., the ear (Figure 4C). Interestingly, the level of active cathepsin B in draining lymph nodes revealed much stronger cathepsin B activity than that in inflamed ear tissue (Figure 4D). Again, CA-074 treatment effectively reduced active cathepsin B levels in draining lymph nodes during cutaneous DTHR, confirming the efficacy of selective, irreversible cathepsin B inhibition by CA-074 (Figure 4D). Nevertheless, active site labeling could not assess the inhibitory effect of inhibitor 17, most likely because of the reversible binding mode of inhibitor 17 to cathepsin B (Figure S3C/D). Most importantly, the expression of cathepsin Z in inflamed ears of CA-074 treated mice remained unaffected (Figure S4).

Role of cathepsin Z in Ctsb$^{-/-}$ mice

Despite the known proinflammatory role of cathepsin B, Ctsb$^{-/-}$ mice revealed an enhanced ear swelling response compared to that of wild-type mice during acute cutaneous DTHR, especially 24 h after challenge (Figure 5A). The absence of cathepsin B may be compensated by another protease. Since cathepsin Z (also known as cathepsin X) is the other carboxypeptidase in the cysteine-type cathepsin family, and because compensatory expression of those proteases has been reported previously [31], we analyzed cathepsin Z in more detail. In sharp contrast to Ctsb$^{-/-}$ mice, Ctsz$^{-/-}$ mice exhibited a trend towards reduced ear swelling responses 12 h and 24 h after TNCB ear challenge compared with those of wild-type mice (Figure 5A). H&E staining of ear tissue obtained from Ctsb$^{-/-}$ mice 24 h after TNCB ear challenge revealed more severe ear swelling, more pronounced edema and a higher density of infiltrating neutrophils than in wild-type mice. However, we could not identify any histopathological differences between Ctsz$^{-/-}$ and wild-type mice (Figure 5B).

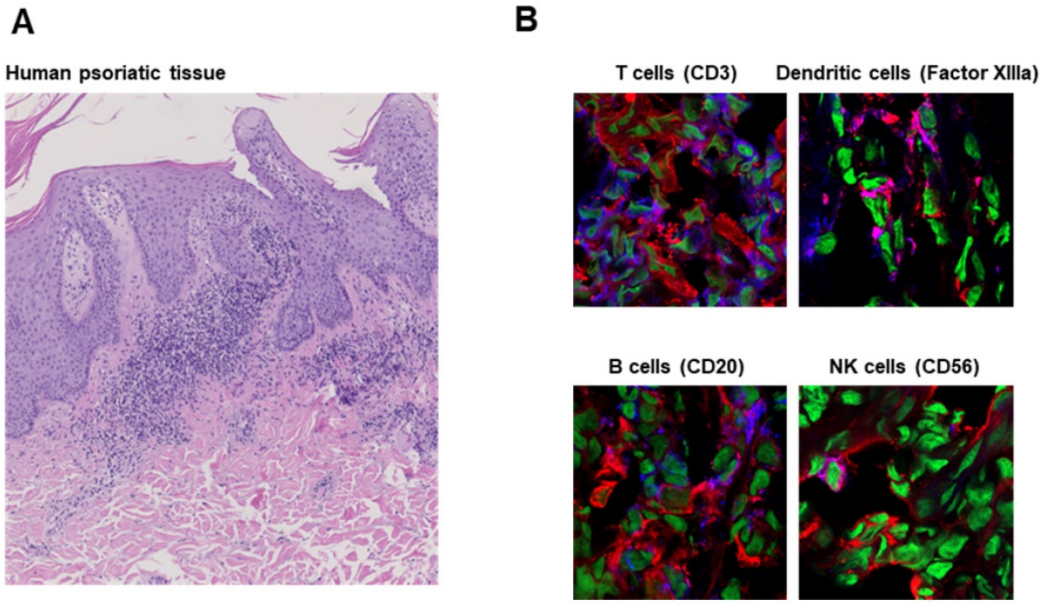

Figure 3: Cathepsin B expression in human inflammatory disease. A: H&E staining of human psoriatic skin tissue obtained from a clinically indicated punch biopsy shows parakeratosis and a dense neutrophil infiltrate. **B:** Immunofluorescence microscopy revealed cathepsin B expression by T cells (CD3), dendritic cells (Factor XIIIa), B cells (CD20) and NK cells (CD56) comparable to that in tissue from mice with experimental acute cutaneous DTHR (Figure 2). Cathepsin B (red); nuclei (green), CD3/Factor XIIIa/CD20/CD56 (blue); cathepsin B and CD3/Factor XIIIa/CD20/CD56 double-positive cells (pink).

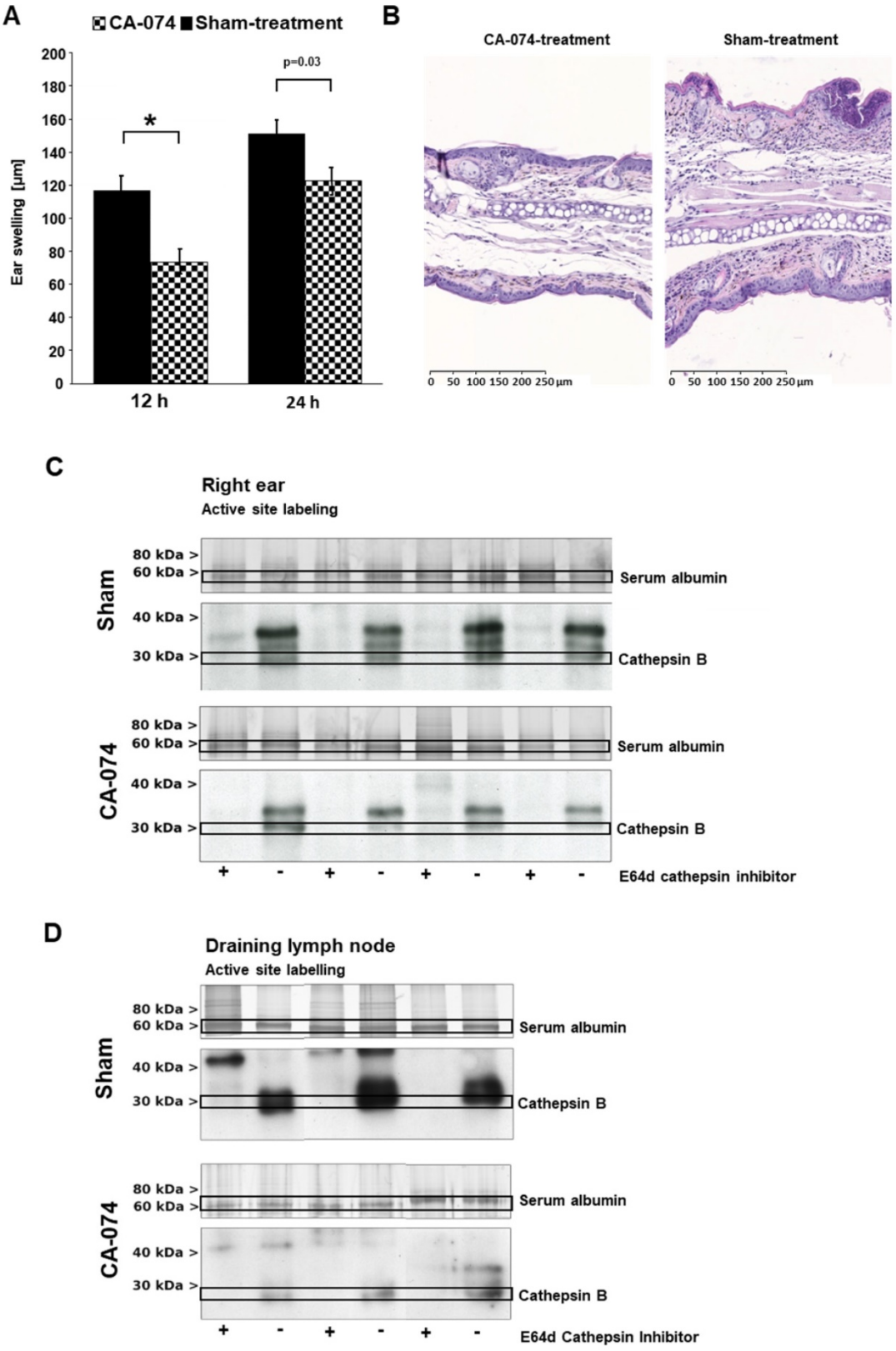

Figure 4: Therapeutic impact of the specific cathepsin B inhibitor CA-074. The specific cathepsin B inhibitor CA-074 or a sham-treatment was applied topically on the right ears daily, starting three days prior the first challenge. **A:** CA-074-treated mice showed a highly significant decrease in ear swelling responses 12 h after the first challenge. Twenty-four hours after the first challenge, the effect on the ear swelling response was lower but still significant (treatment group: n=14; control groups: 12 h, n=28; 24 h, n=25; unpaired, two-tailed Student's t-test; Bonferroni correction for multiple comparisons, significance level p< 0.0125; mean±SEM). **B:** Ear tissue was harvested 24 h after challenge and stained with H&E according to standard protocols. Tissue from CA-074-treated mice showed noticeably reduced ear thickness and reduced edema, hyperkeratosis, acanthosis and inflammatory cell infiltration (magnification 100x). **C:** To analyze active cathepsin B *in vitro* in tissue harvested from inflamed ears and draining lymph nodes of sensitized mice 24 h after TNCB challenge, we used an activity-based probe, which is an analog of broad-spectrum cysteine-type cathepsin inhibitor the E-64. Active site labeling of probes in inflamed ear tissue revealed active cathepsin B during acute cutaneous DTHR in sham-treated mice. Targeted CA-074 treatment reduced active cathepsin B levels very effectively. **D:** CA-074 strongly suppressed cathepsin B activation in draining lymph nodes.

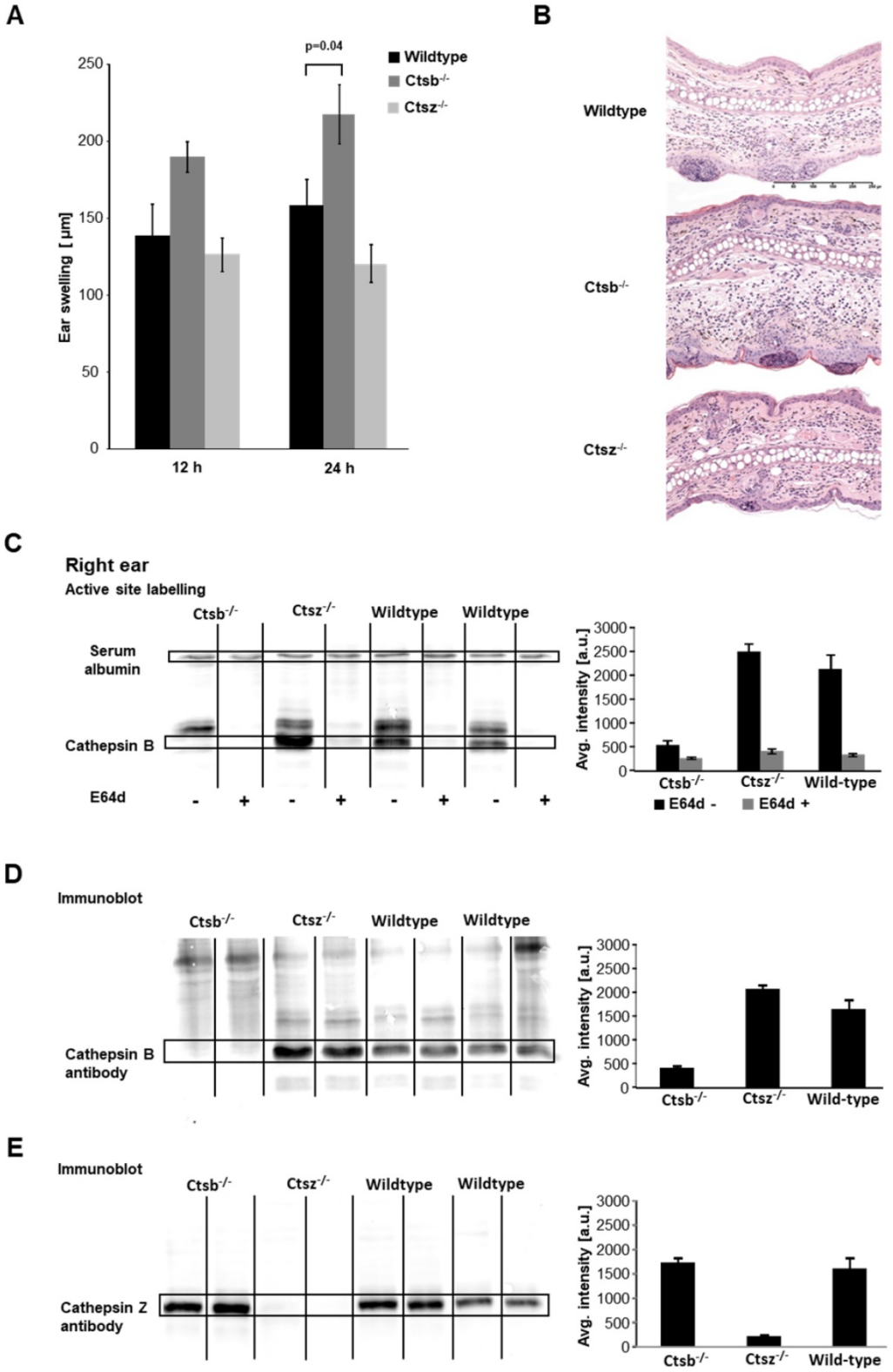

Figure 5: Effect of cathepsin B deficiency. Ctsb$^{-/-}$ mice, Ctsz$^{-/-}$ mice and wild-type mice were sensitized on the abdomen with 5% TNCB and challenged seven days later on the right ear. **A:** We observed significantly enhanced ear swelling in Ctsb$^{-/-}$ mice during acute cutaneous DTHR 24 h after challenge compared to that in wild-type mice, while Ctsz$^{-/-}$ mice showed a trend towards reduced ear swelling compared to that in wild-type mice (wild-type: n=8; Ctsb$^{-/-}$ mice: n=11; Ctsz$^{-/-}$ mice: n=3; two-tailed Student's t-test with Bonferroni correction $p < 0.025$; mean±SEM). **B:** H&E staining of inflamed ear tissue harvested 24 h after TNCB challenge revealed more severe ear swelling, more pronounced edema and a higher density of infiltrating neutrophils in Ctsb$^{-/-}$ mice than in wild-type mice. However, Ctsz$^{-/-}$ and wild-type mice exhibited no histopathological differences. **C:** Active site labeling revealed a diminished cathepsin B-sized band in the lanes corresponding to samples from Ctsb$^{-/-}$ mice. The cathepsin B bands in the lanes corresponding to samples from Ctsb$^{-/-}$ mice were more prominent than those in the lanes corresponding to samples from wild-type mice, suggesting upregulation of cathepsin B expression (Ctsb$^{-/-}$: n=4; Ctsz$^{-/-}$: n=3; wild-type: n=4). **D:** To confirm the identity of the bands detected by active site labeling, we performed immunoblotting on the same gel using a cathepsin B-specific antibody. Immunoblotting indicated a trend towards enhanced cathepsin B expression in Ctsz$^{-/-}$ mice and verified diminished cathepsin B expression in Ctsb$^{-/-}$ mice (Ctsb$^{-/-}$: n=4; Ctsz$^{-/-}$: n=3; wild-type: n=4). **E:** Immunoblotting using a cathepsin Z-specific antibody demonstrated a slight trend towards elevated cathepsin Z expression in some Ctsb$^{-/-}$ mice and virtually no cathepsin Z expression in Ctsz$^{-/-}$ mice (Ctsb$^{-/-}$: n=4; Ctsz$^{-/-}$: n=3; wild-type: n=4).

Optical imaging using the CatB680 probe during acute TNCB-induced cutaneous DTHR revealed a tendency towards increased signal intensity in the inflamed right ears of Ctsb$^{-/-}$ mice compared with that in wild-type mice (Figure S5A), suggesting compensatory effects of other proteases, especially since fluorescence microscopy analysis (Figure S5B) as well as Western blot analysis for cathepsin B expression showed cathepsin B deficiency in the inflamed ears of Ctsb$^{-/-}$ mice (Figure 5D).

One day after the first TNCB ear challenge, DCG-04 labeling of ear tissue from Ctsb$^{-/-}$ mice revealed markedly reduced cysteine-type cathepsin activity in the region where cathepsin B activity was expected, while cathepsin B was detectable in wild-type and Ctsz$^{-/-}$ mice (Figure 5C). Western blot analysis using cathepsin B- and cathepsin Z-specific antibodies clearly identified the cathepsin B- and cathepsin Z-expressing bands that were detected with active site labeling (Figure 5C/D). Interestingly, the cathepsin B immunoblots revealed a trend towards reinforced cathepsin B bands in the lanes corresponding to samples from the inflamed ears of Ctsz$^{-/-}$ mice compared to those of wild-type mice, whereas, consistent with our expectations, no cathepsin B-positive band was detectable in samples from Ctsb$^{-/-}$ mice (Figure 5D). A similar effect was observed on the cathepsin Z immunoblots: We determined a pronounced cathepsin Z band in the lanes corresponding to samples from the inflamed ears of Ctsb$^{-/-}$ mice compared to those of wild-type mice, while Ctsz$^{-/-}$ mice did not express cathepsin Z (Figure 5E). These results suggest a compensatory role for cathepsin Z in Ctsb$^{-/-}$ mice and may explain the proinflammatory effects in Ctsb$^{-/-}$ mice. Analysis of cathepsins in draining lymph nodes revealed a similar level of cathepsin Z expression in Ctsb$^{-/-}$ mice and wild-type mice; similarly, no differences in cathepsin B expression were seen between Ctsz$^{-/-}$ and wild-type mice (Figure S5C-E).

To test whether cathepsin B or cathepsin Z deficiency differentially impairs the immune system of Ctsb$^{-/-}$ and Ctsz$^{-/-}$ mice, we first analyzed the cellular composition of the spleen and the inguinal and axillary lymph nodes at the site of abdominal TNCB sensitization by flow cytometry, mainly focusing on CD4^{+} T helper cells and CD8^{+} cytotoxic T cells. Neither Ctsb$^{-/-}$ nor Ctsz$^{-/-}$ mice (naïve or TNCB-sensitized) exhibited significant alterations in the composition of immune cells or the T cell polarization in the spleen or mesenteric draining lymph nodes (sensitization phase) relative to those factors in wild-type mice with acute cutaneous DTHR (Figure S6).

Discussion

In this study, we examined the importance of the activity of proteases such as cathepsin B in cutaneous DTHR and the resulting implications for future therapeutic strategies.

Proteases play an essential role in different steps of inflammatory process establishment. Cathepsins, a diverse group comprising approximately 15 cysteine, serine or aspartic proteases, are mainly active in the acidic environment of endolysosomes, where they are involved in processing the MHC class II-associated invariant chain and MHC-bound antigens [4]. While cathepsins B and D are not essential for MHC-dependent antigen processing [32], cathepsin S is indispensable for processing antigens and the invariant chain [33]. The ubiquitously expressed cathepsin B is considered a key enzyme in the degradation of immune complexes bound to Fcγ receptors (FcγRs) on antigen-presenting cells (APCs) [34].

In addition to the intracellular roles of cathepsin B, many of its extracellular functions, such as the extracellular matrix degradation and angiogenesis, have been described [8, 9], although the neutral pH outside of the lysosome leads to the inactivation and instability of the cathepsin B molecule [35]. The ability of heparin to prevent pH-dependent cathepsin B degradation has been described [36]. In addition to the proteolytic effect of cathepsin B itself, this enzyme can inactivate inhibitors of MMPs, which are other highly potent mediators of extracellular matrix degradation and angiogenesis [37].

We recently established *in vivo* optical imaging as a tool to noninvasively assess the activity of MMPs in cutaneous DTHR [18]. In this study, we measured high *in vivo* protease activity in ears with chronic cutaneous DTHR using a ProSense probe (Figure 1 A/B). ProSense probes contain an oligo-L-lysine sequence with attached near-infrared fluorochromes and methoxypolyethylene glycol side chains [38]. The oligo-L-lysine sequence is cleaved not only by several cathepsins but also by the proteases trypsin, urokinase and plasmin [37, 39].

Furthermore, we evaluated the CatB680 probe, which is more specific for cathepsins than the ProSense probe [29]. Our measurements revealed a 4-fold enhancement of *in vivo* CatB680 signal intensity in ears (right side) with acute cutaneous DTHR compared with that in healthy control ears (left side). Ears with chronic cutaneous DTHR exhibited a further increase in the CatB680 signal intensity (Figure 1C/D).

CatB680 is cleaved preferentially by cathepsin B; however, Lin et al. reported substantial cleavage by cathepsin S but only a very faint interaction with

cathepsins L, D and K [29]. Cathepsin S is mostly expressed by APCs such as dendritic cells as well as macrophages [4] and is more stable than cathepsin B at neutral pH [40]. Therefore, a considerable contribution of cathepsin S to the cleavage of the CatB680 probe seems plausible.

Various probes for noninvasive *in vivo* imaging of cathepsin B activity are available, for example, nanoparticles with linkers to quenched fluorescent dyes [41], lysosome targeting groups [42] or prodrug-inspired probes [43]. Nevertheless, substrate-like activatable probes are dependent on cleavage sites consisting of peptide sequences that are not exclusively cleaved by one single protease (such as cathepsin B) since active sites are highly conserved throughout the cathepsin family [2, 44]. Caculitan et al. investigated an antibody-drug conjugate with a linker domain designed to be cleaved by cathepsin B, which should lead to the specific release of a cytotoxic drug in the target tissue. Their experiments revealed multiple approaches to produce active catabolites from the antibody-drug conjugate and demonstrated that cathepsin B is dispensable for the cleavage of this linker [45].

Cathepsin inhibitors, antibodies or designed ankyrin repeat proteins (DARPins) [46] labeled with fluorophores or radioactive isotopes can be highly specific but do not reflect the actual proteolytic activity of cysteine-type cathepsins such as cathepsin B. Activity-based probes combine both principles; such probes bind specifically to the protease after activation by proteolytic cleavage [44, 47, 48] but lack signal amplification, as a protease molecule can cleave multiple molecules of a substrate-like activatable probe.

Unfortunately, most of the available probes have not been thoroughly evaluated *in vivo* by specific inhibitor treatment or gene knockout in mice. Our optical imaging experiments revealed a decreasing trend in the CatB680 signal only in draining lymph nodes and not the inflamed ear tissue of CA-074-treated mice (Figure S2B/C; see discussion below). In $Ctsb^{-/-}$ mice, we measured an enhanced CatB680 signal intensity compared with wild-type mice (Figure S5A; see discussion below).

Data concerning the exact cellular sources of cathepsin B during inflammatory processes are scarce. However, immunofluorescence microscopy and flow cytometry analysis identified neutrophils, dendritic cells, macrophages and lymphocytes as the main cathepsin B-expressing cell populations (Figure 2).

Lautwein et al. detected cathepsin B expression in peripheral monocytes, as well as in stimulated and unstimulated dendritic cells [49]. Cathepsin B expression in T cells and monocytic cells is elevated after activation and is involved in the migration of these immune cells [50]. In cytotoxic T cells, cathepsin B is found at the cell surface, suggesting that it protects the cell by cleaving secreted perforin [51]. However, in $Ctsb^{-/-}$ mice, the function and survival of cytotoxic T cells were not impaired [52]. Thus, Pipkin et al. assumed that other cathepsins assume the functions of cathepsin B [53].

The percentage of cathepsin B-expressing cells was much higher in draining lymph nodes (Figure 2C) than in inflamed ear tissue (Figure 2B), suggesting an important role for cathepsin B in adaptive immunity, as in antigen processing.

In particular, a high percentage of macrophages and dendritic cells showed cathepsin B expression. While cathepsin B in macrophages and dendritic cells is known for its involvement in antigen processing, no data exist on whether cathepsin B is involved in lymphocyte expansion, possibly explaining the high numbers of cathepsin B-expressing B and T cells in draining lymph nodes (Figure 2C). Regarding B cells, Cathepsin B has been shown to be involved in lymphopoiesis [54]. High-throughput sequencing of macrophages, monocytes and neutrophils from fresh mouse tissues revealed expression of cathepsin B as well as cathepsin Z in multiple subsets of macrophages and neutrophils [55].

Interestingly, neutrophil elastase leads to an upregulation of cathepsin B and MMP-2 expression in macrophages [56]. Regarding neutrophils, most evidence suggests that the secretion of granule-derived cathepsin G mediates the killing of certain bacteria [57] and activates proinflammatory cytokines [58]. An important inducer of cathepsin B release in neutrophils is fluid shear stress [59]. In addition, cathepsin B was found to control the persistence of memory $CD8^+$ T cells after viral infection [60]. Fewer cells, especially dendritic cells and macrophages, expressed cathepsin B in the lymph nodes of naïve mice than in the lymph nodes of mice with DTHR, suggesting an elevation of cathepsin B expression through inflammatory processes. Only the percentage of cathepsin B-expressing NK cells remained almost unchanged (Figure 2D). NK cell-derived cathepsin B is suggested to protect cells from self-destruction [51].

To elucidate the therapeutic impact of specifically targeting cathepsin B, we treated mice with the selective cathepsin B inhibitor CA-074. In mice with acute cutaneous DTHR, CA-074 reduced the ear swelling 12 h and 24 h after challenge compared with that in sham-treated mice (Figure 4A). The anti-inflammatory effect of CA-074 was confirmed by histological analyses of ear sections, which revealed reductions in ear thickness, edema,

hyperkeratosis, acanthosis and inflammatory cell infiltration in CA-074-treated mice compared with these parameters in sham-treated mice (Figure 4B).

CA-074 binds to the active site and occludes the loop of cathepsin B [61]. CA-074 inhibits cathepsin B most effectively at acidic pH, which is common in lysosomes [62]. The anionic CA-074 molecule was thought to be unable to penetrate the cell membrane and to inhibit only extracellular cathepsin B, but Szpaderska et al. demonstrated that high concentrations of CA-074 can suppress intracellular cathepsin B *in vitro* [63]. Very possibly, cells can ingest increased concentrations of CA-074 via endocytosis. Several *in vivo* experiments confirmed the effectiveness of cathepsin B inhibition by CA-074. In a murine model of leishmaniasis, CA-074 could trigger the switch from a Th2-dominated inflammatory response to a Th1 immune reaction associated with IFN-γ production [64]. In an *in vivo* tumor xenograft model, CA-074 inhibited tumor growth and the metastatic potential of human melanoma [65].

We further analyzed inflamed ear tissue and draining lymph nodes by active site labeling, a highly sensitive *in vitro* method to tag and visualize the active form of enzymes such as cathepsin B [27].

This method revealed the presence of active cathepsin B in inflamed ear tissue (Figure 4C) and even higher levels in draining lymph nodes (Figure 4D). Topical treatment with the cathepsin B inhibitor CA-074 led to a clear reduction in active cathepsin B levels in inflamed ear tissue and draining lymph nodes compared with these levels in sham-treated mice (Figure 4C/D).

The regulatory dynamics of proteases are largely unknown, but it is plausible that in mice treated with a specific inhibitor such as CA-074, compensatory upregulation of other cathepsins may not occur immediately. This delay could explain why the therapeutic effect of CA-074 is present in acute but not in chronic cutaneous DTHR (Figure S2A).

Surprisingly, we observed enhanced acute TNCB-induced cutaneous DTHR in $Ctsb^{-/-}$ mice (Figure 5A), despite the disrupted cathepsin B expression confirmed by immunohistochemistry, active site labeling and Western blotting (Figure 5C/D; Figure S3B-D).

In vivo optical imaging using the CatB680 probe in CA-074-treated mice showed, paradoxically, slightly enhanced cathepsin activity (Figure S2B), whereas *ex vivo* cathepsin activity in the lymph nodes was decreased (Figure S1C/D). These results differed from those of our *ex vivo* active site labeling experiments (Figure 4C/D).

As mentioned above, CatB680 also interacts with cathepsin S, as reported previously [29]. The inhibitor CA-074 acts specifically on cathepsin B; Katunuma reported that CA-074 does not affect cathepsin S [61]. Therefore, cathepsin S may compensate for cathepsin B to cleave the CatB680 probe. However, whether treatment with CA-074 affects the expression of other cathepsins that are able to activate CatB680 has not yet been investigated.

Furthermore, these differences between cathepsin B activity in lymph nodes and ear tissue in our *ex vivo* and *in vivo* studies may also be due to differing cathepsin B activity and expression in diverse cell compartments.

Through tissue homogenization, protease activity in the extracellular space and all intracellular compartments can be detected *in vitro*. Optical imaging of protease-activatable probes was thought to selectively detect extracellular protease activity; nevertheless, Blum et al. showed that a protease-activatable probe could specifically detect protease activity in intracellular lysosomes *in vitro* [16]. Whether protease-activatable optical imaging probes are internalized into lysosomes or can penetrate the cell membrane remains unknown.

Several cathepsins, such as cathepsins S and L, have endopeptidase functions like those of cathepsin B [66]. Orlowski et al. revealed a redundant function of cathepsins B, L, C, S and X in pro-IL-1β synthesis and NLRP3-mediated IL-1β activation [67]. This redundancy suggests that a compensatory function of other cathepsins could be the reason for the undiminished cutaneous DTHR in $Ctsb^{-/-}$ mice. Interestingly, optical imaging using CatB680 in $Ctsb^{-/-}$ mice showed a higher signal intensity than that in wild-type mice (Figure S5A). Lin et al. showed that CatB680 is mainly activated by cathepsin B but also, to a lesser extent, by cathepsin S [29].

Our results suggest that cathepsin Z may compensate for cathepsin B deficiency in $Ctsb^{-/-}$ mice (Figure 5C/D). Both cathepsin Z and cathepsin B are carboxypeptidases in the family of cysteine-type cathepsins and are, therefore, quite similar biochemically [2]. Functionally, cathepsin B is considered an endopeptidase and a carboxydipeptidase [68], whereas cathepsin Z is considered a carboxymonopeptidase [69]. A compensatory role for cathepsin Z in cathepsin B deficiency was previously studied by Vasiljeva et al. [31] and Sevenich et al. [24] in an experimental breast cancer model. To our knowledge, however, this study is the first to investigate the role of cathepsin B and cathepsin Z together in inflammation.

Conclusions

Cysteine-type cathepsins such as cathepsin B are involved in various steps of inflammatory immune

response establishment, especially in draining lymph nodes but also at the site of inflammation. We found that cathepsin B is highly expressed in draining lymph nodes and that the therapeutic effects on active cathepsin B occur mainly in draining lymph nodes. Topical treatment with CA-074, a highly specific cathepsin B inhibitor, revealed a significant anti-inflammatory effect in acute but not chronic cutaneous DTHR. Topically applied cathepsin B inhibitors may reflect a new therapeutic tool for inflammatory skin diseases such as psoriasis.

Abbreviations

ANOVA: analysis of variance; APC: antigen-presenting cells; CHSR: contact hypersensitivity reaction; DARPin: designed ankyrin repeat protein; DC: dendritic cell; DMSO: dimethylsulfoxide; DTHR: delayed-type hypersensitivity reactions; FRET: fluorescence resonance energy transfer; H&E: hematoxylin and eosin; IFN: interferon; MHC: major histocompatibility complex; MMP: matrix metalloproteinase; NLRP: NACHT, LRR and PYD domains-containing protein; PBS: phosphate-buffered saline; ROI: region of interest; SEM: standard error of the mean; SI: signal intensity; Tc: cytotoxic T cell; Th: T helper cell; TLR: Toll-like receptor; TNCB: 2,4,6-trinitrochlorobenzene; TNF: tumor necrosis factor.

Supplementary Material

Supplementary figures.
http://www.thno.org/v09p3903s1.pdf

Acknowledgments

The authors thank Maren Harant, Linda Schramm, Ramona Stumm and Funda Cay for providing excellent technical support, as well as Gregory Bowden for providing language editing.

Funding

This work was supported by the Medical Faculty of the Eberhard Karls University Tübingen ("Promotionskolleg" and "PATE-Programm"), the German Research Foundation (SFB TRR156, TP C03 to M.K. & J.S. and TP B07 to K.G.) and the Werner Siemens-Foundation.

Author contributions

J.S., A.M., B.F., R.M., P.K., N.M., D.H., D.B., J.H., I.G.M and M.K. performed the experiments. J.S., A.M., B.F., R.M., P.K., L.Q.-F. and M.K. analyzed the data. J.S. and M.K. wrote the manuscript. A.M., K.F., C.M.G., M.S., K.G., L.Q.-F., M.G., S.L., T.R., M.R., H.K. and B.J.P. contributed technical expertise and critically edited the manuscript. All authors read and approved the manuscript.

Competing Interests

The authors have declared that no competing interest exists.

References

1. Reiser J, Adair B, Reinheckel T. Specialized roles for cysteine cathepsins in health and disease. J Clin Invest. 2010; 120: 3421-31.
2. Turk V, Stoka V, Vasiljeva O, Renko M, Sun T, Turk B, et al. Cysteine cathepsins: from structure, function and regulation to new frontiers. Biochim Biophys Acta. 2012; 1824: 68-88.
3. Turk V, Stoka V, Vasiljeva O, Renko M, Sun T, Turk B, et al. Cysteine cathepsins: from structure, function and regulation to new frontiers. Biochim Biophys Acta. 2012; 1824: 68-88.
4. Honey K, Rudensky AY. Lysosomal cysteine proteases regulate antigen presentation. Nat Rev Immunol. 2003; 3: 472-82.
5. Conus S, Simon HU. Cathepsins and their involvement in immune responses. Swiss Med Wkly. 2010; 140: w13042.
6. Chwieralski CE, Welte T, Buhling F. Cathepsin-regulated apoptosis. Apoptosis. 2006; 11: 143-9.
7. Ha SD, Martins A, Khazaie K, Han J, Chan BM, Kim SO. Cathepsin B is involved in the trafficking of TNF-alpha-containing vesicles to the plasma membrane in macrophages. J Immunol. 2008; 181: 690-7.
8. Im E, Venkatakrishnan A, Kazlauskas A. Cathepsin B regulates the intrinsic angiogenic threshold of endothelial cells. Mol Biol Cell. 2005; 16: 3488-500.
9. Obermajer N, Jevnikar Z, Doljak B, Kos J. Role of cysteine cathepsins in matrix degradation and cell signalling. Connect Tissue Res. 2008; 49: 193-6.
10. Hashimoto Y, Kakegawa H, Narita Y, Hachiya Y, Hayakawa T, Kos J, et al. Significance of cathepsin B accumulation in synovial fluid of rheumatoid arthritis. Biochem Biophys Res Commun. 2001; 283: 334-9.
11. Bever CT, Jr., Garver DW. Increased cathepsin B activity in multiple sclerosis brain. J Neurol Sci. 1995; 131: 71-3.
12. Van Acker GJ, Saluja AK, Bhagat L, Singh VP, Song AM, Steer ML. Cathepsin B inhibition prevents trypsinogen activation and reduces pancreatitis severity. Am J Physiol Gastrointest Liver Physiol. 2002; 283: G794-800.
13. Mohamed MM, Sloane BF. Cysteine cathepsins: multifunctional enzymes in cancer. Nat Rev Cancer. 2006; 6: 764-75.
14. Hook V, Schechter I, Demuth HU, Hook G. Alternative pathways for production of beta-amyloid peptides of Alzheimer's disease. Biol Chem. 2008; 389: 993-1006.
15. Ntziachristos V, Tung CH, Bremer C, Weissleder R. Fluorescence molecular tomography resolves protease activity in vivo. Nat Med. 2002; 8: 757-60.
16. Blum G, von Degenfeld G, Merchant MJ, Blau HM, Bogyo M. Noninvasive optical imaging of cysteine protease activity using fluorescently quenched activity-based probes. Nat Chem Biol. 2007; 3: 668-77.
17. Kneilling M, Mailhammer R, Hultner L, Schonberger T, Fuchs K, Schaller M, et al. Direct crosstalk between mast cell-TNF and TNFR1-expressing endothelia mediates local tissue inflammation. Blood. 2009; 114: 1696-706.
18. Schwenck J, Griessinger CM, Fuchs K, Bukala D, Bauer N, Eichner M, et al. In vivo optical imaging of matrix metalloproteinase activity detects acute and chronic contact hypersensitivity reactions and enables monitoring of the antiinflammatory effects of N-acetylcysteine. Mol Imaging. 2014: 1-12.
19. Pichler BJ, Kneilling M, Haubner R, Braumuller H, Schwaiger M, Rocken M, et al. Imaging of delayed-type hypersensitivity reaction by PET and 18F-galacto-RGD. J Nucl Med. 2005; 46: 184-9.
20. Murata M, Miyashita S, Yokoo C, Tamai M, Hanada K, Hatayama K, et al. Novel epoxysuccinyl peptides. Selective inhibitors of cathepsin B, in vitro. FEBS Lett. 1991; 280: 307-10.
21. Montaser M, Lalmanach G, Mach L. CA-074, but not its methyl ester CA-074Me, is a selective inhibitor of cathepsin B within living cells. Biol Chem. 2002; 383: 1305-8.
22. Schmitz J, Li T, Bartz U, Gutschow M. Cathepsin B Inhibitors: Combining Dipeptide Nitriles with an Occluding Loop Recognition Element by Click Chemistry. ACS Med Chem Lett. 2016; 7: 211-6.
23. Halangk W, Lerch MM, Brandt-Nedelev B, Roth W, Ruthenbuerger M, Reinheckel T, et al. Role of cathepsin B in intracellular trypsinogen activation and the onset of acute pancreatitis. J Clin Invest. 2000; 106: 773-81.
24. Sevenich L, Schurigt U, Sachse K, Gajda M, Werner F, Muller S, et al. Synergistic antitumor effects of combined cathepsin B and cathepsin Z deficiencies on breast cancer progression and metastasis in mice. Proc Natl Acad Sci U S A. 2010; 107: 2497-502.
25. Schmitz J, Li TW, Bartz U, Gutschow M. Cathepsin B Inhibitors: Combining Dipeptide Nitriles with an Occluding Loop Recognition Element by Click Chemistry. Acs Med Chem Lett. 2016; 7: 211-6.
26. Biedermann T, Kneilling M, Mailhammer R, Maier K, Sander CA, Kollias G, et al. Mast cells control neutrophil recruitment during T cell-mediated delayed-type hypersensitivity reactions through tumor necrosis factor and macrophage inflammatory protein 2. J Exp Med. 2000; 192: 1441-52.

27. Lutzner N, Kalbacher H. Quantifying cathepsin S activity in antigen presenting cells using a novel specific substrate. J Biol Chem. 2008; 283: 36185-94.
28. Nahrendorf M, Waterman P, Thurber G, Groves K, Rajopadhye M, Panizzi P, et al. Hybrid in vivo FMT-CT imaging of protease activity in atherosclerosis with customized nanosensors. Arterioscler Thromb Vasc Biol. 2009; 29: 1444-51.
29. Lin SA, Patel M, Suresch D, Connolly B, Bao B, Groves K, et al. Quantitative Longitudinal Imaging of Vascular Inflammation and Treatment by Ezetimibe in apoE Mice by FMT Using New Optical Imaging Biomarkers of Cathepsin Activity and alpha(v)beta(3) Integrin. Int J Mol Imaging. 2012; 2012: 189254.
30. Greenbaum D, Medzihradszky KF, Burlingame A, Bogyo M. Epoxide electrophiles as activity-dependent cysteine protease profiling and discovery tools. Chem Biol. 2000; 7: 569-81.
31. Vasiljeva O, Papazoglou A, Kruger A, Brodoefel H, Korovin M, Deussing J, et al. Tumor cell-derived and macrophage-derived cathepsin B promotes progression and lung metastasis of mammary cancer. Cancer Res. 2006; 66: 5242-50.
32. Deussing J, Roth W, Saftig P, Peters C, Ploegh HL, Villadangos JA. Cathepsins B and D are dispensable for major histocompatibility complex class II-mediated antigen presentation. Proc Natl Acad Sci U S A. 1998; 95: 4516-21.
33. Riese RJ, Wolf PR, Bromme D, Natkin LR, Villadangos JA, Ploegh HL, et al. Essential role for cathepsin S in MHC class II-associated invariant chain processing and peptide loading. Immunity. 1996; 4: 357-66.
34. Driessen C, Lennon-Dumenil AM, Ploegh HL. Individual cathepsins degrade immune complexes internalized by antigen-presenting cells via Fcgamma receptors. Eur J Immunol. 2001; 31: 1592-601.
35. Puzer L, Cotrin SS, Cezari MH, Hirata IY, Juliano MA, Stefe I, et al. Recombinant human cathepsin X is a carboxymonopeptidase only: a comparison with cathepsins B and L. Biological chemistry. 2005; 386: 1191-5.
36. Costa MGS, Batista PR, Shida CS, Robert CH, Bisch PM, Pascutti PG. How does heparin prevent the pH inactivation of cathepsin B? Allosteric mechanism elucidated by docking and molecular dynamics. Bmc Genomics. 2010; 11.
37. Kostoulas G, Lang A, Nagase H, Baici A. Stimulation of angiogenesis through cathepsin B inactivation of the tissue inhibitors of matrix metalloproteinases. FEBS Lett. 1999; 455: 286-90.
38. Weissleder R, Tung CH, Mahmood U, Bogdanov A, Jr. In vivo imaging of tumors with protease-activated near-infrared fluorescent probes. Nat Biotechnol. 1999; 17: 375-8.
39. Costa MG, Batista PR, Shida CS, Robert CH, Bisch PM, Pascutti PG. How does heparin prevent the pH inactivation of cathepsin B? Allosteric mechanism elucidated by docking and molecular dynamics. BMC Genomics. 2010; 11 Suppl 5: S5.
40. Bromme D, Bonneau PR, Lachance P, Wiederanders B, Kirschke H, Peters C, et al. Functional expression of human cathepsin S in Saccharomyces cerevisiae. Purification and characterization of the recombinant enzyme. J Biol Chem. 1993; 268: 4832-8.
41. Ryu JH, Kim SA, Koo H, Yhee JY, Lee A, Na JH, et al. Cathepsin B-sensitive nanoprobe for in vivo tumor diagnosis. J Mater Chem. 2011; 21: 17631-4.
42. Wang YQ, Li JB, Feng LD, Yu JF, Zhang Y, Ye DJ, et al. Lysosome-Targeting Fluorogenic Probe for Cathepsin B Imaging in Living Cells. Anal Chem. 2016; 88: 12403-10.
43. Chowdhury MA, Moya IA, Bhilocha S, McMillan CC, Vigliarolo BG, Zehbe I, et al. Prodrug-inspired probes selective to cathepsin B over other cysteine cathepsins. J Med Chem. 2014; 57: 6092-104.
44. Watzke A, Kosec G, Kindermann M, Jeske V, Nestler HP, Turk V, et al. Selective activity-based probes for cysteine cathepsins. Angew Chem Int Ed Engl. 2008; 47: 406-9.
45. Caculitan NG, Dela Cruz Chuh J, Ma Y, Zhang D, Kozak KR, Liu Y, et al. Cathepsin B Is Dispensable for Cellular Processing of Cathepsin B-Cleavable Antibody-Drug Conjugates. Cancer Res. 2017; 77: 7027-37.
46. Kramer L, Renko M, Zavrsnik J, Turk D, Seeger MA, Vasiljeva O, et al. Non-invasive in vivo imaging of tumour-associated cathepsin B by a highly selective inhibitory DARPin. Theranostics. 2017; 7: 2806-21.
47. Edem PE, Czorny S, Valliant JF. Synthesis and Evaluation of Radioiodinated Acyloxymethyl Ketones as Activity-Based Probes for Cathepsin B. Journal of Medicinal Chemistry. 2014; 57: 9564-77.
48. Ren G, Blum G, Verdoes M, Liu HG, Syed S, Edgington LE, et al. Non-Invasive Imaging of Cysteine Cathepsin Activity in Solid Tumors Using a Cu-64-Labeled Activity-Based Probe. Plos One. 2011; 6.
49. Lautwein A, Burster T, Lennon-Dumenil AM, Overkleeft HS, Weber E, Kalbacher H, et al. Inflammatory stimuli recruit cathepsin activity to late endosomal compartments in human dendritic cells. Eur J Immunol. 2002; 32: 3348-57.
50. Staun-Ram E, Miller A. Cathepsins (S and B) and their inhibitor Cystatin C in immune cells: modulation by interferon-beta and role played in cell migration. J Neuroimmunol. 2011; 232: 200-6.
51. Balaji KN, Schaschke N, Machleidt W, Catalfamo M, Henkart PA. Surface cathepsin B protects cytotoxic lymphocytes from self-destruction after degranulation. J Exp Med. 2002; 196: 493-503.
52. Baran K, Ciccone A, Peters C, Yagita H, Bird PI, Villadangos JA, et al. Cytotoxic T lymphocytes from cathepsin B-deficient mice survive normally in vitro and in vivo after encountering and killing target cells. J Biol Chem. 2006; 281: 30485-91.
53. Pipkin ME, Lieberman J. Delivering the kiss of death: progress on understanding how perforin works. Curr Opin Immunol. 2007; 19: 301-8.
54. Lalanne AI, Moraga I, Hao Y, Pereira JP, Alves NL, Huntington ND, et al. CpG inhibits pro-B cell expansion through a cathepsin B-dependent mechanism. J Immunol. 2010; 184: 5678-85.
55. Lavin Y, Winter D, Blecher-Gonen R, David E, Keren-Shaul H, Merad M, et al. Tissue-resident macrophage enhancer landscapes are shaped by the local microenvironment. Cell. 2014; 159: 1312-26.
56. Geraghty P, Rogan MP, Greene CM, Boxio RMM, Poiriert T, O'Mahony M, et al. Neutrophil elastase up-regulates cathepsin B and matrix metalloprotease-2 expression. Journal of Immunology. 2007; 178: 5871-8.
57. van der Windt D, Bootsma HJ, Burghout P, van der Gaast-de Jongh CE, Hermans PW, van der Flier M. Nonencapsulated Streptococcus pneumoniae resists extracellular human neutrophil elastase- and cathepsin G-mediated killing. FEMS Immunol Med Microbiol. 2012; 66: 445-8.
58. Henry CM, Sullivan GP, Clancy DM, Afonina IS, Kulms D, Martin SJ. Neutrophil-Derived Proteases Escalate Inflammation through Activation of IL-36 Family Cytokines. Cell Rep. 2016; 14: 708-22.
59. Akenhead ML, Fukuda S, Schmid-Schonbein GW, Shin HY. Fluid shear-induced cathepsin B release in the control of Mac1-dependent neutrophil adhesion. J Leukoc Biol. 2017; 102: 117-26.
60. Byrne SM, Aucher A, Alyahya S, Elder M, Olson ST, Davis DM, et al. Cathepsin B controls the persistence of memory CD8+ T lymphocytes. J Immunol. 2012; 189: 1133-43.
61. Katunuma N. Structure-based development of specific inhibitors for individual cathepsins and their medical applications. Proc Jpn Acad Ser B Phys Biol Sci. 2011; 87: 29-39.
62. Linebaugh BE, Sameni M, Day NA, Sloane BF, Keppler D. Exocytosis of active cathepsin B enzyme activity at pH 7.0, inhibition and molecular mass. Eur J Biochem. 1999; 264: 100-9.
63. Szpaderska AM, Frankfater A. An intracellular form of cathepsin B contributes to invasiveness in cancer. Cancer Res. 2001; 61: 3493-500.
64. Maekawa Y, Himeno K, Ishikawa H, Hisaeda H, Sakai T, Dainichi T, et al. Switch of CD4+ T cell differentiation from Th2 to Th1 by treatment with cathepsin B inhibitor in experimental leishmaniasis. J Immunol. 1998; 161: 2120-7.
65. Matarrese P, Ascione B, Ciarlo L, Vona R, Leonetti C, Scarsella M, et al. Cathepsin B inhibition interferes with metastatic potential of human melanoma: an in vitro and in vivo study. Mol Cancer. 2010; 9: 207.
66. Olson OC, Joyce JA. Cysteine cathepsin proteases: regulators of cancer progression and therapeutic response. Nat Rev Cancer. 2015; 15: 712-29.
67. Orlowski GM, Colbert JD, Sharma S, Bogyo M, Robertson SA, Rock KL. Multiple Cathepsins Promote Pro-IL-1beta Synthesis and NLRP3-Mediated IL-1beta Activation. J Immunol. 2015; 195: 1685-97.
68. Musil D, Zucic D, Turk D, Engh RA, Mayr I, Huber R, et al. The refined 2.15 A X-ray crystal structure of human liver cathepsin B: the structural basis for its specificity. EMBO J. 1991; 10: 2321-30.
69. Guncar G, Klemencic I, Turk B, Turk V, Karaoglanovic-Carmona A, Juliano L, et al. Crystal structure of cathepsin X: a flip-flop of the ring of His23 allows carboxy-monopeptidase and carboxy-dipeptidase activity of the protease. Structure. 2000; 8: 305-13.

Cysteine-type cathepsins promote the effector phase of acute cutaneous delayed-type hypersensitivity reactions

Johannes Schwenck[1,2], Andreas Maurer[1,3], Birgit Fehrenbacher[4], Roman Mehling[1], Philipp Knopf[1], Natalie Mucha[1], Dennis Haupt[1], Kerstin Fuchs[1], Christoph M. Griessinger[1], Daniel Bukala[1], Julia Holstein[4], Martin Schaller[4], Irene Gonzalez Menendez[5], Kamran Ghoreschi[4], Leticia Quintanilla-Martinez[5], Michael Gütschow[6], Stefan Laufer[7], Thomas Reinheckel[8], Martin Röcken[4], Hubert Kalbacher[3], Bernd J Pichler[1], Manfred Kneilling[1,4*]

[1] Werner Siemens Imaging Center, Department of Preclinical Imaging and Radiopharmacy, Eberhard Karls University, 72076 Tübingen, Germany
[2] Department of Nuclear Medicine and Clinical Molecular Imaging, Eberhard Karls University, 72076 Tübingen, Germany
[3] Interfaculty Institute of Biochemistry, Eberhard Karls University, 72076 Tübingen, Germany
[4] Department of Dermatology, Eberhard Karls University, 72076 Tübingen, Germany
[5] Department of Pathology, Eberhard Karls University, 72076 Tübingen, Germany
[6] Pharmaceutical Institute, Pharmaceutical Chemistry I, University of Bonn, 53121 Bonn, Germany
[7] Department of Pharmaceutical and Medicinal Chemistry, Institute of Pharmacy, Eberhard Karls University, 72076 Tübingen, Germany
[8] Institute of Molecular Medicine and Cell Research, Medical Faculty, Albert-Ludwigs University, 79085 Freiburg, Germany

* corresponding author email: manfred.kneilling@med.uni-tuebingen.de
telephone: +49-7071-29-83427
fax: +49-7071-29-4451

Keywords: inflammation, proteases, cathepsin B, optical imaging, delayed type hypersensitivity

Supplementary Figures

Supplementary Fig. 1

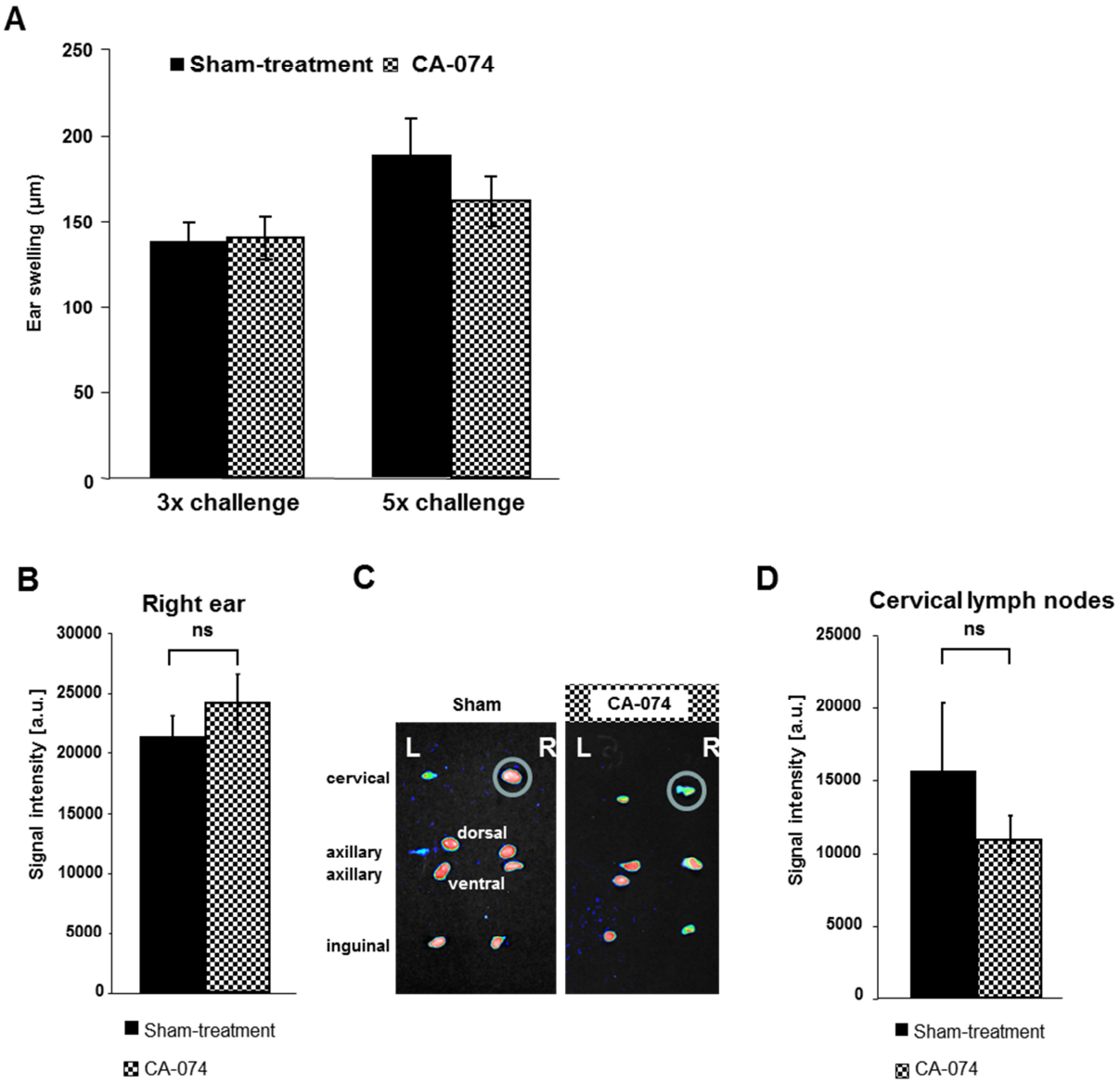

A: In chronic CHSR after three or five TNCB challenges no significant differences in ear swelling response between sham- and CA-074 treated mice were observed (n=7). **B:** *In vivo* optical imaging with the cathepsin-activatable probe CatB680 displayed no significant difference in signal-intensity between mice treated with CA-074 and sham-treatment in the right ear (n=4). **C:** *Ex*

vivo optical imaging yielded a reduced CatB680 signal-intensity in the draining cervical LNs of CA-074 treated mice. Axillary and inguinal LNs showed high signal intensities in both groups. **D:** *Ex vivo* CatB680 signal intensity of the cervical draining lymph nodes was slightly lower in CA-074-treated mice (n=4).

Supplementary Fig. 2

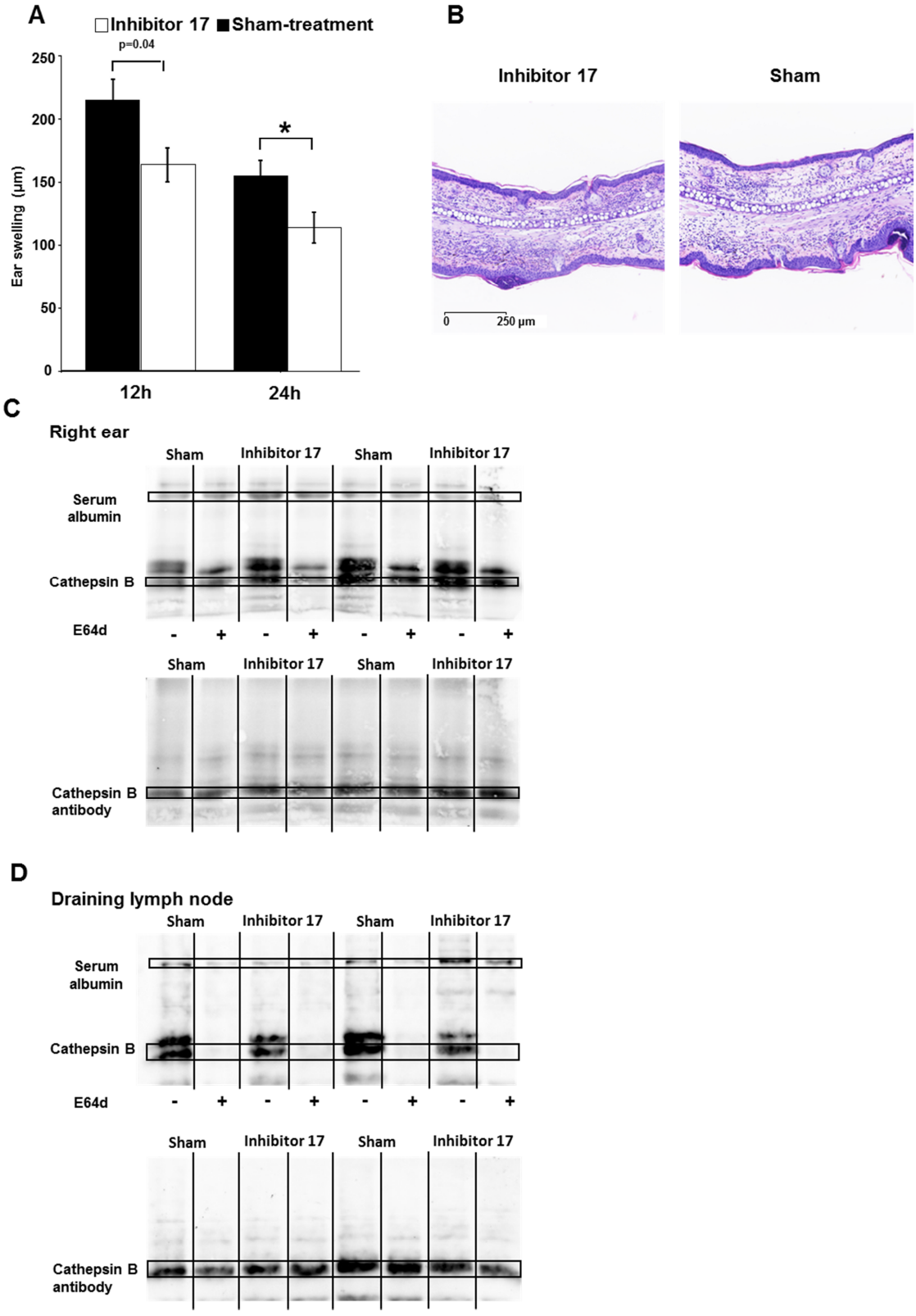

A: Topical treatment with Inhibitor 17 reduced ear swelling 12 h and 24 h after TNCB challenge compared to sham treated mice (n=8). **B:** H&E histology of ear tissue derived from Inhibitor 17 and sham treated mice 24 h after challenge revealed a reduced edema and leukocyte infiltration as a consequence of Inhibitor 17 treatment. **C/D:** Active site labelling and immune blotting of ear tissue as well as the draining lymph nodes was not able to assess differences between inhibitor 17 and sham treated mice, most probably because of the reversible covalent binding of inhibitor 17 to cathepsin B (n=8).

Supplementary Fig. 3

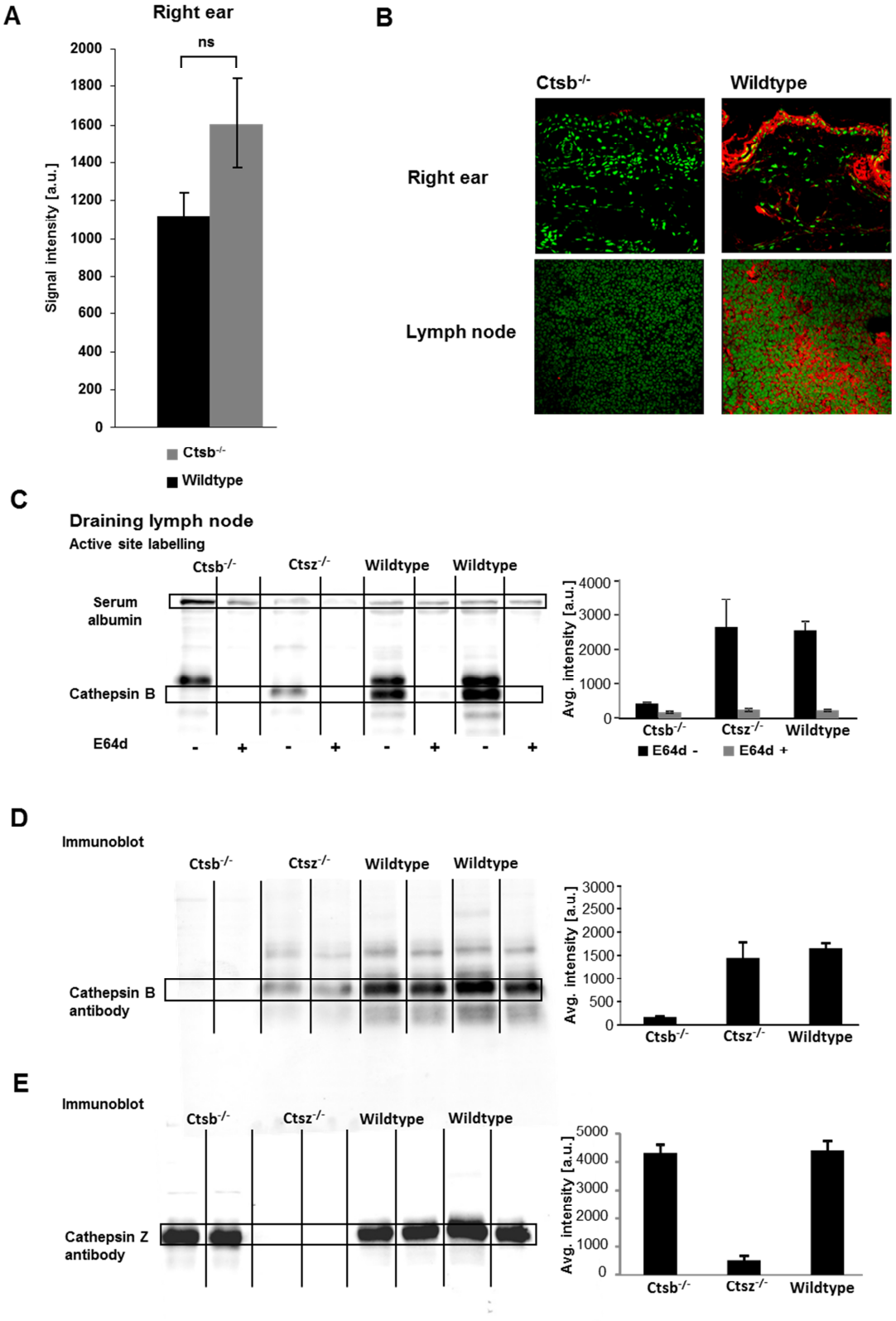

A: Optical imaging of Ctsb$^{-/-}$ mice and wildtype mice using CatB680 revealed a higher SI in cathepsin B deficient mice after the first challenge (1x challenge n=10; 1x/3x challenge n=7). **B:** Immune fluorescence staining of cathepsin B (red) of right ear tissue and the draining lymph node of sensitized Ctsb$^{-/-}$ and wildtype mice 24 h after TNCB-challenge revealed suppressed cathepsin B expression in Ctsb$^{-/-}$ mice (goat anti–cathepsin B Ab 1:20; R&D Systems, Minneapolis, USA; visualized using Cy3-donkey anti-goat Ab; Dianova). **C:** Active site labeling of the draining lymph node derived from Ctsb$^{-/-}$ mice revealed a diminished cathepsin B band but equivalent Cathepsin B expression in Ctsz$^{-/-}$ mice compared to wildtype mice (Ctsb$^{-/-}$ n=4; Ctsz$^{-/-}$ n=3; wildtype n=4). **D:** Immunoblotting using a cathepsin B specific antibody on the same confirmed the bands detected by active site labeling and indicated normal cathepsin B expression in the draining lymph nodes of Ctsz$^{-/-}$ mice while cathepsin B expression in Ctsb$^{-/-}$ mice was diminished (Ctsb$^{-/-}$ n=4; Ctsz$^{-/-}$ n=3; wildtype n=4). **E:** Cathepsin Z expression detected by immunoblotting using a cathepsin Z specific antibody was similar in the draining lymph nodes of Ctsb$^{-/-}$ and wildtype mice, while cathepsin Z was virtually absent in Ctsz$^{-/-}$ mice (Ctsb$^{-/-}$ n=4; Ctsz$^{-/-}$ n=3; wildtype n=4).

Supplementary Fig. 4

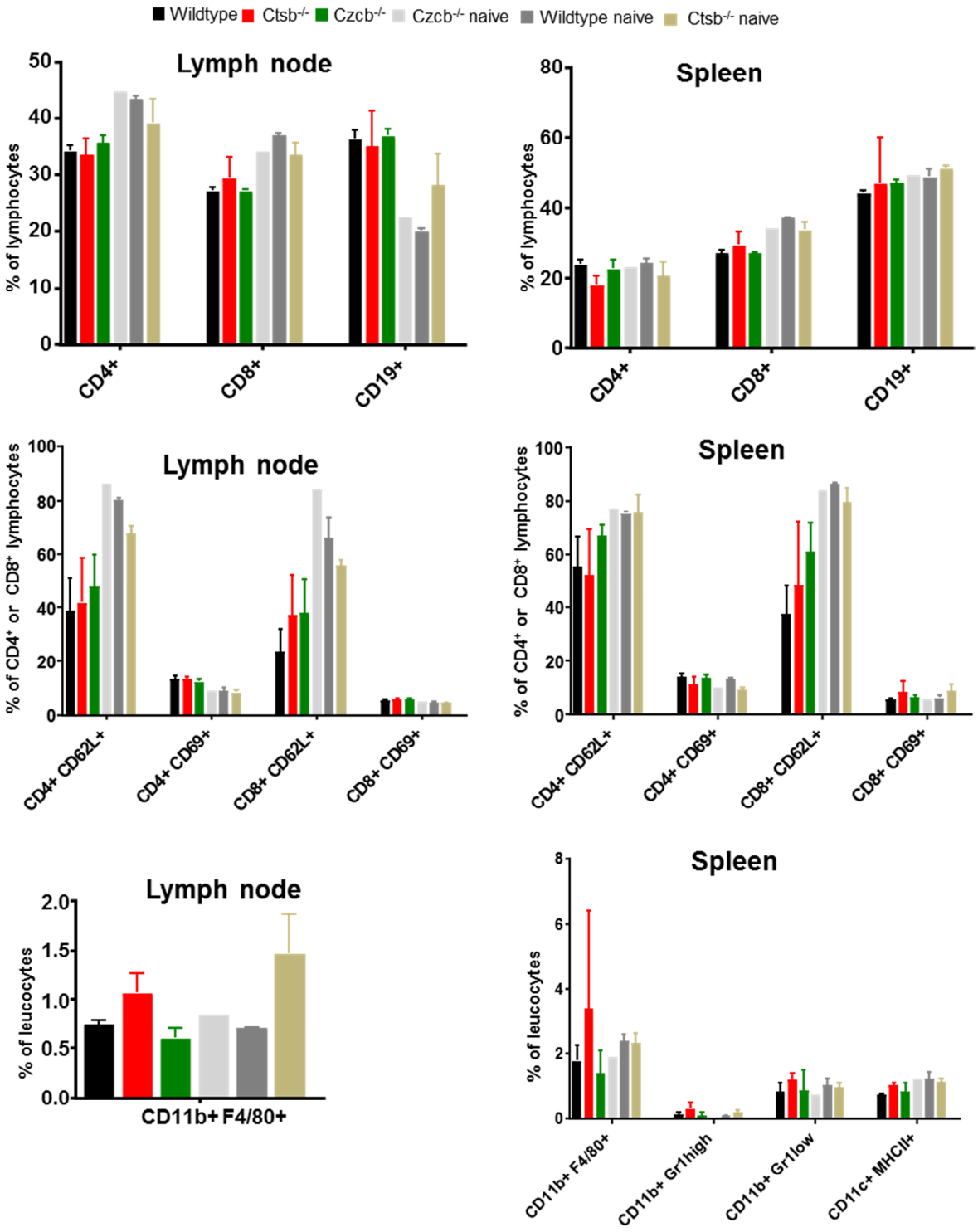

We performed flow cytometry analysis of inguinal and axillary lymph nodes (TNCB-sensitization at the abdomen) and spleen tissue derived from naïve

and TNCB-sensitized and challenged wild-type, $Ctsb^{-/-}$, and $Czsb^{-/-}$ mice. Neither $Ctsb^{-/-}$ or $Ctsz^{-/-}$ mice showed significant alterations in the cellular composition of immune cells in the spleen or the lymph nodes compared to wildtype mice in naïve state or 24 h after the challenge (TNCB-sensitized and challenged mice: n = 3-4; naïve mice: n = 1-3).

Supplementary Fig. 5

A

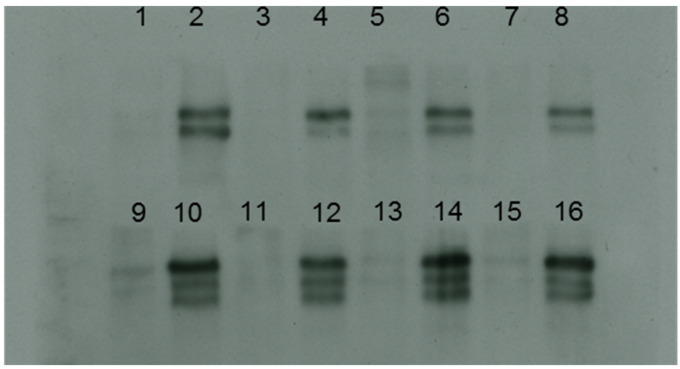

B

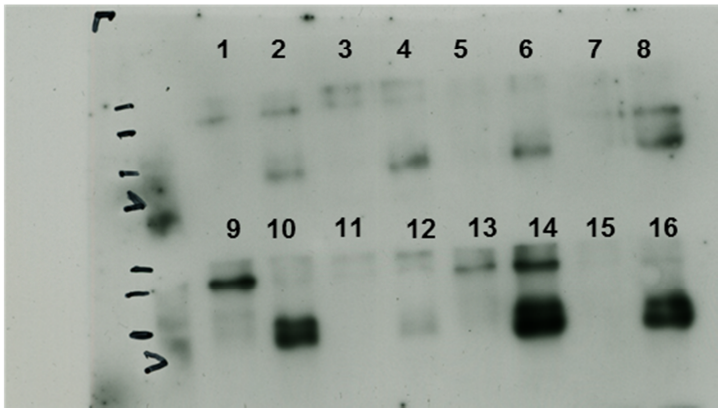

Original blots from Figure 4 C/D. **A:** Blot active site labelling (shown in Fig 4C): lane 1 CA-074 treatment + E64d, lane 2 CA-074 treatment, lane 3 CA-074 treatment + E64d, lane 4 CA-074 treatment, lane 5 CA-074 treatment + E64d, lane 6 CA-074 treatment, lane 7 CA-074 treatment + E64d, lane 8 CA-074 treatment, lane 9 sham treatment + E64d, lane 10 sham treatment, lane 11 sham treatment + E64d, lane 12 sham treatment, lane 13 sham treatment + E64d, lane 14 sham treatment, lane 15 sham treatment + E64d, lane 16 sham treatment. **B:** Blot active site labelling (shown in Fig 4D): lane 1 CA-074

treatment + E64d, lane 2 CA-074 treatment, lane 3 CA-074 treatment + E64d, lane 4 CA-074 treatment, lane 5 CA-074 treatment + E64d, lane 6 CA-074 treatment, lane 7 CA-074 treatment + E64d, lane 8 CA-074 treatment, lane 9 sham treatment + E64d, lane 10 sham treatment, lane 11 sham treatment + E64d (no proteases detectable, data not shown in Fig. 4D), lane 12 sham treatment (no proteases detectable, data not shown in Fig. 4D), lane 13 sham treatment + E64d, lane 14 sham treatment, lane 15 sham treatment + E64d, lane 16 sham treatment.

Supplementary Fig. 6

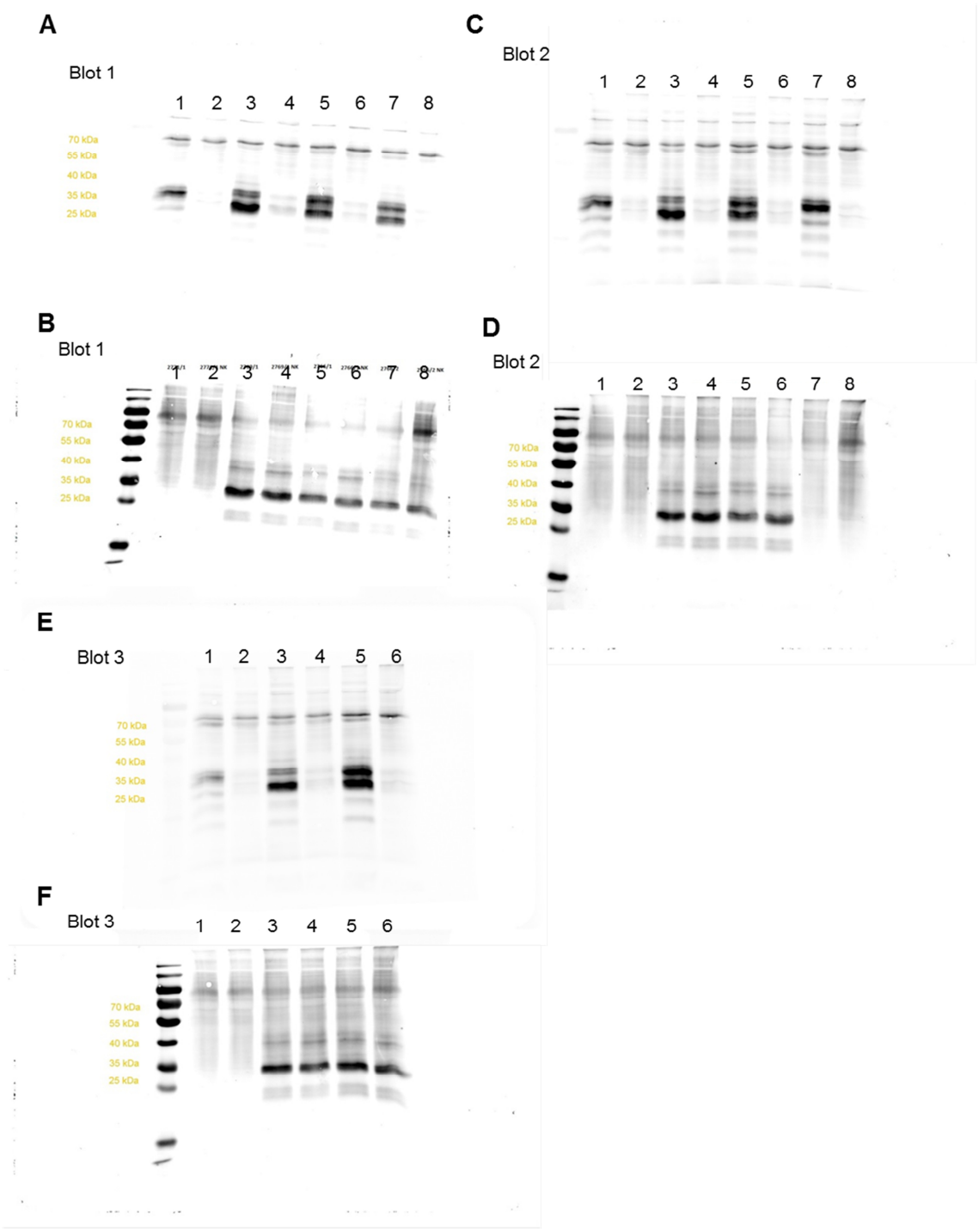

Original blots from Figure 5 C/D. **A:** Blot 1 active site labelling (shown in Fig 5C): lane 1 Ctsb$^{-/-}$, lane 2 Ctsb$^{-/-}$ + E64d, lane 3 Ctsz$^{-/-}$, lane 4 Ctsz$^{-/-}$ + E64d, lane 5 wildtype, lane 6 wildtype + E64d, lane 7 wildtype, lane 8 wildtype +

E64d. **B:** Blot 1 cathepsin B Western blot (shown in Fig 5D): lane 1 $Ctsb^{-/-}$, lane 2 $Ctsb^{-/-}$ + E64d, lane 3 $Ctsz^{-/-}$, lane 4 $Ctsz^{-/-}$ + E64d, lane 5 wildtype, lane 6 wildtype + E64d, lane 7 wildtype, lane 8 wildtype + E64d. **C:** Membrane 2 active site labelling: lane 1 $Ctsb^{-/-}$, lane 2 $Ctsb^{-/-}$ + E64d, lane 3 $Ctsz^{-/-}$, lane 4 $Ctsz^{-/-}$ + E64d, lane 5 wildtype, lane 6 wildtype + E64d, lane 7 $Ctsb^{-/-}$, lane 8 $Ctsb^{-/-}$ + E64d. **D:** Blot 2 cathepsin B Western blot: lane 1 $Ctsb^{-/-}$, lane 2 $Ctsb^{-/-}$ + E64d, lane 3 $Ctsz^{-/-}$, lane 4 $Ctsz^{-/-}$ + E64d, lane 5 wildtype, lane 6 wildtype + E64d, lane 7 $Ctsb^{-/-}$, lane 8 $Ctsb^{-/-}$ + E64d. **E:** Blot 3 active site labelling: lane 1 $Ctsb^{-/-}$, lane 2 $Ctsb^{-/-}$ + E64d, lane 3 $Ctsz^{-/-}$, lane 4 $Ctsz^{-/-}$ + E64d, lane 5 wildtype, lane 6 wildtype + E64d. **F:** Blot 3 cathepsin B Western blot: lane 1 $Ctsb^{-/-}$, lane 2 $Ctsb^{-/-}$ + E64d, lane 3 $Ctsz^{-/-}$, lane 4 $Ctsz^{-/-}$ + E64d, lane 5 wildtype, lane 6 wildtype + E64d.

Supplementary Fig. 7

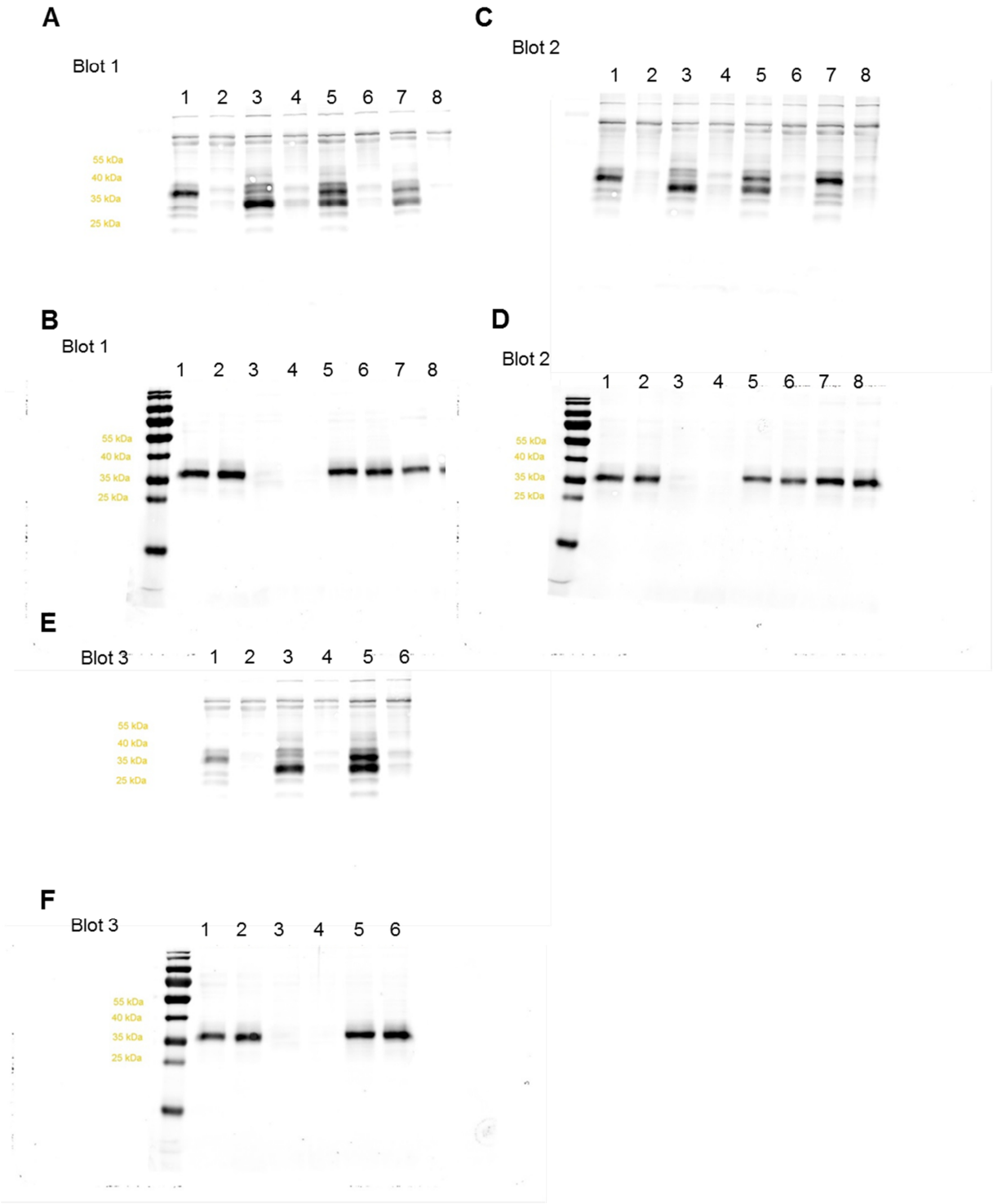

Original blots from Figure 5 E. **A:** Blot 1 active site labelling: lane 1 $Ctsb^{-/-}$, lane 2 $Ctsb^{-/-}$ + E64d, lane 3 $Ctsz^{-/-}$, lane 4 $Ctsz^{-/-}$ + E64d, lane 5 wildtype, lane

6 wildtype + E64d, lane 7 wildtype, lane 8 wildtype + E64d. **B:** Blot 1 cathepsin Z Western blot (shown in Figure 5 E): lane 1 $Ctsb^{-/-}$, lane 2 $Ctsb^{-/-}$ + E64d, lane 3 $Ctsz^{-/-}$, lane 4 $Ctsz^{-/-}$ + E64d, lane 5 wildtype, lane 6 wildtype + E64d, lane 7 wildtype, lane 8 wildtype + E64d. **C:** Blot 2 active site labelling: lane 1 $Ctsb^{-/-}$, lane 2 $Ctsb^{-/-}$ + E64d, lane 3 $Ctsz^{-/-}$, lane 4 $Ctsz^{-/-}$ + E64d, lane 5 wildtype, lane 6 wildtype + E64d, lane 7 $Ctsb^{-/-}$, lane 8 $Ctsb^{-/-}$ + E64d. **D:** Blot 2 cathepsin Z Western blot: lane 1 $Ctsb^{-/-}$, lane 2 $Ctsb^{-/-}$ + E64d, lane 3 $Ctsz^{-/-}$, lane 4 $Ctsz^{-/-}$ + E64d, lane 5 wildtype, lane 6 wildtype + E64d, lane 7 $Ctsb^{-/-}$, lane 8 $Ctsb^{-/-}$ + E64d. **E:** Blot 3 active site labelling: lane 1 $Ctsb^{-/-}$, lane 2 $Ctsb^{-/-}$ + E64d, lane 3 $Ctsz^{-/-}$, lane 4 $Ctsz^{-/-}$ + E64d, lane 5 wildtype, lane 6 wildtype + E64d. **F:** Blot 3 cathepsin Z Western blot: lane 1 $Ctsb^{-/-}$, lane 2 $Ctsb^{-/-}$ + E64d, lane 3 $Ctsz^{-/-}$, lane 4 $Ctsz^{-/-}$ + E64d, lane 5 wildtype, lane 6 wildtype + E64d.

Supplementary Fig. 8

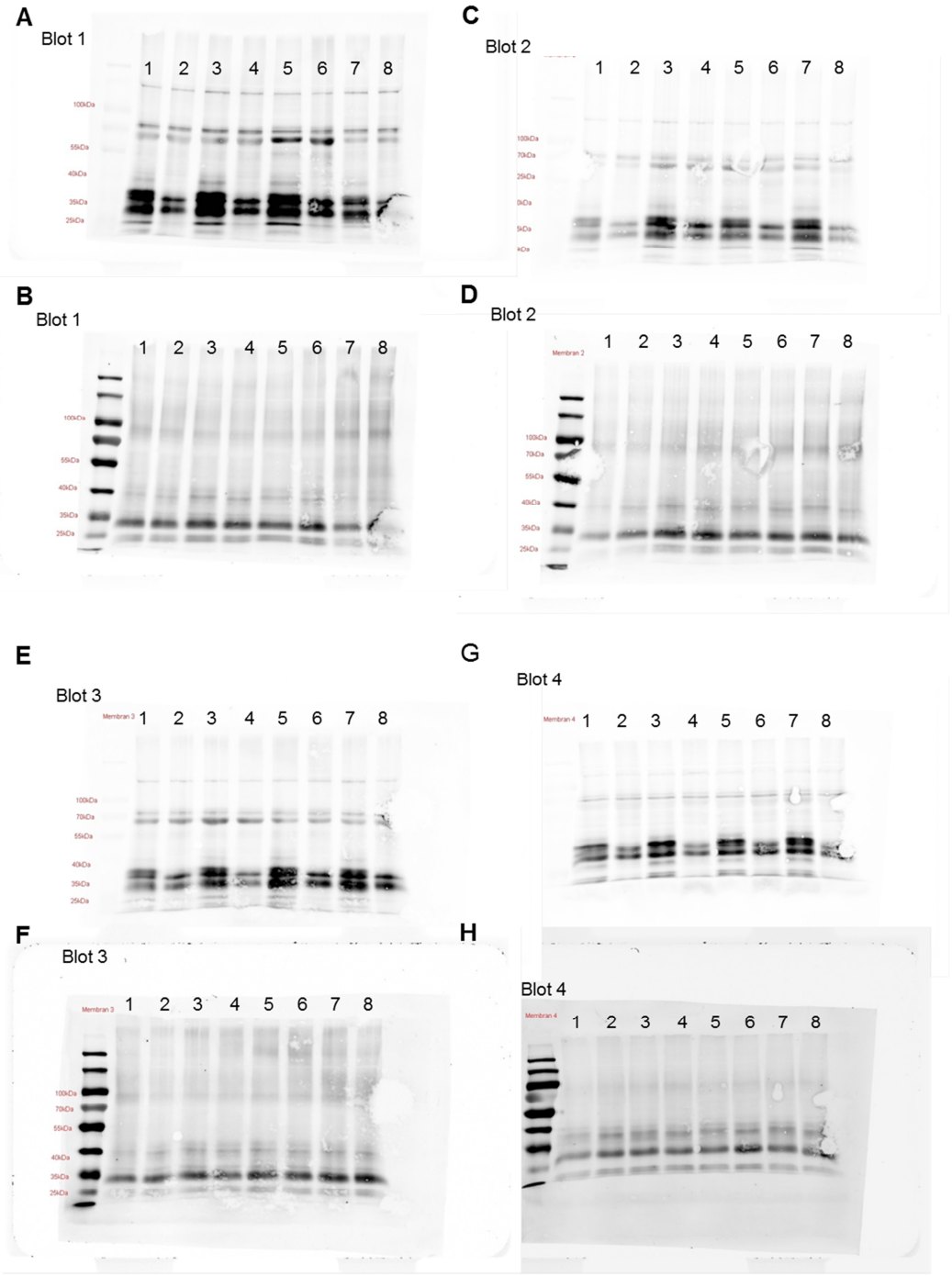

Original blots from Supplementary Fig. 2 C. **A:** Blot 1 active site labelling: lane 1 sham treatment, lane 2 sham treatment + E64d, lane 3 inhibitor 17, lane 4 inhibitor 17 + E64d, lane 5 sham treatment, lane 6 sham treatment + E64d,

lane 7 inhibitor 17, lane 8 inhibitor 17 + E64d. **B:** Blot 1 cathepsin B Western blot: lane 1 sham treatment, lane 2 sham treatment + E64d, lane 3 inhibitor 17, lane 4 inhibitor 17 + E64d, lane 5 sham treatment, lane 6 sham treatment + E64d, lane 7 inhibitor 17, lane 8 inhibitor 17+ E64d. **C:** Blot 2 active site labelling: : lane 1 sham treatment, lane 2 sham treatment + E64d, lane 3 inhibitor 17, lane 4 inhibitor 17 + E64d, lane 5 sham treatment, lane 6 sham treatment + E64d, lane 7 inhibitor 17, lane 8 inhibitor 17 + E64d. **D:** Blot 2 cathepsin B Western blot: lane 1 sham treatment, lane 2 sham treatment + E64d, lane 3 inhibitor 17, lane 4 inhibitor 17 + E64d, lane 5 sham treatment, lane 6 sham treatment + E64d, lane 7 inhibitor 17, lane 8 inhibitor 17 + E64d. **E:** Blot 3 active site labelling: lane 1 sham treatment, lane 2 sham treatment + E64d, lane 3 inhibitor 17, lane 4 inhibitor 17 + E64d, lane 5 sham treatment, lane 6 sham treatment + E64d, lane 7 inhibitor 17, lane 8 inhibitor 17 + E64d. **F:** Blot 3 cathepsin Z Western blot: cathepsin B Western blot: lane 1 sham treatment, lane 2 sham treatment + E64d, lane 3 inhibitor 17, lane 4 inhibitor 17 + E64d, lane 5 sham treatment, lane 6 sham treatment + E64d, lane 7 inhibitor 17, lane 8 inhibitor 17 + E64d. **G:** Blot 3 active site labelling: lane 1 sham treatment, lane 2 sham treatment + E64d, lane 3 inhibitor 17, lane 4 inhibitor 17 + E64d, lane 5 sham treatment, lane 6 sham treatment + E64d, lane 7 inhibitor 17, lane 8 inhibitor 17 + E64d. **H:** Blot 3 cathepsin Z Western blot: cathepsin B Western blot: lane 1 sham treatment, lane 2 sham treatment + E64d, lane 3 inhibitor 17, lane 4 inhibitor 17 + E64d, lane 5 sham treatment, lane 6 sham treatment + E64d, lane 7 inhibitor 17, lane 8 inhibitor 17 + E64d.

Supplementary Fig. 9

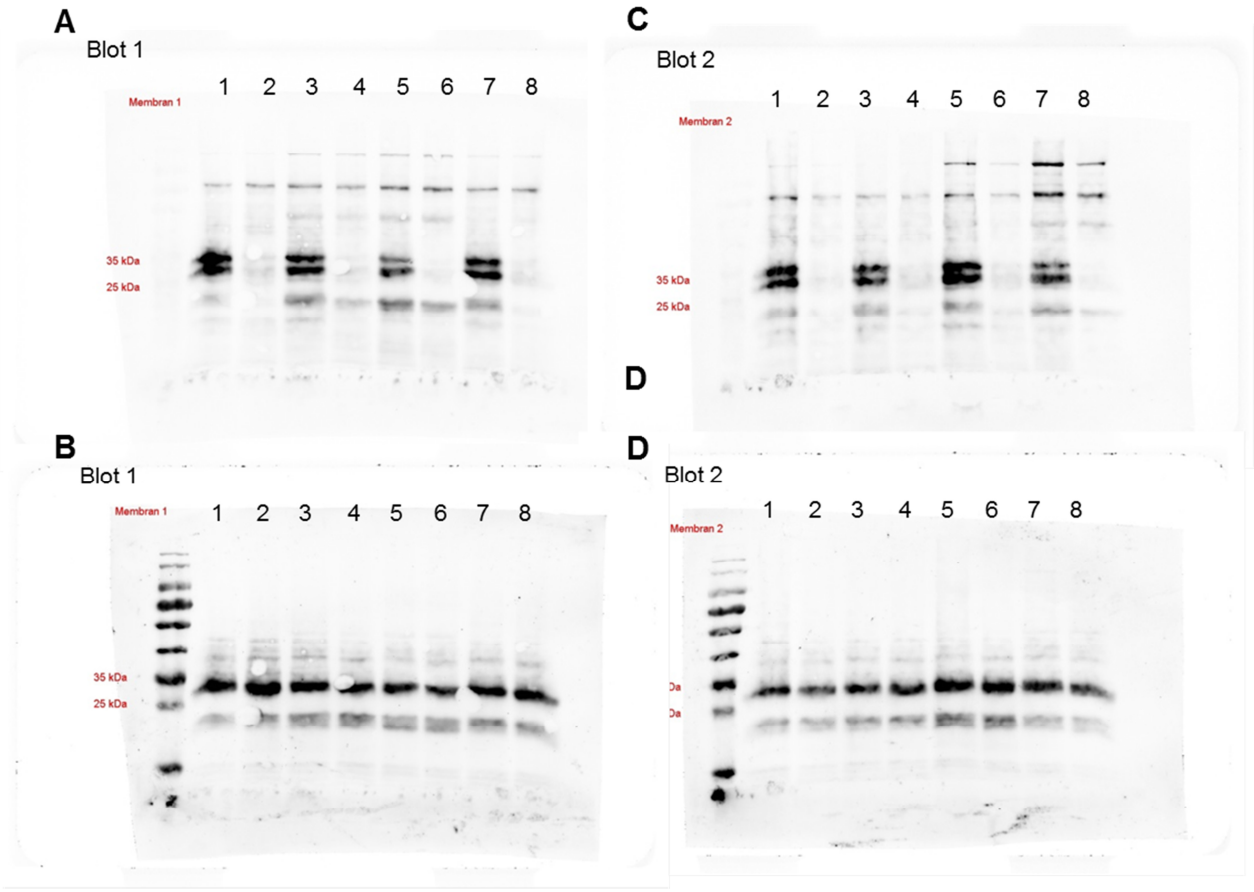

Original blots from Supplementary Fig. 2 D. **A:** Blot 1 active site labelling: lane 1 sham treatment, lane 2 sham treatment + E64d, lane 3 inhibitor 17, lane 4 inhibitor 17 + E64d, lane 5 sham treatment, lane 6 sham treatment + E64d, lane 7 inhibitor 17, lane 8 inhibitor 17 + E64d. **B:** Blot 1 cathepsin B Western blot: lane 1 sham treatment, lane 2 sham treatment + E64d, lane 3 inhibitor 17, lane 4 inhibitor 17 + E64d, lane 5 sham treatment, lane 6 sham treatment + E64d, lane 7 inhibitor 17, lane 8 inhibitor 17+ E64d. **C:** Blot 2 active site labelling: : lane 1 sham treatment, lane 2 sham treatment + E64d, lane 3 inhibitor 17, lane 4 inhibitor 17 + E64d, lane 5 sham treatment, lane 6 sham treatment + E64d, lane 7 inhibitor 17, lane 8 inhibitor 17 + E64d. **D:** Blot 2 cathepsin B Western blot: lane 1 sham treatment, lane 2 sham treatment +

E64d, lane 3 inhibitor 17, lane 4 inhibitor 17 + E64d, lane 5 sham treatment, lane 6 sham treatment + E64d, lane 7 inhibitor 17, lane 8 inhibitor 17 + E64d.

Supplementary Fig. 10

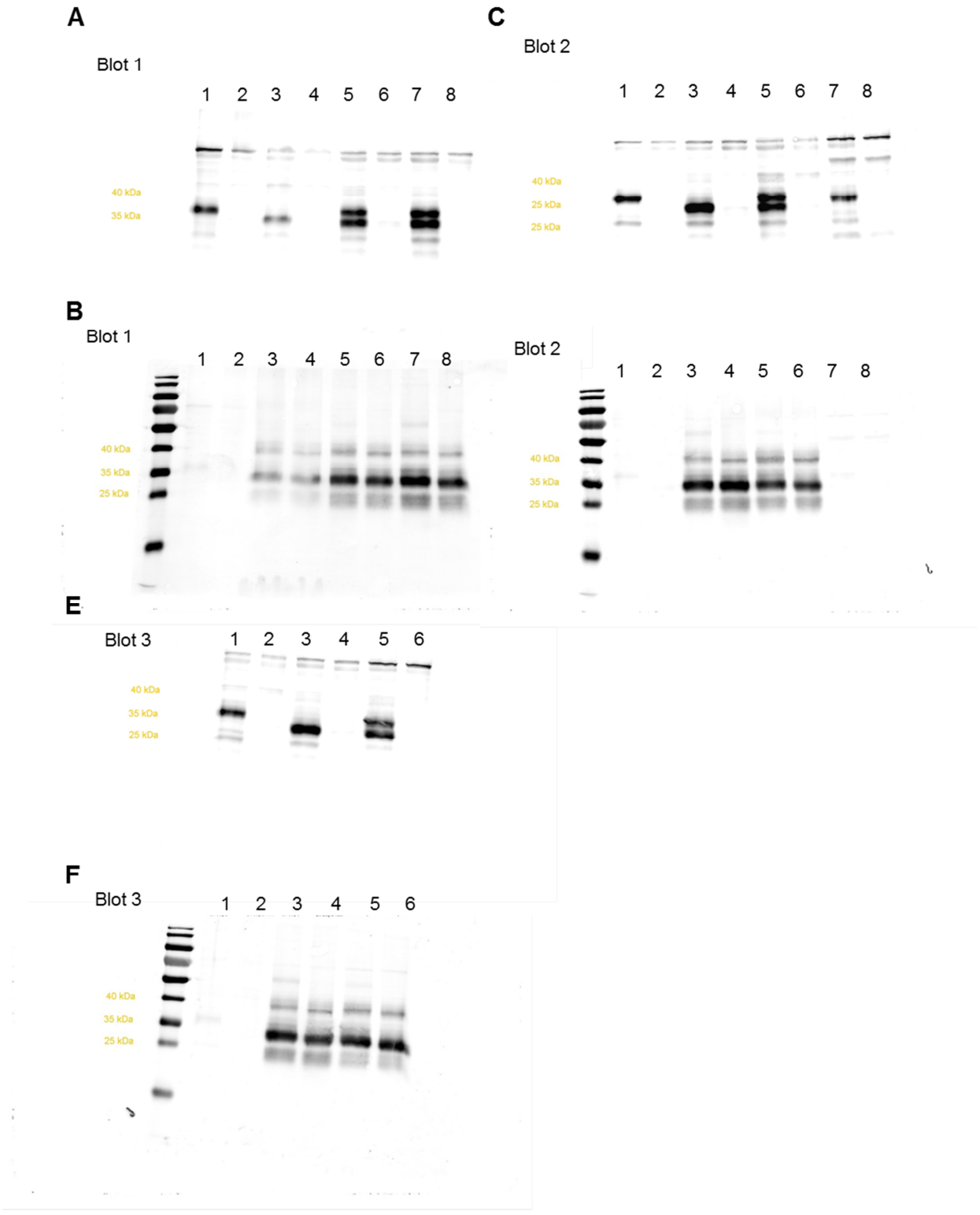

Original blots from Supplementary Fig. 3 C/D. **A:** Blot 1 active site labelling (shown in Supplementary Fig 3C): lane 1 $Ctsb^{-/-}$, lane 2 $Ctsb^{-/-}$ + E64d, lane 3

Ctsz$^{-/-}$, lane 4 Ctsz$^{-/-}$ + E64d, lane 5 wildtype, lane 6 wildtype + E64d, lane 7 wildtype, lane 8 wildtype + E64d. **B:** Blot 1 cathepsin B Western blot (shown in Supplementary Fig 3D): lane 1 Ctsb$^{-/-}$, lane 2 Ctsb$^{-/-}$ + E64d, lane 3 Ctsz$^{-/-}$, lane 4 Ctsz$^{-/-}$ + E64d, lane 5 wildtype, lane 6 wildtype + E64d, lane 7 wildtype, lane 8 wildtype + E64d. **C:** Membrane 2 active site labelling: lane 1 Ctsb$^{-/-}$, lane 2 Ctsb$^{-/-}$ + E64d, lane 3 Ctsz$^{-/-}$, lane 4 Ctsz$^{-/-}$ + E64d, lane 5 wildtype, lane 6 wildtype + E64d, lane 7 Ctsb$^{-/-}$, lane 8 Ctsb$^{-/-}$ + E64d. **D:** Blot 2 cathepsin B Western blot: lane 1 Ctsb$^{-/-}$, lane 2 Ctsb$^{-/-}$ + E64d, lane 3 Ctsz$^{-/-}$, lane 4 Ctsz$^{-/-}$ + E64d, lane 5 wildtype, lane 6 wildtype + E64d, lane 7 Ctsb$^{-/-}$, lane 8 Ctsb$^{-/-}$ + E64d. **E:** Blot 3 active site labelling: lane 1 Ctsb$^{-/-}$, lane 2 Ctsb$^{-/-}$ + E64d, lane 3 Ctsz$^{-/-}$, lane 4 Ctsz$^{-/-}$ + E64d, lane 5 wildtype, lane 6 wildtype + E64d. **F:** Blot 3 cathepsin B Western blot: lane 1 Ctsb$^{-/-}$, lane 2 Ctsb$^{-/-}$ + E64d, lane 3 Ctsz$^{-/-}$, lane 4 Ctsz$^{-/-}$ + E64d, lane 5 wildtype, lane 6 wildtype + E64d.

Supplementary Fig. 11

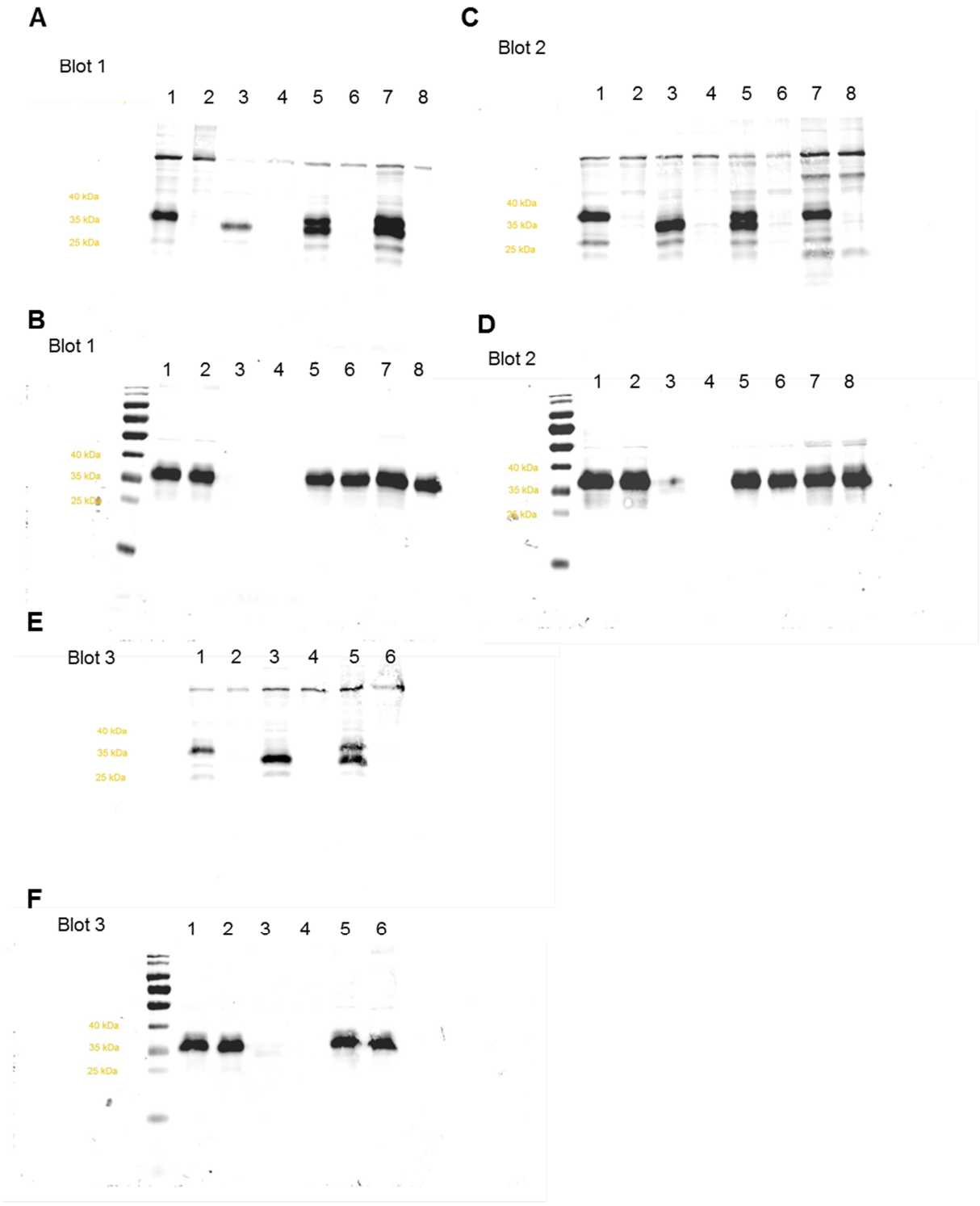

Original blots from Supplementary Fig. 3 E. **A:** Blot 1 active site labelling: lane 1 Ctsb$^{-/-}$, lane 2 Ctsb$^{-/-}$ + E64d, lane 3 Ctsz$^{-/-}$, lane 4 Ctsz$^{-/-}$ + E64d, lane 5

wildtype, lane 6 wildtype + E64d, lane 7 wildtype, lane 8 wildtype + E64d. **B:** Blot 1 cathepsin Z Western blot (shown in Figure 5 E): lane 1 $Ctsb^{-/-}$, lane 2 $Ctsb^{-/-}$ + E64d, lane 3 $Ctsz^{-/-}$, lane 4 $Ctsz^{-/-}$ + E64d, lane 5 wildtype, lane 6 wildtype + E64d, lane 7 wildtype, lane 8 wildtype + E64d. **C:** Blot 2 active site labelling: lane 1 $Ctsb^{-/-}$, lane 2 $Ctsb^{-/-}$ + E64d, lane 3 $Ctsz^{-/-}$, lane 4 $Ctsz^{-/-}$ + E64d, lane 5 wildtype, lane 6 wildtype + E64d, lane 7 $Ctsb^{-/-}$, lane 8 $Ctsb^{-/-}$ + E64d. **D:** Blot 2 cathepsin Z Western blot: lane 1 $Ctsb^{-/-}$, lane 2 $Ctsb^{-/-}$ + E64d, lane 3 $Ctsz^{-/-}$, lane 4 $Ctsz^{-/-}$ + E64d, lane 5 wildtype, lane 6 wildtype + E64d, lane 7 $Ctsb^{-/-}$, lane 8 $Ctsb^{-/-}$ + E64d. **E:** Blot 3 active site labelling: lane 1 $Ctsb^{-/-}$, lane 2 $Ctsb^{-/-}$ + E64d, lane 3 $Ctsz^{-/-}$, lane 4 $Ctsz^{-/-}$ + E64d, lane 5 wildtype, lane 6 wildtype + E64d. **F:** Blot 3 cathepsin Z Western blot: lane 1 $Ctsb^{-/-}$, lane 2 $Ctsb^{-/-}$ + E64d, lane 3 $Ctsz^{-/-}$, lane 4 $Ctsz^{-/-}$ + E64d, lane 5 wildtype, lane 6 wildtype + E64d.

3. Discussion

Various complex mechanisms are involved in the development, regulation and resolution of inflammatory processes. A comprehensive network of interactions is needed to fine tune these mechanisms in order to avoid on the one hand insufficient inflammatory responses and on the other hand overreactions of the immune system leading to tissue destruction and finally to organ failure. Targeted therapeutic interventions are necessary to modulate the inflammatory response especially in autoimmune diseases like rheumatoid arthritis. Molecular imaging represents an important tool to investigate potential targets for therapeutic interventions particularly as timing in the highly dynamic inflammatory processes is critical.

Here in this thesis, important players in the inflammatory mechanisms with very different biochemical and functional properties were investigated during the time course of acute and chronic TNCB-induced DTHR by molecular imaging.

In the acute cutaneous DTHR a strong induction of ROS/RNS expression, NF-κB activation and cathepsin B activity was detected 12h after the first TNCB challenge (168, 169). During the early chronic DTHR after the third TNCB challenge and in chronic DTHR after the fifth TNCB challenge the peak of ROS/RNS expression and NF-κB activation shifted to earlier time points. Thus, the maximum ROS/RNS production and NF-κB activation was already measured 12 h after the third repetitive TNCB ear challenge whereas the peak

in ROS/RNS production and NF-κB activation during chronic cutaneous DTHR could be observed as early as 4-12 h after the fifth TNCB challenge (168) (Fig. 2a/b).

Although all probes were injected at 12h after the TNCB challenges, the assessment of cathepsin B activity might represent different temporal characteristics. The chemiluminescence probe L-012 and the transgene NF-κB-luciferase reporter system allow a very rapid measurement already 5 min after injection (168), while the cathepsin B activity can be detected by optical imaging only 24 h after injection using the fluorescence activated optical imaging probe CatB680 (169). Thus, a distinct assessment of the cathepsin B activity 4-24h after challenge was not possible with the cathepsin B activatable optical imaging probe because of the long uptake time on the one side and the dynamic changes of the inflammatory response in the TNCB induced DTHR on the other side. Therefore, only a steady increase of cathepsin B activity from acute (after the first challenge) to early chronic (after the third challenge) and chronic DTHR (after the fifth challenge) was observed. The measurement of the peak cathepsin B activity after the respective challenges was not possible *in vivo* using this optical imaging technique (169).

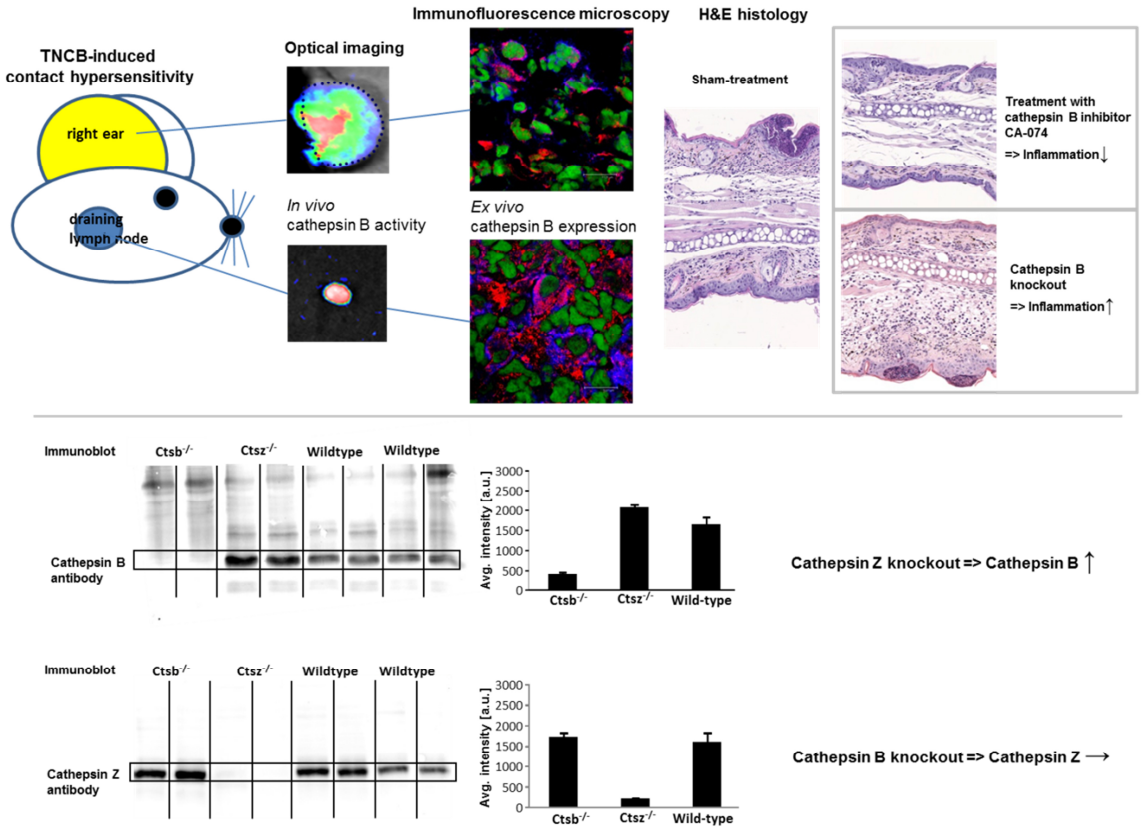

Figure 4: Noninvasive *in vivo* optical imaging displayed an intense activity of cysteine-type cathepsins in the inflamed ears as well as the draining lymph nodes of mice with acute cutaneous DTHR. Fluorescence microscopy revealed the cathepsin B expression by neutrophils, dendritic cells, macrophages, B, T and natural killer (NK) cells in inflamed ears and draining lymph nodes during acute DTHR. The topically applied cathepsin B inhibitor CA-074 significantly reduced ear swelling in acute DTHR, while $Ctsb^{-/-}$ mice exhibited an enhanced ear swelling response during acute DTHR compared with wild-type mice despite a lack of cathepsin B expression. Cathepsin Z, a protease closely related to cathepsin B, revealed compensatory expression in inflamed ears of $Ctsb^{-/-}$ mice, while cathepsin B expression was reciprocally elevated in $Ctsz^{-/-}$ mice (169).

To prevent pathological tissue destruction a tightly regulated balance between ROS/RNS and antioxidants needs to be maintained (200). Remarkably, pro- and anti-inflammatory roles are associated with the expression of ROS/RNS,

which can provoke both tissue-destructive or -protective effects (201). Interactions with signaling pathways like the nuclear factor (erythroid-derived 2)-like 2 (NRF2) or the p38 MAP kinase (185, 187, 188, 202, 203), but also the direct biocidal activity e.g. against bacteria (204, 205) are some examples of many described pro–inflammatory effects. The pathway with the most described interactions with ROS is NF-κB, which in return induces the expression of multiple genes with pro- or antioxidative effects (63).

Furthermore, in acute TNCB-specific DTHR ROS are involved in the degradation of a hyaluronic acid, a component of the extracellular matrix (206). The fragments of the hyaluronic acid are known TLR-2 and -4 agonists with consecutive pro-inflammatory effects leading to innate immune activation (207, 208). ROS/RNS are also affecting the metabolism of T-cells, in particular the aerobic glycolysis which is associated with activation and proliferation of T cells (106). Furthermore, T cell receptor signaling as well as antigen presentation is modulated by ROS and RNS (106).

The anti-inflammatory effects of ROS are less studied, but evidence for these effects is given e.g. by experiments with NCF1 deficient mice, where a reduced ROS production results in increased experimental arthritis and autoimmune encephalomyelitis (209-212). ROS reduced also the *in vitro* expression of pro-inflammatory IL-1β, IL-6, IL-8, iNOS and cyclooxygenase-2 in chondrocytes (213, 214). Inherit mutations of the NADPHoxidase in patients is causing the chronic granulomatous disease (CGD), where patients are suffering from recurrent bacterial and fungal infections (215), but also an

increased incidence of autoimmune diseases such as rheumatoid arthritis was observed (216, 217).

Optical imaging revealed a very similar temporal dynamic of ROS expression and NF-κB activation in acute and early chronic DTHR. Only in chronic DTHR after five TNCB challenges the peak of ROS expression seems to be shifted to 4h while the NF-κB activation peak was observed 12h after the fifth challenge (168). In *in vitro* experiments the prolonged expression of ROS inactivated 50–80% of the proteasomes, which resulted in decreased NF-κB activation because less NF-κB inhibiting IκBα was degraded by the proteasome (218). If this might be a reason for the shift of the ROS expression peak to 4h after challenge in our experiments, is debatable (168). Treatment with the antioxidative and NF-κB inhibiting drug NAC decreased the inflammatory response assessed by the ear swelling response in acute and chronic DTHR. However, *in vivo* optical imaging revealed an inconclusive influence on the ROS/RNS production measured by L-012 and NF-κB activation in NF-κB-reporter mice during acute and chronic DTHR.
Although the activity of cathepsin B were increasing drastically from acute to chronic DTHR in our experiments (169), the peaks of ROS/RNS expression and NF-κB activation stayed on the same level, but were reached earlier after challenge (168).

The function of proteases in an inflammatory environment can be described rather as a proteolytic network than the result of the activity from a single

protease. By cleavage of inactive pro-forms proteases are able to regulate each others proteolytic activity (43). This close interaction between several proteases and their inhibitors is needed to prevent, for example, unintended tissue destruction.

A major hub of this proteolytic network is the cysteine protease cathepsin B (43). For instance, cathepsin B is able to degrade MMP inhibiting molecules and thereby regulate extracellular matrix degradation and angiogenesis induced by MMPs (219), which play an important role in acute and chronic TNCB-induced DTHR (8).

In the proteolytic network deficiency of a specific protease can be compensated by other proteases (43). Cathepsin B is primarily cleaving the activatable fluorescence probe CatB680, which we facilitated in our optical imaging experiments. Nevertheless CatB680 is also cleaved by active cathepsin S (220) which is expressed by many APCs like DCs and macrophages (92) and has a higher stability at neutral pH than cathepsin B (221). Consequently, the measured CatB680 signal intensity is probably also influenced by cathepsin S to a certain extent. This could explain the trend towards a higher CatB680 signal intensity in mice treated with the specific cathepsin B inhibitor CA-074 (Figure S2B) (169), because CA-074 does not interfere with cathepsin S (222), but may lead to an compensatory upregulation of cathepsin S. The contribution of other cathepsins like cathepsin L, D or K to the cleavage of CatB680 is probably very little (220).

In our experiments, cathepsin B deficient mice ($Ctsb^{-/-}$) revealed an enhanced acute DTHR along with a trend towards increased CatB680 signal intensity

when compared to inflamed ears of wildtype mice (169). Active site labeling suggested that cathepsin Z may compensate the lack of cathepsin B activity in the inflamed tissue (Figure 5C/D) (169). The effect that cathepsin Z is compensating the cathepsin B deficiency was already proven in the microenvironment of an experimental breast cancer model (91, 223). Flow cytometry analysis revealed no alterations in the immune cell composition of cathepsin B deficient mice (169), which is in line with previously published results, where function and survival of cathepsin B deficient $CD8^+$ T cells was not influenced (224).

Treatment with the specific cathepsin B inhibitor CA-074 reduced acute DTHR but no significant effect during chronic DTHR was observed after the third and fifth TNCB challenge (Fig. S2A) (169). This might be explained by compensatory mechanisms, e.g. via cathepsin Z upregulation as discussed above, but no according data are available yet.

In the acute TNCB induced DTHR, especially neutrophilic granulocytes, dendritic cells, macrophages and lymphocytes expressed cathepsin B according to immunohistochemistry and flow cytometry results (Figure 2; Supplementary Fig. 1) (169). The highest amount of cathepsin B-expressing cells (dendritic cells, macrophages and lymphocytes) was located in the lymph nodes, which are draining the inflamed tissue (Figure 2C)(169). Especially cathepsin B expression in macrophages and dendritic cells was induced during acute DTHR compared to naïve controls (169), where cathepsins are highly involved in antigen processing (225, 226). In $CD8^+$ T cells, cathepsin B can be detected at the cell surface, where a protective mechanism against the

secreted perforin is discussed (227, 228). Cathepsin B and other cathepsins are also important for the migration of immune cells (229).

Controversial results have been reported lately regarding the interaction between ROS and cathepsins. Cysteine cathepsins require a reducing redox potential for optimal cleaving conditions (230). Therefore, the activity of cathepsins are impaired by ROS because of oxidization and consecutive inactivation of the enzymes (83). In contrary, Bai et al. reported that the ROS species H_2O_2 leads to enhanced cathepsin B activity, which induces the secretion of IL-1β depending on the NLRP3 inflammasome (231). Nevertheless, cathepsin B is also influencing ROS generation as Ni et al. detected reduced ROS production in cathepsin B deficient mice (232). Cathepsins are also interfering with signaling pathways such as NF-κB, as for example the inhibition of cathepsin B and S is reducing the NF-κB signaling in hepatic cell lines (233).

An important pivot in the inflammatory cascade is the NLRP3 inflammasome. Inflammasomes are intracellular complexes, which form large supramolecular structures consisting of sensor molecules, adapter molecules and the protease caspase 1 as effector molecule (234). Disrupted lysosomes might lead to release of lysosomal cathepsin B into the intracellular space where it interacts with the NLRP3 inflammasome (234-236). Several groups confirmed either a role of ROS (234, 237, 238) or cathepsin B (234, 235, 239) in the activation of the NLRP3 inflammasome, while Bai et al. even suggested that

the NLRP3 inflammasome might serve as a crucial link between these molecular effectors (231).

The cathepsin B inhibitor CA-074-Me suppressed the activation of the NLRP3 inflammasome in several experiments, while in macrophages from cathepsin B-deficient mice only a slight or no effect on the NLRP3 inflammasome activation could be observed (240). Like shown in this thesis (169), a compensatory role of other cathepsins, like cathepsin Z might be a reason for this effect (241). Some experiments also suggest a non-redundant role of cathepsin Z in the activation of the NLRP3 inflammasome (242, 243). The effect of ROS on the activation of the NLRP3 inflammasome is associated with mitochondrial dysfunction (234) and different anti-oxidative treatments like NAC are reducing the NLRP3 inflammasome activation (244).

NF-κB induces the expression of pro-IL-1β and NLRP3 which are necessary to form the NLRP3-inflammasome, but it also limits the inflammasome activation by p62 dependent disruption of damaged mitochondria (245).

Beside its important role in inflammation, inflammasome activation have been also associated with carcinogenesis and tumor progression, especially in skin cancer, although no distinct mechanism could be figured out yet (246).

The investigated *in vivo* cathepsin activity, NF-κB signaling and ROS production are involved in cellular stress responses like autophagy and senescence, which are accompanied with inflammation (247-252). Oh et al. observed that the inhibition of cathepsin B leads to cellular senescence associated with increased glycogen synthase induction (253). Also deficiency

of cathepsin Z, which may possesses redundant functions to cathepsin B (169, 241), induces cellular senescence detected by β-galactosidase activity in fibroblasts (254).

Mitochondrial ROS is involved in the induction of cellular senescence via several mechanisms e.g. interactions with p53, NF-κB and the p38 MAP kinase signaling pathway (255). In addition, the NF-κB pathway is highly activated in senescent cells and was also shown to induce the senescence associated secretory phenotype (SASP) (256).

Autophagy is a cellular response to stress with whom the cell e.g. tries to maintain energy homeostasis, to control the quality of proteins and organelles or to dispose intracellular pathogens (251). ROS is a well known inducer of autophagy (251), while cathepsin B is an essential player in the lysosome and therefore an important regulator of autophagy (257, 258).

The NF-κB signaling pathway is inducing autophagy-associated proteins like beclin 1 (BECN1) or SQSTM1. However, autophagy is inhibiting NF-κB signaling by degradation of IKK as negative feed back loop (256). Furthermore, NF-κB seems to link autophagy to senescence via the transcription factor GATA4, but also other mechanisms like the mechanistic Target of Rapamycin (mtor) complex are involved in these processes (259, 260). Moreover, Capparelli et al. revealed that cathepsin B expression was induced in cancer associated fibroblasts during both senescence and autophagy, which can lead to tumor progression (261). Nevertheless, the interplay between senescence and autophagy seems to be dependent on its temporal dynamic (262).

As inflammation is driving the pathogenesis of many diseases, the investigated dynamic role of cathepsin B, NF-κB and ROS in acute and chronic DTHR (168, 169) might be also important in diseases, which are not primarily associated with cutaneous inflammation. Cathepsin B, NF-κB and ROS are playing a crucial role in carcinogenesis and tumor progression (51, 256, 263).

An important example for carcinogenesis in the context of chronic inflammation is the non alcoholic steatohepatitis (NASH), a disease of fast growing importance, which is already a leading cause of hepatocellular carcinoma (HCC) worldwide (264-266). In this disease, a T cell driven chronic inflammation, induced by a high caloric diet, leading to an irreversible transformation of the liver tissue and finally to carcinogenesis (267-272). NF-κB signaling might link the conversion from inflammatory NASH to the carcinogenesis of HCC (268, 273). ROS are highly involved in this process, but the exact mechanism as well as the temporal dynamics are largely unknown (274-277). Moreover, Cathepsin B is essentially involved in these transformations leading to NASH and HCC (233, 278, 279), possibly because of its role in autophagy and senescence (253, 280). However, the exact role during the time course of NASH and HCC development is not entirely clear yet, which would be of paramount importance for therapeutic targeting especially in the clinical setting.

Here in this thesis, the complex regulatory mechanisms and their temporal dynamics during acute and chronic TNCB induced DTHR were investigated. Especially the effects of targeted therapeutic interventions were studied in this experimental model of cutaneous inflammation. This knowledge might be helpful to understand and treat other T cell driven diseases like rheumatoid arthritis or NASH. Furthermore, the ability of molecular imaging e.g. optical imaging is of tremendous importance to understand the underlying biological mechanisms during the time course of acute and chronic inflammation, but also to understand subsequent processes like carcinogenesis and tumor progression. Moreover, molecular imaging helps to identify relevant treatment targets and is able to find appropriate windows of opportunity for successful therapeutic interventions.

4. Summary

Inflammatory responses are involving a complex interplay between molecular and cellular mechanisms. Here in this thesis, different players within the inflammatory tissue and draining lymph nodes such as cathepsin B, reactive oxygen species (ROS) and reactive nitrogen species (RNS) as well as the NF-κB pathway were investigated in a model of acute and chronic delayed type hypersensitivity reaction (DTHR) by non invasive *in vivo* optical imaging. Cathepsin B represents an important intra- and extracellular protease, which is of immense importance during the establishment of an immune response e.g. in antigen processing. ROS and RNS are a byproduct of cellular metabolism but are also produced as effector and signaling molecule mainly by neutrophilic granulocytes. NF-κB is an important signaling pathway which is sensing inflammatory stimuli and leads to the expression of many genes involved in the immune response.

The T-cell driven acute cutaneous DTHR was induced by sensitizing mice at the abdomen and eliciting the inflammatory response 7 days later at the right ear using the hapten 2,4,6-trinitrochlorobenzene (TNCB). Repetitive application of TNCB at the right ear for up to five times induced chronic DTHR. Beside wild-type C57BL/6 mice, we used cathepsin B-deficient ($Ctsb^{-/-}$), cathepsin Z-deficient ($Ctsz^{-/-}$) and NF-κB-luciferase-reporter mice to induce the acute and chronic TNCB specific DTHR. Cathepsin B activity, ROS/RNS production and NF-κB activation were measured noninvasively by optical imaging employing protease-activatable fluorescence probes, the ROS-

sensitive chemiluminescence probe L-012 and luciferin for bioluminescence imaging in NF-κB-luciferase-reporter mice.

Extensive *ex vivo* validation was performed including histopathology, immunohistochemistry, flow cytometry, fluorescence microscopy, RT-PCR as well as active site labeling of proteases and Western blotting. Furthermore, the therapeutic effects of N-acetylcysteine (NAC) and the cathepsin-inhibitors CA-074 and Inhibitor 17 were investigated.

In acute cutaneous DTHR *in vivo* optical imaging detected an intense cathepsin B activity as well as ROS/RNS production and NF-κB activation peaking at 24 h after the 1st TNCB ear challenge. In chronic DTHR the cathepsin B activity further increased while the peaks of ROS/RNS production and NF-κB activation were shifted to an earlier timepoint.

NAC treatment decreased the ear swelling response in acute and chronic DTHR while the influence on the ROS/RNS production and NF-κB activation during acute and chronic DTHR assessed by *in vivo* optical imaging was divergent.

The cathepsin B inhibitors CA-074 and Inhibitor 17 reduced inflammation in acute but not in chronic DTHR, while Ctsb$^{-/-}$ mice exhibited an even enhanced ear swelling response during acute DTHR caused by a compensatory expression of cathepsin Z. *Ex vivo* analysis revealed enhanced cathepsin B expression in neutrophilic granulocytes, dendritic cells, macrophages, B, T and natural killer (NK) cells within inflamed ears and draining lymph nodes.

The investigated mechanisms are an essential part of the multifaceted interplay which is needed to establish and maintain inflammatory immune responses. Molecular imaging involving optical imaging is a highly capable tool to monitor these mechanisms *in vivo* and to asses targeted therapeutic interventions. These results could be of high importance not only to modulate inflammatory autoimmune diseases like rheumatoid arthritis but also to prevent carcinogenesis in chronic inflammation like non alcoholic steatohepatitis.

5. German summary

Entzündungsreaktionen beruhen auf einer komplexen Wechselwirkung zwischen molekularen und zellulären Mechanismen. In dieser Arbeit wurden verschiedene Akteure im entzündeten Gewebe und in den drainierenden Lymphknoten wie Cathepsin B, reaktive Sauerstoffspezies (ROS) und reaktive Stickstoffspezies (RNS) sowie der NF-κB-Signalweg in einem experimentellen Mausmodell der akuten und chronischen Kontaktallergiereaktion vom verzögerten Typ (delayed type hypersensitivity reaction; DTHR) durch nicht-invasive optische Bildgebung *in vivo* untersucht. Cathepsin B stellt eine wichtige intra- und extrazelluläre Protease dar, die z.B. bei der Antigenprozessierung von immenser Bedeutung ist. ROS und RNS können als Nebenprodukt des zellulären Metabolismus anfallen, werden aber auch z.B. von neutrophilen Granulozyten gezielt als Effektor- und Signalmolekül produziert. NF-κB ist ein wichtiger Signalweg, der auf Entzündungsreize reagiert und zur Expression vieler, an der Immunantwort beteiligter Gene führt.

Um eine akute kutane DTHR zu induzieren wurden Mäuse am Abdomen mit dem Hapten 2,4,6-Trinitrochlorobenzen (TNCB) sensibilisiert und 7 Tage später die Entzündungsreaktion am rechten Ohr durch erneutes Auftragen einer TNCB-Lösung ausgelöst. Die chronische DTHR wurde durch wiederholte Applikation der TNCB-Lösung am rechten Ohr induziert. Neben Wildtyp-C57BL/6-Mäusen verwendeten wir Cathepsin-B-defiziente ($Ctsb^{-/-}$), Cathepsin-Z-defiziente ($Ctsz^{-/-}$) und NF-κB-Luciferase-transgene Reportermäuse. Die Cathepsin-B-Aktivität, die ROS/RNS-Produktion und die

NF-κB-Aktivierung wurden nicht-invasiv durch optische Bildgebung unter Verwendung von Protease-aktivierbaren Fluoreszenzmarkern, dem ROS-sensitiven Chemilumineszenzmarker L-012 und Luciferin, welches mit der Luciferase der NF-κB-Reportermäusen reagiert, gemessen.

Die Ergebnisse wurden durch umfassende *ex vivo* Experimente mittels Histopathologie, Immunhistochemie, Durchflusszytometrie, Fluoreszenzmikroskopie, RT-PCR sowie active site labelling und Western Blotting der Proteasen validiert. Darüber hinaus wurden die therapeutischen Effekte von N-Acetylcystein (NAC) sowie der Cathepsin-Inhibitoren CA-074 und Inhibitor 17 untersucht.

Während der akuten kutanen DTHR zeigte die optische *in vivo* Bildgebung eine intensive Cathepsin-B-Aktivität, ROS/RNS-Produktion und NF-κB-Aktivierung. Nach Auslösen der chronischen DTHR stieg die Cathepsin-B-Aktivität weiter an, während die maximale ROS/RNS-Produktion sowie die maximale NF-κB-Aktivierung schon zu einem früheren Zeitpunkt gemessen werden konnte.

Die Therapie mit NAC verringerte die TNCB-spezifische Ohrschwellungsreaktion während der akuten und chronischen DTHR. Der Einfluss der NAC Therapie auf die ROS/RNS-Produktion und die NF-κB-Aktivierung während der akuten und chronischen DTHR folgte jedoch nicht eindeutig diesem Trend.

In der akuten DTHR konnte im entzündeten Ohrgewebe und in den drainierenden Lymphknoten eine erhöhte Cathepsin B Expression in neutrophilen Granulozyten, dendritischen Zellen, Makrophagen, B-, T- und

natürlichen Killerzellen (NK-Zellen) nachgewiesen werden. Die Cathepsin B-Inhibitoren CA-074 und Inhibitor 17 reduzierten die akute, jedoch nicht die chronische DTHR. Dahingegen zeigten $Ctsb^{-/-}$ Mäuse während der akuten DTHR eine verstärkte Ohrschwellungsreaktion, die durch eine kompensatorische Expression von Cathepsin Z verursacht wurde.

Die untersuchten Mechanismen sind ein wesentlicher Bestandteil des komplexen Zusammenspiels molekularer Prozesse, welche für die Entstehung und Aufrechterhaltung von Entzündungsreaktionen erforderlich sind. Die molekulare optische Bildgebung ist ein sehr leistungsfähiges Instrument zur Untersuchung dieser regulatorischen Mechanismen und zur Beurteilung des Einflusses gezielter therapeutischer Interventionen. Diese Ergebnisse können nicht nur für die Behandlung von Autoimmunkrankheiten wie der rheumatoiden Arthritis von großer Bedeutung sein, sondern auch z.B. zur Prävention der Karzinogenese beitragen, welche durch chronische Entzündungsprozesse wie der nichtalkoholischen Steatohepatitis ausgelöst werden kann.

6. References

1. Takeuchi O, and Akira S. Pattern recognition receptors and inflammation. *Cell.* 2010;140(6):805-20.
2. Medzhitov R. Origin and physiological roles of inflammation. *Nature.* 2008;454(7203):428-35.
3. Esser PR, and Martin SF. Pathomechanisms of Contact Sensitization. *Curr Allergy Asthma Rep.* 2017;17(12):83.
4. Thieblemont N, Wright HL, Edwards SW, and Witko-Sarsat V. Human neutrophils in auto-immunity. *Semin Immunol.* 2016;28(2):159-73.
5. Chaplin DD. Overview of the immune response. *J Allergy Clin Immunol.* 2010;125(2 Suppl 2):S3-23.
6. Greten FR, and Grivennikov SI. Inflammation and Cancer: Triggers, Mechanisms, and Consequences. *Immunity.* 2019;51(1):27-41.
7. Coussens LM, and Werb Z. Inflammation and cancer. *Nature.* 2002;420(6917):860-7.
8. Schwenck J, Griessinger CM, Fuchs K, Bukala D, Bauer N, Eichner M, et al. In vivo optical imaging of matrix metalloproteinase activity detects acute and chronic contact hypersensitivity reactions and enables monitoring of the antiinflammatory effects of N-acetylcysteine. *Mol Imaging.* 2014;13.
9. Kneilling M, Mailhammer R, Hultner L, Schonberger T, Fuchs K, Schaller M, et al. Direct crosstalk between mast cell-TNF and TNFR1-expressing endothelia mediates local tissue inflammation. *Blood.* 2009;114(8):1696-706.
10. Biedermann T, Kneilling M, Mailhammer R, Maier K, Sander CA, Kollias G, et al. Mast cells control neutrophil recruitment during T cell-mediated delayed-type hypersensitivity reactions through tumor necrosis factor and macrophage inflammatory protein 2. *J Exp Med.* 2000;192(10):1441-52.
11. Asada H, Linton J, and Katz SI. Cytokine gene expression during the elicitation phase of contact sensitivity: regulation by endogenous IL-4. *J Invest Dermatol.* 1997;108(4):406-11.
12. Martin SF, Esser PR, Weber FC, Jakob T, Freudenberg MA, Schmidt M, et al. Mechanisms of chemical-induced innate immunity in allergic contact dermatitis. *Allergy.* 2011;66(9):1152-63.
13. Martin SF, Dudda JC, Bachtanian E, Lembo A, Liller S, Durr C, et al. Toll-like receptor and IL-12 signaling control susceptibility to contact hypersensitivity. *J Exp Med.* 2008;205(9):2151-62.
14. Kaplan DH, Igyarto BZ, and Gaspari AA. Early immune events in the induction of allergic contact dermatitis. *Nat Rev Immunol.* 2012;12(2):114-24.
15. Weber FC, Esser PR, Muller T, Ganesan J, Pellegatti P, Simon MM, et al. Lack of the purinergic receptor P2X(7) results in resistance to contact hypersensitivity. *J Exp Med.* 2010;207(12):2609-19.

16. Watanabe H, Gaide O, Petrilli V, Martinon F, Contassot E, Roques S, et al. Activation of the IL-1beta-processing inflammasome is involved in contact hypersensitivity. *J Invest Dermatol.* 2007;127(8):1956-63.
17. Yazdi AS, Ghoreschi K, and Rocken M. Inflammasome activation in delayed-type hypersensitivity reactions. *J Invest Dermatol.* 2007;127(8):1853-5.
18. Watanabe H, Gehrke S, Contassot E, Roques S, Tschopp J, Friedmann PS, et al. Danger signaling through the inflammasome acts as a master switch between tolerance and sensitization. *J Immunol.* 2008;180(9):5826-32.
19. Kaplan DH, Igyarto BZ, and Gaspari AA. Early immune events in the induction of allergic contact dermatitis. *Nat Rev Immunol.* 2012;12(2):114-24.
20. Kripke ML, Munn CG, Jeevan A, Tang JM, and Bucana C. Evidence that cutaneous antigen-presenting cells migrate to regional lymph nodes during contact sensitization. *J Immunol.* 1990;145(9):2833-8.
21. Kobayashi Y. Langerhans' cells produce type IV collagenase (MMP-9) following epicutaneous stimulation with haptens. *Immunology.* 1997;90(4):496-501.
22. Banchereau J, and Steinman RM. Dendritic cells and the control of immunity. *Nature.* 1998;392(6673):245-52.
23. Bouloc A, Cavani A, and Katz SI. Contact hypersensitivity in MHC class II-deficient mice depends on CD8 T lymphocytes primed by immunostimulating Langerhans cells. *J Invest Dermatol.* 1998;111(1):44-9.
24. Krasteva M, Kehren J, Ducluzeau MT, Sayag M, Cacciapuoti M, Akiba H, et al. Contact dermatitis I. Pathophysiology of contact sensitivity. *Eur J Dermatol.* 1999;9(1):65-77.
25. Grabbe S, and Schwarz T. Immunoregulatory mechanisms involved in elicitation of allergic contact hypersensitivity. *Immunol Today.* 1998;19(1):37-44.
26. Okazaki F, Kanzaki H, Fujii K, Arata J, Akiba H, Tsujii K, et al. Initial recruitment of interferon-gamma-producing CD8+ effector cells, followed by infiltration of CD4+ cells in 2,4,6-trinitro-1-chlorobenzene (TNCB)-induced murine contact hypersensitivity reactions. *J Dermatol.* 2002;29(11):699-708.
27. Bouloc A, Cavani A, and Katz SI. Contact hypersensitivity in MHC class II-deficient mice depends on CD8 T lymphocytes primed by immunostimulating Langerhans cells. *J Invest Dermatol.* 1998;111(1):44-9.
28. O'Leary JG, Goodarzi M, Drayton DL, and von Andrian UH. T cell- and B cell-independent adaptive immunity mediated by natural killer cells. *Nat Immunol.* 2006;7(5):507-16.
29. Nakae S, Komiyama Y, Nambu A, Sudo K, Iwase M, Homma I, et al. Antigen-specific T cell sensitization is impaired in IL-17-deficient mice, causing suppression of allergic cellular and humoral responses. *Immunity.* 2002;17(3):375-87.

30. Staite ND, Justen JM, Sly LM, Beaudet AL, and Bullard DC. Inhibition of delayed-type contact hypersensitivity in mice deficient in both E-selectin and P-selectin. *Blood.* 1996;88(8):2973-9.
31. Tamagawa-Mineoka R, Katoh N, Ueda E, Takenaka H, Kita M, and Kishimoto S. The role of platelets in leukocyte recruitment in chronic contact hypersensitivity induced by repeated elicitation. *Am J Pathol.* 2007;170(6):2019-29.
32. Shimada Y, Hasegawa M, Kaburagi Y, Hamaguchi Y, Komura K, Saito E, et al. L-selectin or ICAM-1 deficiency reduces an immediate-type hypersensitivity response by preventing mast cell recruitment in repeated elicitation of contact hypersensitivity. *J Immunol.* 2003;170(8):4325-34.
33. Ogawa A, Yoshizaki A, Yanaba K, Ogawa F, Hara T, Muroi E, et al. The differential role of L-selectin and ICAM-1 in Th1-type and Th2-type contact hypersensitivity. *J Invest Dermatol.* 2010;130(6):1558-70.
34. Komura K, Hasegawa M, Hamaguchi Y, Saito E, Kaburagi Y, Yanaba K, et al. Ultraviolet light exposure suppresses contact hypersensitivity by abrogating endothelial intercellular adhesion molecule-1 up-regulation at the elicitation site. *J Immunol.* 2003;171(6):2855-62.
35. McHale JF, Harari OA, Marshall D, and Haskard DO. Vascular endothelial cell expression of ICAM-1 and VCAM-1 at the onset of eliciting contact hypersensitivity in mice: evidence for a dominant role of TNF-alpha. *J Immunol.* 1999;162(3):1648-55.
36. Steeber DA, Tang ML, Green NE, Zhang XQ, Sloane JE, and Tedder TF. Leukocyte entry into sites of inflammation requires overlapping interactions between the L-selectin and ICAM-1 pathways. *J Immunol.* 1999;163(4):2176-86.
37. Ohmatsu H, Kadono T, Sugaya M, Tomita M, Kai H, Miyagaki T, et al. alpha 4 beta 7 Integrin is essential for contact hypersensitivity by regulating migration of T cells to skin. *J Allergy Clin Immun.* 2010;126(6):1267-76.
38. Biedermann T, Kneilling M, Mailhammer R, Maier K, Sander CA, Kollias G, et al. Mast cells control neutrophil recruitment during T cell-mediated delayed-type hypersensitivity reactions through tumor necrosis factor and macrophage inflammatory protein 2. *J Exp Med.* 2000;192(10):1441-52.
39. Ring S, Schafer SC, Mahnke K, Lehr HA, and Enk AH. CD4+ CD25+ regulatory T cells suppress contact hypersensitivity reactions by blocking influx of effector T cells into inflamed tissue. *Eur J Immunol.* 2006;36(11):2981-92.
40. Schwarz A, Grabbe S, Riemann H, Aragane Y, Simon M, Manon S, et al. In vivo effects of interleukin-10 on contact hypersensitivity and delayed-type hypersensitivity reactions. *J Invest Dermatol.* 1994;103(2):211-6.
41. Ring S, Oliver SJ, Cronstein BN, Enk AH, and Mahnke K. CD4+CD25+ regulatory T cells suppress contact hypersensitivity reactions through a CD39, adenosine-dependent mechanism. *J Allergy Clin Immunol.* 2009;123(6):1287-96 e2.

42. Tomura M, Honda T, Tanizaki H, Otsuka A, Egawa G, Tokura Y, et al. Activated regulatory T cells are the major T cell type emigrating from the skin during a cutaneous immune response in mice. *J Clin Invest.* 2010;120(3):883-93.
43. Mason SD, and Joyce JA. Proteolytic networks in cancer. *Trends Cell Biol.* 2011;21(4):228-37.
44. Visse R, and Nagase H. Matrix metalloproteinases and tissue inhibitors of metalloproteinases: structure, function, and biochemistry. *Circ Res.* 2003;92(8):827-39.
45. Agewall S. Matrix metalloproteinases and cardiovascular disease. *Eur Heart J.* 2006;27(2):121-2.
46. Liu P, Sun M, and Sader S. Matrix metalloproteinases in cardiovascular disease. *Can J Cardiol.* 2006;22 Suppl B:25B-30B.
47. Churg A, Zhou S, and Wright JL. Series "matrix metalloproteinases in lung health and disease": Matrix metalloproteinases in COPD. *Eur Respir J.* 2012;39(1):197-209.
48. Egeblad M, and Werb Z. New functions for the matrix metalloproteinases in cancer progression. *Nat Rev Cancer.* 2002;2(3):161-74.
49. Deryugina EI, and Quigley JP. Matrix metalloproteinases and tumor metastasis. *Cancer Metastasis Rev.* 2006;25(1):9-34.
50. Shuman Moss LA, Jensen-Taubman S, and Stetler-Stevenson WG. Matrix metalloproteinases: changing roles in tumor progression and metastasis. *Am J Pathol.* 2012;181(6):1895-9.
51. Mijanovic O, Brankovic A, Panin AN, Savchuk S, Timashev P, Ulasov I, et al. Cathepsin B: A sellsword of cancer progression. *Cancer Lett.* 2019;449:207-14.
52. Burrage PS, Mix KS, and Brinckerhoff CE. Matrix metalloproteinases: role in arthritis. *Front Biosci.* 2006;11:529-43.
53. van Hinsbergh VW, and Koolwijk P. Endothelial sprouting and angiogenesis: matrix metalloproteinases in the lead. *Cardiovasc Res.* 2008;78(2):203-12.
54. Klein T, and Bischoff R. Physiology and pathophysiology of matrix metalloproteases. *Amino Acids.* 2011;41(2):271-90.
55. Visse R, and Nagase H. Matrix metalloproteinases and tissue inhibitors of metalloproteinases: structure, function, and biochemistry. *Circ Res.* 2003;92(8):827-39.
56. Grote K, Flach I, Luchtefeld M, Akin E, Holland SM, Drexler H, et al. Mechanical stretch enhances mRNA expression and proenzyme release of matrix metalloproteinase-2 (MMP-2) via NAD(P)H oxidase-derived reactive oxygen species. *Circ Res.* 2003;92(11):e80-6.
57. Kessenbrock K, Plaks V, and Werb Z. Matrix metalloproteinases: regulators of the tumor microenvironment. *Cell.* 2010;141(1):52-67.
58. Chakrabarti S, Zee JM, and Patel KD. Regulation of matrix metalloproteinase-9 (MMP-9) in TNF-stimulated neutrophils: novel pathways for tertiary granule release. *J Leukoc Biol.* 2006;79(1):214-22.

59. Ardi VC, Kupriyanova TA, Deryugina EI, and Quigley JP. Human neutrophils uniquely release TIMP-free MMP-9 to provide a potent catalytic stimulator of angiogenesis. *Proc Natl Acad Sci U S A.* 2007;104(51):20262-7.
60. Warner RL, Bhagavathula N, Nerusu KC, Lateef H, Younkin E, Johnson KJ, et al. Matrix metalloproteinases in acute inflammation: induction of MMP-3 and MMP-9 in fibroblasts and epithelial cells following exposure to pro-inflammatory mediators in vitro. *Exp Mol Pathol.* 2004;76(3):189-95.
61. Norrby K. Mast cells and angiogenesis. *Apmis.* 2002;110(5):355-71.
62. Adya R, Tan BK, Chen J, and Randeva HS. Nuclear factor-kappaB induction by visfatin in human vascular endothelial cells: its role in MMP-2/9 production and activation. *Diabetes Care.* 2008;31(4):758-60.
63. Pahl HL. Activators and target genes of Rel/NF-kappaB transcription factors. *Oncogene.* 1999;18(49):6853-66.
64. Han YP, Tuan TL, Wu H, Hughes M, and Garner WL. TNF-alpha stimulates activation of pro-MMP2 in human skin through NF-(kappa)B mediated induction of MT1-MMP. *J Cell Sci.* 2001;114(Pt 1):131-9.
65. Li J, Lau GK, Chen L, Dong SS, Lan HY, Huang XR, et al. Interleukin 17A promotes hepatocellular carcinoma metastasis via NF-kB induced matrix metalloproteinases 2 and 9 expression. *PLoS One.* 2011;6(7):e21816.
66. Bond M, Chase AJ, Baker AH, and Newby AC. Inhibition of transcription factor NF-kappaB reduces matrix metalloproteinase-1, -3 and -9 production by vascular smooth muscle cells. *Cardiovasc Res.* 2001;50(3):556-65.
67. Esparza J, Vilardell C, Calvo J, Juan M, Vives J, Urbano-Marquez A, et al. Fibronectin upregulates gelatinase B (MMP-9) and induces coordinated expression of gelatinase A (MMP-2) and its activator MT1-MMP (MMP-14) by human T lymphocyte cell lines. A process repressed through RAS/MAP kinase signaling pathways. *Blood.* 1999;94(8):2754-66.
68. Ringshausen I, Dechow T, Schneller F, Weick K, Oelsner M, Peschel C, et al. Constitutive activation of the MAPkinase p38 is critical for MMP-9 production and survival of B-CLL cells on bone marrow stromal cells. *Leukemia.* 2004;18(12):1964-70.
69. Liacini A, Sylvester J, Li WQ, and Zafarullah M. Inhibition of interleukin-1-stimulated MAP kinases, activating protein-1 (AP-1) and nuclear factor kappa B (NF-kappa B) transcription factors down-regulates matrix metalloproteinase gene expression in articular chondrocytes. *Matrix Biol.* 2002;21(3):251-62.
70. Kurata H, Thant AA, Matsuo S, Senga T, Okazaki K, Hotta N, et al. Constitutive activation of MAP kinase kinase (MEK1) is critical and sufficient for the activation of MMP-2. *Exp Cell Res.* 2000;254(1):180-8.
71. Rundhaug JE. Matrix metalloproteinases and angiogenesis. *J Cell Mol Med.* 2005;9(2):267-85.

72. Collen A, Hanemaaijer R, Lupu F, Quax PH, van Lent N, Grimbergen J, et al. Membrane-type matrix metalloproteinase-mediated angiogenesis in a fibrin-collagen matrix. *Blood.* 2003;101(5):1810-7.
73. Carmeliet P, and Jain RK. Molecular mechanisms and clinical applications of angiogenesis. *Nature.* 2011;473(7347):298-307.
74. Lee S, Jilani SM, Nikolova GV, Carpizo D, and Iruela-Arispe ML. Processing of VEGF-A by matrix metalloproteinases regulates bioavailability and vascular patterning in tumors. *J Cell Biol.* 2005;169(4):681-91.
75. Vempati P, Mac Gabhann F, and Popel AS. Quantifying the proteolytic release of extracellular matrix-sequestered VEGF with a computational model. *PLoS One.* 2010;5(7):e11860.
76. Kalluri R. Basement membranes: structure, assembly and role in tumour angiogenesis. *Nat Rev Cancer.* 2003;3(6):422-33.
77. Cornelius LA, Nehring LC, Harding E, Bolanowski M, Welgus HG, Kobayashi DK, et al. Matrix metalloproteinases generate angiostatin: effects on neovascularization. *J Immunol.* 1998;161(12):6845-52.
78. O'Reilly MS, Wiederschain D, Stetler-Stevenson WG, Folkman J, and Moses MA. Regulation of angiostatin production by matrix metalloproteinase-2 in a model of concomitant resistance. *J Biol Chem.* 1999;274(41):29568-71.
79. Reiser J, Adair B, and Reinheckel T. Specialized roles for cysteine cathepsins in health and disease. *J Clin Invest.* 2010;120(10):3421-31.
80. Turk V, Stoka V, Vasiljeva O, Renko M, Sun T, Turk B, et al. Cysteine cathepsins: from structure, function and regulation to new frontiers. *Biochim Biophys Acta.* 2012;1824(1):68-88.
81. Katunuma N. Posttranslational processing and modification of cathepsins and cystatins. *J Signal Transduct.* 2010;2010:375345.
82. Nissler K, Strubel W, Kreusch S, Rommerskirch W, Weber E, and Wiederanders B. The half-life of human procathepsin S. *Eur J Biochem.* 1999;263(3):717-25.
83. Lalmanach G, Saidi A, Bigot P, Chazeirat T, Lecaille F, and Wartenberg M. Regulation of the Proteolytic Activity of Cysteine Cathepsins by Oxidants. *Int J Mol Sci.* 2020;21(6).
84. Turk V, Stoka V, Vasiljeva O, Renko M, Sun T, Turk B, et al. Cysteine cathepsins: from structure, function and regulation to new frontiers. *Biochim Biophys Acta.*1824(1):68-88.
85. Hashimoto Y, Kakegawa H, Narita Y, Hachiya Y, Hayakawa T, Kos J, et al. Significance of cathepsin B accumulation in synovial fluid of rheumatoid arthritis. *Biochem Biophys Res Commun.* 2001;283(2):334-9.
86. Bever CT, Jr., and Garver DW. Increased cathepsin B activity in multiple sclerosis brain. *J Neurol Sci.* 1995;131(1):71-3.
87. Van Acker GJ, Saluja AK, Bhagat L, Singh VP, Song AM, and Steer ML. Cathepsin B inhibition prevents trypsinogen activation and reduces pancreatitis severity. *Am J Physiol Gastrointest Liver Physiol.* 2002;283(3):G794-800.

88. Mohamed MM, and Sloane BF. Cysteine cathepsins: multifunctional enzymes in cancer. *Nat Rev Cancer.* 2006;6(10):764-75.
89. Hook V, Schechter I, Demuth HU, and Hook G. Alternative pathways for production of beta-amyloid peptides of Alzheimer's disease. *Biol Chem.* 2008;389(8):993-1006.
90. Shree T, Olson OC, Elie BT, Kester JC, Garfall AL, Simpson K, et al. Macrophages and cathepsin proteases blunt chemotherapeutic response in breast cancer. *Genes Dev.* 2011;25(23):2465-79.
91. Vasiljeva O, Papazoglou A, Kruger A, Brodoefel H, Korovin M, Deussing J, et al. Tumor cell-derived and macrophage-derived cathepsin B promotes progression and lung metastasis of mammary cancer. *Cancer Res.* 2006;66(10):5242-50.
92. Honey K, and Rudensky AY. Lysosomal cysteine proteases regulate antigen presentation. *Nat Rev Immunol.* 2003;3(6):472-82.
93. Deussing J, Roth W, Saftig P, Peters C, Ploegh HL, and Villadangos JA. Cathepsins B and D are dispensable for major histocompatibility complex class II-mediated antigen presentation. *Proc Natl Acad Sci U S A.* 1998;95(8):4516-21.
94. Riese RJ, Wolf PR, Bromme D, Natkin LR, Villadangos JA, Ploegh HL, et al. Essential role for cathepsin S in MHC class II-associated invariant chain processing and peptide loading. *Immunity.* 1996;4(4):357-66.
95. Driessen C, Lennon-Dumenil AM, and Ploegh HL. Individual cathepsins degrade immune complexes internalized by antigen-presenting cells via Fcgamma receptors. *Eur J Immunol.* 2001;31(5):1592-601.
96. Conus S, and Simon HU. Cathepsins and their involvement in immune responses. *Swiss Med Wkly.*140:w13042.
97. Chwieralski CE, Welte T, and Buhling F. Cathepsin-regulated apoptosis. *Apoptosis.* 2006;11(2):143-9.
98. Ha SD, Martins A, Khazaie K, Han J, Chan BM, and Kim SO. Cathepsin B is involved in the trafficking of TNF-alpha-containing vesicles to the plasma membrane in macrophages. *J Immunol.* 2008;181(1):690-7.
99. Obermajer N, Jevnikar Z, Doljak B, and Kos J. Role of cysteine cathepsins in matrix degradation and cell signalling. *Connect Tissue Res.* 2008;49(3):193-6.
100. Im E, Venkatakrishnan A, and Kazlauskas A. Cathepsin B regulates the intrinsic angiogenic threshold of endothelial cells. *Mol Biol Cell.* 2005;16(8):3488-500.
101. Murata M, Miyashita S, Yokoo C, Tamai M, Hanada K, Hatayama K, et al. Novel epoxysuccinyl peptides. Selective inhibitors of cathepsin B, in vitro. *FEBS Lett.* 1991;280(2):307-10.
102. Montaser M, Lalmanach G, and Mach L. CA-074, but not its methyl ester CA-074Me, is a selective inhibitor of cathepsin B within living cells. *Biol Chem.* 2002;383(7-8):1305-8.
103. Schmitz J, Li T, Bartz U, and Gutschow M. Cathepsin B Inhibitors: Combining Dipeptide Nitriles with an Occluding Loop Recognition Element by Click Chemistry. *ACS Med Chem Lett.* 2016;7(3):211-6.

104. Ray PD, Huang BW, and Tsuji Y. Reactive oxygen species (ROS) homeostasis and redox regulation in cellular signaling. *Cell Signal.* 2012;24(5):981-90.
105. Winterbourn CC, Kettle AJ, and Hampton MB. Reactive Oxygen Species and Neutrophil Function. *Annu Rev Biochem.* 2016;85:765-92.
106. Forrester SJ, Kikuchi DS, Hernandes MS, Xu Q, and Griendling KK. Reactive Oxygen Species in Metabolic and Inflammatory Signaling. *Circ Res.* 2018;122(6):877-902.
107. Adams L, Franco MC, and Estevez AG. Reactive nitrogen species in cellular signaling. *Exp Biol Med (Maywood).* 2015;240(6):711-7.
108. Aruoma OI, Halliwell B, Hoey BM, and Butler J. The antioxidant action of N-acetylcysteine: its reaction with hydrogen peroxide, hydroxyl radical, superoxide, and hypochlorous acid. *Free Radic Biol Med.* 1989;6(6):593-7.
109. Hong SY, Gil HW, Yang JO, Lee EY, Kim HK, Kim SH, et al. Effect of high-dose intravenous N-acetylcysteine on the concentration of plasma sulfur-containing amino acids. *Korean J Intern Med.* 2005;20(3):217-23.
110. Sarnstrand B, Tunek A, Sjodin K, and Hallberg A. Effects of N-acetylcysteine stereoisomers on oxygen-induced lung injury in rats. *Chem Biol Interact.* 1995;94(2):157-64.
111. Hou L, Xie K, Qin M, Peng D, Ma S, Shang L, et al. Effects of reactive oxygen species scavenger on the protective action of 100% oxygen treatment against sterile inflammation in mice. *Shock.* 2010;33(6):646-54.
112. Zhang F, Lau SS, and Monks TJ. The cytoprotective effect of N-acetyl-L-cysteine against ROS-induced cytotoxicity is independent of its ability to enhance glutathione synthesis. *Toxicol Sci.* 2011;120(1):87-97.
113. Verhasselt V, Vanden Berghe W, Vanderheyde N, Willems F, Haegeman G, and Goldman M. N-acetyl-L-cysteine inhibits primary human T cell responses at the dendritic cell level: association with NF-kappaB inhibition. *J Immunol.* 1999;162(5):2569-74.
114. Senaldi G, Pointaire P, Piguet PF, and Grau GE. Protective effect of N-acetylcysteine in hapten-induced irritant and contact hypersensitivity reactions. *J Invest Dermatol.* 1994;102(6):934-7.
115. Wang BJ, Guo YL, Chang HY, Sheu HM, Pan MH, Lee YH, et al. N-acetylcysteine inhibits chromium hypersensitivity in coadjuvant chromium-sensitized albino guinea pigs by suppressing the effects of reactive oxygen species. *Exp Dermatol.*19(8):e191-200.
116. Tsuji F, Miyake Y, Aono H, Kawashima Y, and Mita S. Effects of bucillamine and N-acetyl-L-cysteine on cytokine production and collagen-induced arthritis (CIA). *Clin Exp Immunol.* 1999;115(1):26-31.
117. Paterson RL, Galley HF, and Webster NR. The effect of N-acetylcysteine on nuclear factor-kappa B activation, interleukin-6, interleukin-8, and intercellular adhesion molecule-1 expression in patients with sepsis. *Crit Care Med.* 2003;31(11):2574-8.
118. Spapen H, Zhang H, Demanet C, Vleminckx W, Vincent JL, and Huyghens L. Does N-acetyl-L-cysteine influence cytokine response during early human septic shock? *Chest.* 1998;113(6):1616-24.

119. Heller AR, Groth G, Heller SC, Breitkreutz R, Nebe T, Quintel M, et al. N-acetylcysteine reduces respiratory burst but augments neutrophil phagocytosis in intensive care unit patients. *Crit Care Med.* 2001;29(2):272-6.
120. Tirouvanziam R, Conrad CK, Bottiglieri T, Herzenberg LA, and Moss RB. High-dose oral N-acetylcysteine, a glutathione prodrug, modulates inflammation in cystic fibrosis. *Proc Natl Acad Sci U S A.* 2006;103(12):4628-33.
121. Grassi C, and Morandini GC. A controlled trial of intermittent oral acetylcysteine in the long-term treatment of chronic bronchitis. *Eur J Clin Pharmacol.* 1976;09(5-6):393-6.
122. Grandjean EM, Berthet P, Ruffmann R, and Leuenberger P. Efficacy of oral long-term N-acetylcysteine in chronic bronchopulmonary disease: a meta-analysis of published double-blind, placebo-controlled clinical trials. *Clin Ther.* 2000;22(2):209-21.
123. Oral N-acetylcysteine and exacerbation rates in patients with chronic bronchitis and severe airways obstruction. British Thoracic Society Research Committee. *Thorax.* 1985;40(11):832-5.
124. Millar AB, Pavia D, Agnew JE, Lopez-Vidriero MT, Lauque D, and Clarke SW. Effect of oral N-acetylcysteine on mucus clearance. *Br J Dis Chest.* 1985;79(3):262-6.
125. Ratjen F, Wonne R, Posselt HG, Stover B, Hofmann D, and Bender SW. A double-blind placebo controlled trial with oral ambroxol and N-acetylcysteine for mucolytic treatment in cystic fibrosis. *Eur J Pediatr.* 1985;144(4):374-8.
126. Perkins ND. Integrating cell-signalling pathways with NF-kappaB and IKK function. *Nat Rev Mol Cell Biol.* 2007;8(1):49-62.
127. Hayden MS, and Ghosh S. Signaling to NF-kappaB. *Genes Dev.* 2004;18(18):2195-224.
128. Wu ZH, and Miyamoto S. Many faces of NF-kappaB signaling induced by genotoxic stress. *J Mol Med (Berl).* 2007;85(11):1187-202.
129. O'Dea E, and Hoffmann A. The regulatory logic of the NF-kappaB signaling system. *Cold Spring Harb Perspect Biol.* 2010;2(1):a000216.
130. Hayden MS, and Ghosh S. Shared principles in NF-kappaB signaling. *Cell.* 2008;132(3):344-62.
131. Sha WC, Liou HC, Tuomanen EI, and Baltimore D. Targeted disruption of the p50 subunit of NF-kappa B leads to multifocal defects in immune responses. *Cell.* 1995;80(2):321-30.
132. Bonizzi G, and Karin M. The two NF-kappaB activation pathways and their role in innate and adaptive immunity. *Trends Immunol.* 2004;25(6):280-8.
133. Brown KD, Claudio E, and Siebenlist U. The roles of the classical and alternative nuclear factor-kappaB pathways: potential implications for autoimmunity and rheumatoid arthritis. *Arthritis Res Ther.* 2008;10(4):212.
134. Sun SC. Non-canonical NF-kappaB signaling pathway. *Cell Res.* 2011;21(1):71-85.

135. Luftig M, Yasui T, Soni V, Kang MS, Jacobson N, Cahir-McFarland E, et al. Epstein-Barr virus latent infection membrane protein 1 TRAF-binding site induces NIK/IKK alpha-dependent noncanonical NF-kappaB activation. *Proc Natl Acad Sci U S A.* 2004;101(1):141-6.
136. Droebner K, Klein B, Paxian S, Schmid R, Stitz L, and Planz O. The alternative NF-kappaB signalling pathway is a prerequisite for an appropriate immune response against lymphocytic choriomeningitis virus infection. *Viral Immunol.* 2010;23(3):295-308.
137. Shih VF, Tsui R, Caldwell A, and Hoffmann A. A single NFkappaB system for both canonical and non-canonical signaling. *Cell Res.* 2011;21(1):86-102.
138. Basak S, Shih VF, and Hoffmann A. Generation and activation of multiple dimeric transcription factors within the NF-kappaB signaling system. *Mol Cell Biol.* 2008;28(10):3139-50.
139. Rao P, Hayden MS, Long M, Scott ML, West AP, Zhang D, et al. IkappaBbeta acts to inhibit and activate gene expression during the inflammatory response. *Nature.* 2010;466(7310):1115-9.
140. Madge LA, and May MJ. Classical NF-kappaB activation negatively regulates noncanonical NF-kappaB-dependent CXCL12 expression. *J Biol Chem.* 2010;285(49):38069-77.
141. Ghosh G, Wang VY, Huang DB, and Fusco A. NF-kappaB regulation: lessons from structures. *Immunol Rev.* 2012;246(1):36-58.
142. Verstrepen L, Bekaert T, Chau TL, Tavernier J, Chariot A, and Beyaert R. TLR-4, IL-1R and TNF-R signaling to NF-kappa B: variations on a common theme. *Cell Mol Life Sci.* 2008;65(19):2964-78.
143. Gerondakis S, and Siebenlist U. Roles of the NF-kappaB pathway in lymphocyte development and function. *Cold Spring Harb Perspect Biol.* 2010;2(5):a000182.
144. Weil R, and Israel A. T-cell-receptor- and B-cell-receptor-mediated activation of NF-kappaB in lymphocytes. *Curr Opin Immunol.* 2004;16(3):374-81.
145. Tas SW, Vervoordeldonk MJ, Hajji N, Schuitemaker JH, van der Sluijs KF, May MJ, et al. Noncanonical NF-kappaB signaling in dendritic cells is required for indoleamine 2,3-dioxygenase (IDO) induction and immune regulation. *Blood.* 2007;110(5):1540-9.
146. Oka S, Kamata H, Kamata K, Yagisawa H, and Hirata H. N-acetylcysteine suppresses TNF-induced NF-kappaB activation through inhibition of IkappaB kinases. *FEBS Lett.* 2000;472(2-3):196-202.
147. Ntziachristos V, Ripoll J, and Weissleder R. Would near-infrared fluorescence signals propagate through large human organs for clinical studies? *Opt Lett.* 2002;27(5):333-5.
148. Ntziachristos V, Bremer C, and Weissleder R. Fluorescence imaging with near-infrared light: new technological advances that enable in vivo molecular imaging. *Eur Radiol.* 2003;13(1):195-208.
149. Schwenck J, Maier FC, Kneilling M, Wiehr S, and Fuchs K. Non-invasive In Vivo Fluorescence Optical Imaging of Inflammatory MMP Activity Using an Activatable Fluorescent Imaging Agent. *J Vis Exp.* 2017(123).

150. Ntziachristos V, Tung CH, Bremer C, and Weissleder R. Fluorescence molecular tomography resolves protease activity in vivo. *Nat Med.* 2002;8(7):757-60.
151. Blum G, von Degenfeld G, Merchant MJ, Blau HM, and Bogyo M. Noninvasive optical imaging of cysteine protease activity using fluorescently quenched activity-based probes. *Nat Chem Biol.* 2007;3(10):668-77.
152. Kielland A, Blom T, Nandakumar KS, Holmdahl R, Blomhoff R, and Carlsen H. In vivo imaging of reactive oxygen and nitrogen species in inflammation using the luminescent probe L-012. *Free Radic Biol Med.* 2009;47(6):760-6.
153. Zielonka J, Lambeth JD, and Kalyanaraman B. On the use of L-012, a luminol-based chemiluminescent probe, for detecting superoxide and identifying inhibitors of NADPH oxidase: a reevaluation. *Free Radic Biol Med.* 2013;65:1310-4.
154. Boutagy NE, Wu J, Cai Z, Zhang W, Booth CJ, Kyriakides TC, et al. In Vivo Reactive Oxygen Species Detection With a Novel Positron Emission Tomography Tracer, (18)F-DHMT, Allows for Early Detection of Anthracycline-Induced Cardiotoxicity in Rodents. *JACC Basic Transl Sci.* 2018;3(3):378-90.
155. Carroll V, Michel BW, Blecha J, VanBrocklin H, Keshari K, Wilson D, et al. A boronate-caged [(1)(8)F]FLT probe for hydrogen peroxide detection using positron emission tomography. *J Am Chem Soc.* 2014;136(42):14742-5.
156. Carroll VN, Truillet C, Shen B, Flavell RR, Shao X, Evans MJ, et al. [(11)C]Ascorbic and [(11)C]dehydroascorbic acid, an endogenous redox pair for sensing reactive oxygen species using positron emission tomography. *Chem Commun (Camb).* 2016;52(27):4888-90.
157. Chu W, Chepetan A, Zhou D, Shoghi KI, Xu J, Dugan LL, et al. Development of a PET radiotracer for non-invasive imaging of the reactive oxygen species, superoxide, in vivo. *Org Biomol Chem.* 2014;12(25):4421-31.
158. Okamura T, Okada M, Kikuchi T, Wakizaka H, and Zhang MR. A (1)(1)C-labeled 1,4-dihydroquinoline derivative as a potential PET tracer for imaging of redox status in mouse brain. *J Cereb Blood Flow Metab.* 2015;35(12):1930-6.
159. Zhang W, Cai Z, Li L, Ropchan J, Lim K, Boutagy NE, et al. Optimized and Automated Radiosynthesis of [(18)F]DHMT for Translational Imaging of Reactive Oxygen Species with Positron Emission Tomography. *Molecules.* 2016;21(12).
160. Goiffon RJ, Martinez SC, and Piwnica-Worms D. A rapid bioluminescence assay for measuring myeloperoxidase activity in human plasma. *Nat Commun.* 2015;6:6271.
161. Daiber A, Oelze M, August M, Wendt M, Sydow K, Wieboldt H, et al. Detection of superoxide and peroxynitrite in model systems and mitochondria by the luminol analogue L-012. *Free Radic Res.* 2004;38(3):259-69.

162. Imada I, Sato EF, Miyamoto M, Ichimori Y, Minamiyama Y, Konaka R, et al. Analysis of reactive oxygen species generated by neutrophils using a chemiluminescence probe L-012. *Anal Biochem.* 1999;271(1):53-8.
163. Carlsen H, Moskaug JO, Fromm SH, and Blomhoff R. In vivo imaging of NF-kappa B activity. *J Immunol.* 2002;168(3):1441-6.
164. Notebaert S, Carlsen H, Janssen D, Vandenabeele P, Blomhoff R, and Meyer E. In vivo imaging of NF-kappaB activity during Escherichia coli-induced mammary gland infection. *Cell Microbiol.* 2008;10(6):1249-58.
165. Bowles RD, Mata BA, Bell RD, Mwangi TK, Huebner JL, Kraus VB, et al. In vivo luminescence imaging of NF-kappaB activity and serum cytokine levels predict pain sensitivities in a rodent model of osteoarthritis. *Arthritis Rheumatol.* 2014;66(3):637-46.
166. Badr CE, Niers JM, Tjon-Kon-Fat LA, Noske DP, Wurdinger T, and Tannous BA. Real-time monitoring of nuclear factor kappaB activity in cultured cells and in animal models. *Mol Imaging.* 2009;8(5):278-90.
167. Kolberg M, Pedersen S, Mitake M, Holm KL, Bohn SK, Blomhoff HK, et al. Coffee inhibits nuclear factor-kappa B in prostate cancer cells and xenografts. *J Nutr Biochem.* 2016;27:153-63.
168. Schwenck J, Mehling R, Thaiss WM, Kramer D, Menendez IG, Oz HH, et al. Temporal Dynamics of Reactive Oxygen and Nitrogen Species and NF-kappaB Activation During Acute and Chronic T Cell-Driven Inflammation. *Mol Imaging Biol.* 2019.
169. Schwenck J, Maurer A, Fehrenbacher B, Mehling R, Knopf P, Mucha N, et al. Cysteine-type cathepsins promote the effector phase of acute cutaneous delayed-type hypersensitivity reactions. *Theranostics.* 2019;9(13):3903-17.
170. Fuchs K, Kuehn A, Mahling M, Guenthoer P, Hector A, Schwenck J, et al. In Vivo Hypoxia PET Imaging Quantifies the Severity of Arthritic Joint Inflammation in Line with Overexpression of Hypoxia-Inducible Factor and Enhanced Reactive Oxygen Species Generation. *J Nucl Med.* 2017;58(5):853-60.
171. Perkins ND. Integrating cell-signalling pathways with NF-kappaB and IKK function. *Nat Rev Mol Cell Biol.* 2007;8(1):49-62.
172. Hayden MS, and Ghosh S. Signaling to NF-kappaB. *Genes Dev.* 2004;18(18):2195-224.
173. Bonizzi G, and Karin M. The two NF-kappaB activation pathways and their role in innate and adaptive immunity. *Trends Immunol.* 2004;25(6):280-8.
174. Brown KD, Claudio E, and Siebenlist U. The roles of the classical and alternative nuclear factor-kappaB pathways: potential implications for autoimmunity and rheumatoid arthritis. *Arthritis Res Ther.* 2008;10(4):212.
175. Sun SC. Non-canonical NF-kappaB signaling pathway. *Cell Res.* 2011;21(1):71-85.
176. Luftig M, Yasui T, Soni V, Kang MS, Jacobson N, Cahir-McFarland E, et al. Epstein-Barr virus latent infection membrane protein 1 TRAF-

binding site induces NIK/IKK alpha-dependent noncanonical NF-kappaB activation. *Proc Natl Acad Sci U S A.* 2004;101(1):141-6.
177. Droebner K, Klein B, Paxian S, Schmid R, Stitz L, and Planz O. The alternative NF-kappaB signalling pathway is a prerequisite for an appropriate immune response against lymphocytic choriomeningitis virus infection. *Viral Immunol.* 2010;23(3):295-308.
178. O'Dea E, and Hoffmann A. The regulatory logic of the NF-kappaB signaling system. *Cold Spring Harb Perspect Biol.* 2010;2(1):a000216.
179. Shih VF, Tsui R, Caldwell A, and Hoffmann A. A single NFkappaB system for both canonical and non-canonical signaling. *Cell Res.* 2011;21(1):86-102.
180. Basak S, Shih VF, and Hoffmann A. Generation and activation of multiple dimeric transcription factors within the NF-kappaB signaling system. *Mol Cell Biol.* 2008;28(10):3139-50.
181. Madge LA, and May MJ. Classical NF-kappaB activation negatively regulates noncanonical NF-kappaB-dependent CXCL12 expression. *J Biol Chem.* 2010;285(49):38069-77.
182. Zhang Q, Lenardo MJ, and Baltimore D. 30 Years of NF-kappaB: A Blossoming of Relevance to Human Pathobiology. *Cell.* 2017;168(1-2):37-57.
183. Karin M. NF-kappaB as a critical link between inflammation and cancer. *Cold Spring Harb Perspect Biol.* 2009;1(5):a000141.
184. Mincheva-Tasheva S, and Soler RM. NF-kappaB signaling pathways: role in nervous system physiology and pathology. *Neuroscientist.* 2013;19(2):175-94.
185. D'Autreaux B, and Toledano MB. ROS as signalling molecules: mechanisms that generate specificity in ROS homeostasis. *Nat Rev Mol Cell Biol.* 2007;8(10):813-24.
186. Morgan MJ, and Liu ZG. Crosstalk of reactive oxygen species and NF-kappaB signaling. *Cell Res.* 2011;21(1):103-15.
187. Dolado I, Swat A, Ajenjo N, De Vita G, Cuadrado A, and Nebreda AR. p38alpha MAP kinase as a sensor of reactive oxygen species in tumorigenesis. *Cancer Cell.* 2007;11(2):191-205.
188. Torres M, and Forman HJ. Redox signaling and the MAP kinase pathways. *Biofactors.* 2003;17(1-4):287-96.
189. Michiels C, Minet E, Mottet D, and Raes M. Regulation of gene expression by oxygen: NF-kappaB and HIF-1, two extremes. *Free Radic Biol Med.* 2002;33(9):1231-42.
190. Hughes G, Murphy MP, and Ledgerwood EC. Mitochondrial reactive oxygen species regulate the temporal activation of nuclear factor kappaB to modulate tumour necrosis factor-induced apoptosis: evidence from mitochondria-targeted antioxidants. *Biochem J.* 2005;389(Pt 1):83-9.
191. Lingappan K. NF-kappaB in Oxidative Stress. *Curr Opin Toxicol.* 2018;7:81-6.
192. Liu J, Yoshida Y, and Yamashita U. DNA-binding activity of NF-kappaB and phosphorylation of p65 are induced by N-acetylcysteine through phosphatidylinositol (PI) 3-kinase. *Mol Immunol.* 2008;45(15):3984-9.

193. Kamata H, Manabe T, Kakuta J, Oka S, and Hirata H. Multiple redox regulation of the cellular signaling system linked to AP-1 and NFkappaB: effects of N-acetylcysteine and H2O2 on the receptor tyrosine kinases, the MAP kinase cascade, and IkappaB kinases. *Ann N Y Acad Sci.* 2002;973:419-22.
194. Wuyts WA, Vanaudenaerde BM, Dupont LJ, Demedts MG, and Verleden GM. N-acetylcysteine reduces chemokine release via inhibition of p38 MAPK in human airway smooth muscle cells. *Eur Respir J.* 2003;22(1):43-9.
195. Hashimoto S, Gon Y, Matsumoto K, Takeshita I, and Horie T. N-acetylcysteine attenuates TNF-alpha-induced p38 MAP kinase activation and p38 MAP kinase-mediated IL-8 production by human pulmonary vascular endothelial cells. *Br J Pharmacol.* 2001;132(1):270-6.
196. Dong C, Davis RJ, and Flavell RA. MAP kinases in the immune response. *Annu Rev Immunol.* 2002;20:55-72.
197. Ashwell JD. The many paths to p38 mitogen-activated protein kinase activation in the immune system. *Nat Rev Immunol.* 2006;6(7):532-40.
198. Verhasselt V, Vanden Berghe W, Vanderheyde N, Willems F, Haegeman G, and Goldman M. N-acetyl-L-cysteine inhibits primary human T cell responses at the dendritic cell level: association with NF-kappaB inhibition. *J Immunol.* 1999;162(5):2569-74.
199. Bruchhausen S, Zahn S, Valk E, Knop J, and Becker D. Thiol antioxidants block the activation of antigen-presenting cells by contact sensitizers. *J Invest Dermatol.* 2003;121(5):1039-44.
200. Niki E. Oxidative stress and antioxidants: Distress or eustress? *Arch Biochem Biophys.* 2016;595:19-24.
201. Hultqvist M, Olsson LM, Gelderman KA, and Holmdahl R. The protective role of ROS in autoimmune disease. *Trends Immunol.* 2009;30(5):201-8.
202. D'Autreaux B, and Toledano MB. ROS as signalling molecules: mechanisms that generate specificity in ROS homeostasis. *Nat Rev Mol Cell Biol.* 2007;8(10):813-24.
203. Mizuashi M, Ohtani T, Nakagawa S, and Aiba S. Redox imbalance induced by contact sensitizers triggers the maturation of dendritic cells. *J Invest Dermatol.* 2005;124(3):579-86.
204. Smith JA. Neutrophils, host defense, and inflammation: a double-edged sword. *J Leukoc Biol.* 1994;56(6):672-86.
205. Valko M, Leibfritz D, Moncol J, Cronin MT, Mazur M, and Telser J. Free radicals and antioxidants in normal physiological functions and human disease. *Int J Biochem Cell Biol.* 2007;39(1):44-84.
206. Esser PR, Wolfle U, Durr C, von Loewenich FD, Schempp CM, Freudenberg MA, et al. Contact Sensitizers Induce Skin Inflammation via ROS Production and Hyaluronic Acid Degradation. *PLoS One.*7(7):e41340.
207. Termeer C, Benedix F, Sleeman J, Fieber C, Voith U, Ahrens T, et al. Oligosaccharides of Hyaluronan activate dendritic cells via toll-like receptor 4. *J Exp Med.* 2002;195(1):99-111.

208. Scheibner KA, Lutz MA, Boodoo S, Fenton MJ, Powell JD, and Horton MR. Hyaluronan fragments act as an endogenous danger signal by engaging TLR2. *J Immunol.* 2006;177(2):1272-81.
209. Naik E, and Dixit VM. Mitochondrial reactive oxygen species drive proinflammatory cytokine production. *J Exp Med.* 2011;208(3):417-20.
210. Hultqvist M, Olsson LM, Gelderman KA, and Holmdahl R. The protective role of ROS in autoimmune disease. *Trends Immunol.* 2009;30(5):201-8.
211. Olofsson P, Holmberg J, Tordsson J, Lu S, Akerstrom B, and Holmdahl R. Positional identification of Ncf1 as a gene that regulates arthritis severity in rats. *Nat Genet.* 2003;33(1):25-32.
212. Hultqvist M, Olofsson P, Holmberg J, Backstrom BT, Tordsson J, and Holmdahl R. Enhanced autoimmunity, arthritis, and encephalomyelitis in mice with a reduced oxidative burst due to a mutation in the Ncf1 gene. *Proc Natl Acad Sci U S A.* 2004;101(34):12646-51.
213. Mathy-Hartert M, Martin G, Devel P, Deby-Dupont G, Pujol JP, Reginster JY, et al. Reactive oxygen species downregulate the expression of pro-inflammatory genes by human chondrocytes. *Inflamm Res.* 2003;52(3):111-8.
214. Mathy-Hartert M, Deby-Dupont GP, Reginster JY, Ayache N, Pujol JP, and Henrotin YE. Regulation by reactive oxygen species of interleukin-1beta, nitric oxide and prostaglandin E(2) production by human chondrocytes. *Osteoarthritis Cartilage.* 2002;10(7):547-55.
215. Segal BH, Leto TL, Gallin JI, Malech HL, and Holland SM. Genetic, biochemical, and clinical features of chronic granulomatous disease. *Medicine (Baltimore).* 2000;79(3):170-200.
216. Magnani A, Brosselin P, Beaute J, de Vergnes N, Mouy R, Debre M, et al. Inflammatory manifestations in a single-center cohort of patients with chronic granulomatous disease. *J Allergy Clin Immunol.* 2014;134(3):655-62 e8.
217. De Ravin SS, Naumann N, Cowen EW, Friend J, Hilligoss D, Marquesen M, et al. Chronic granulomatous disease as a risk factor for autoimmune disease. *J Allergy Clin Immunol.* 2008;122(6):1097-103.
218. Wu M, Bian Q, Liu Y, Fernandes AF, Taylor A, Pereira P, et al. Sustained oxidative stress inhibits NF-kappaB activation partially via inactivating the proteasome. *Free Radic Biol Med.* 2009;46(1):62-9.
219. Kostoulas G, Lang A, Nagase H, and Baici A. Stimulation of angiogenesis through cathepsin B inactivation of the tissue inhibitors of matrix metalloproteinases. *FEBS Lett.* 1999;455(3):286-90.
220. Lin SA, Patel M, Suresch D, Connolly B, Bao B, Groves K, et al. Quantitative Longitudinal Imaging of Vascular Inflammation and Treatment by Ezetimibe in apoE Mice by FMT Using New Optical Imaging Biomarkers of Cathepsin Activity and alpha(v)beta(3) Integrin. *Int J Mol Imaging.* 2012;2012:189254.
221. Bromme D, Bonneau PR, Lachance P, Wiederanders B, Kirschke H, Peters C, et al. Functional expression of human cathepsin S in Saccharomyces cerevisiae. Purification and characterization of the recombinant enzyme. *J Biol Chem.* 1993;268(7):4832-8.

222. Katunuma N. Structure-based development of specific inhibitors for individual cathepsins and their medical applications. *Proc Jpn Acad Ser B Phys Biol Sci.* 2011;87(2):29-39.
223. Sevenich L, Schurigt U, Sachse K, Gajda M, Werner F, Muller S, et al. Synergistic antitumor effects of combined cathepsin B and cathepsin Z deficiencies on breast cancer progression and metastasis in mice. *Proc Natl Acad Sci U S A.* 2010;107(6):2497-502.
224. Baran K, Ciccone A, Peters C, Yagita H, Bird PI, Villadangos JA, et al. Cytotoxic T lymphocytes from cathepsin B-deficient mice survive normally in vitro and in vivo after encountering and killing target cells. *J Biol Chem.* 2006;281(41):30485-91.
225. Matthews SP, Werber I, Deussing J, Peters C, Reinheckel T, and Watts C. Distinct protease requirements for antigen presentation in vitro and in vivo. *J Immunol.* 2010;184(5):2423-31.
226. Zhang T, Maekawa Y, Hanba J, Dainichi T, Nashed BF, Hisaeda H, et al. Lysosomal cathepsin B plays an important role in antigen processing, while cathepsin D is involved in degradation of the invariant chain inovalbumin-immunized mice. *Immunology.* 2000;100(1):13-20.
227. Balaji KN, Schaschke N, Machleidt W, Catalfamo M, and Henkart PA. Surface cathepsin B protects cytotoxic lymphocytes from self-destruction after degranulation. *J Exp Med.* 2002;196(4):493-503.
228. Perisic Nanut M, Sabotic J, Jewett A, and Kos J. Cysteine cathepsins as regulators of the cytotoxicity of NK and T cells. *Front Immunol.* 2014;5:616.
229. Staun-Ram E, and Miller A. Cathepsins (S and B) and their inhibitor Cystatin C in immune cells: modulation by interferon-beta and role played in cell migration. *J Neuroimmunol.*232(1-2):200-6.
230. Pillay CS, Elliott E, and Dennison C. Endolysosomal proteolysis and its regulation. *Biochem J.* 2002;363(Pt 3):417-29.
231. Bai H, Yang B, Yu W, Xiao Y, Yu D, and Zhang Q. Cathepsin B links oxidative stress to the activation of NLRP3 inflammasome. *Exp Cell Res.* 2018;362(1):180-7.
232. Ni J, Wu Z, Stoka V, Meng J, Hayashi Y, Peters C, et al. Increased expression and altered subcellular distribution of cathepsin B in microglia induce cognitive impairment through oxidative stress and inflammatory response in mice. *Aging Cell.* 2019;18(1):e12856.
233. de Mingo A, de Gregorio E, Moles A, Tarrats N, Tutusaus A, Colell A, et al. Cysteine cathepsins control hepatic NF-kappaB-dependent inflammation via sirtuin-1 regulation. *Cell Death Dis.* 2016;7(11):e2464.
234. Mangan MSJ, Olhava EJ, Roush WR, Seidel HM, Glick GD, and Latz E. Targeting the NLRP3 inflammasome in inflammatory diseases. *Nat Rev Drug Discov.* 2018;17(8):588-606.
235. Guo H, Callaway JB, and Ting JP. Inflammasomes: mechanism of action, role in disease, and therapeutics. *Nat Med.* 2015;21(7):677-87.
236. Tschopp J, and Schroder K. NLRP3 inflammasome activation: The convergence of multiple signalling pathways on ROS production? *Nat Rev Immunol.* 2010;10(3):210-5.

237. Abais JM, Xia M, Zhang Y, Boini KM, and Li PL. Redox regulation of NLRP3 inflammasomes: ROS as trigger or effector? *Antioxid Redox Signal.* 2015;22(13):1111-29.
238. Latz E, Xiao TS, and Stutz A. Activation and regulation of the inflammasomes. *Nat Rev Immunol.* 2013;13(6):397-411.
239. Chen N, Ou Z, Zhang W, Zhu X, Li P, and Gong J. Cathepsin B regulates non-canonical NLRP3 inflammasome pathway by modulating activation of caspase-11 in Kupffer cells. *Cell Prolif.* 2018;51(6):e12487.
240. He Y, Hara H, and Nunez G. Mechanism and Regulation of NLRP3 Inflammasome Activation. *Trends Biochem Sci.* 2016;41(12):1012-21.
241. Orlowski GM, Colbert JD, Sharma S, Bogyo M, Robertson SA, and Rock KL. Multiple Cathepsins Promote Pro-IL-1beta Synthesis and NLRP3-Mediated IL-1beta Activation. *J Immunol.* 2015;195(4):1685-97.
242. Campden RI, and Zhang Y. The role of lysosomal cysteine cathepsins in NLRP3 inflammasome activation. *Arch Biochem Biophys.* 2019;670:32-42.
243. Orlowski GM, Sharma S, Colbert JD, Bogyo M, Robertson SA, Kataoka H, et al. Frontline Science: Multiple cathepsins promote inflammasome-independent, particle-induced cell death during NLRP3-dependent IL-1beta activation. *J Leukoc Biol.* 2017;102(1):7-17.
244. Sho T, and Xu J. Role and mechanism of ROS scavengers in alleviating NLRP3-mediated inflammation. *Biotechnol Appl Biochem.* 2019;66(1):4-13.
245. Zhong Z, Umemura A, Sanchez-Lopez E, Liang S, Shalapour S, Wong J, et al. NF-kappaB Restricts Inflammasome Activation via Elimination of Damaged Mitochondria. *Cell.* 2016;164(5):896-910.
246. Ciazynska M, Bednarski IA, Wodz K, Narbutt J, and Lesiak A. NLRP1 and NLRP3 inflammasomes as a new approach to skin carcinogenesis. *Oncol Lett.* 2020;19(3):1649-56.
247. Jurk D, Wilson C, Passos JF, Oakley F, Correia-Melo C, Greaves L, et al. Chronic inflammation induces telomere dysfunction and accelerates ageing in mice. *Nat Commun.* 2014;2:4172.
248. Ren JL, Pan JS, Lu YP, Sun P, and Han J. Inflammatory signaling and cellular senescence. *Cell Signal.* 2009;21(3):378-83.
249. Freund A, Orjalo AV, Desprez PY, and Campisi J. Inflammatory networks during cellular senescence: causes and consequences. *Trends Mol Med.* 2010;16(5):238-46.
250. Qian M, Fang X, and Wang X. Autophagy and inflammation. *Clin Transl Med.* 2017;6(1):24.
251. Levine B, Mizushima N, and Virgin HW. Autophagy in immunity and inflammation. *Nature.* 2011;469(7330):323-35.
252. Deretic V, and Levine B. Autophagy balances inflammation in innate immunity. *Autophagy.* 2018;14(2):243-51.
253. Oh SS, Park S, Lee KW, Madhi H, Park SG, Lee HG, et al. Extracellular cystatin SN and cathepsin B prevent cellular senescence by inhibiting abnormal glycogen accumulation. *Cell Death Dis.* 2017;8(4):e2729.

254. Kraus S, Bunsen T, Schuster S, Cichon MA, Tacke M, Reinheckel T, et al. Cellular senescence induced by cathepsin X downregulation. *Eur J Cell Biol.* 2011;90(8):678-86.
255. Wei W, and Ji S. Cellular senescence: Molecular mechanisms and pathogenicity. *J Cell Physiol.* 2018;233(12):9121-35.
256. Taniguchi K, and Karin M. NF-kappaB, inflammation, immunity and cancer: coming of age. *Nat Rev Immunol.* 2018;18(5):309-24.
257. Lamore SD, and Wondrak GT. Autophagic-lysosomal dysregulation downstream of cathepsin B inactivation in human skin fibroblasts exposed to UVA. *Photochem Photobiol Sci.* 2012;11(1):163-72.
258. Man SM, and Kanneganti TD. Regulation of lysosomal dynamics and autophagy by CTSB/cathepsin B. *Autophagy.* 2016;12(12):2504-5.
259. Kang C, Xu Q, Martin TD, Li MZ, Demaria M, Aron L, et al. The DNA damage response induces inflammation and senescence by inhibiting autophagy of GATA4. *Science.* 2015;349(6255):aaa5612.
260. Gewirtz DA. Autophagy and senescence: a partnership in search of definition. *Autophagy.* 2013;9(5):808-12.
261. Capparelli C, Chiavarina B, Whitaker-Menezes D, Pestell TG, Pestell RG, Hulit J, et al. CDK inhibitors (p16/p19/p21) induce senescence and autophagy in cancer-associated fibroblasts, "fueling" tumor growth via paracrine interactions, without an increase in neo-angiogenesis. *Cell Cycle.* 2012;11(19):3599-610.
262. Kwon Y, Kim JW, Jeoung JA, Kim MS, and Kang C. Autophagy Is Pro-Senescence When Seen in Close-Up, but Anti-Senescence in Long-Shot. *Mol Cells.* 2017;40(9):607-12.
263. Reinheckel T, Peters C, Kruger A, Turk B, and Vasiljeva O. Differential Impact of Cysteine Cathepsins on Genetic Mouse Models of De novo Carcinogenesis: Cathepsin B as Emerging Therapeutic Target. *Front Pharmacol.* 2012;3:133.
264. Dongiovanni P, Romeo S, and Valenti L. Hepatocellular carcinoma in nonalcoholic fatty liver: role of environmental and genetic factors. *World J Gastroenterol.* 2014;20(36):12945-55.
265. Starley BQ, Calcagno CJ, and Harrison SA. Nonalcoholic fatty liver disease and hepatocellular carcinoma: a weighty connection. *Hepatology.* 2010;51(5):1820-32.
266. Takuma Y, and Nouso K. Nonalcoholic steatohepatitis-associated hepatocellular carcinoma: our case series and literature review. *World J Gastroenterol.* 2010;16(12):1436-41.
267. Friedman CF, Proverbs-Singh TA, and Postow MA. Treatment of the Immune-Related Adverse Effects of Immune Checkpoint Inhibitors: A Review. *JAMA Oncol.* 2016;2(10):1346-53.
268. Wolf MJ, Adili A, Piotrowitz K, Abdullah Z, Boege Y, Stemmer K, et al. Metabolic activation of intrahepatic CD8+ T cells and NKT cells causes nonalcoholic steatohepatitis and liver cancer via cross-talk with hepatocytes. *Cancer Cell.* 2014;26(4):549-64.
269. Wolf MJ, Seleznik GM, and Heikenwalder M. Lymphotoxin's link to carcinogenesis: friend or foe? from lymphoid neogenesis to

hepatocellular carcinoma and prostate cancer. *Adv Exp Med Biol.* 2011;691:231-49.
270. Finkin S, Yuan D, Stein I, Taniguchi K, Weber A, Unger K, et al. Ectopic lymphoid structures function as microniches for tumor progenitor cells in hepatocellular carcinoma. *Nat Immunol.* 2015;16(12):1235-44.
271. Ringelhan M, Pfister D, O'Connor T, Pikarsky E, and Heikenwalder M. The immunology of hepatocellular carcinoma. *Nat Immunol.* 2018;19(3):222-32.
272. Endig J, Buitrago-Molina LE, Marhenke S, Reisinger F, Saborowski A, Schutt J, et al. Dual Role of the Adaptive Immune System in Liver Injury and Hepatocellular Carcinoma Development. *Cancer Cell.* 2016;30(2):308-23.
273. Luedde T, Beraza N, Kotsikoris V, van Loo G, Nenci A, De Vos R, et al. Deletion of NEMO/IKKgamma in liver parenchymal cells causes steatohepatitis and hepatocellular carcinoma. *Cancer Cell.* 2007;11(2):119-32.
274. Kastl L, Sauer SW, Ruppert T, Beissbarth T, Becker MS, Suss D, et al. TNF-alpha mediates mitochondrial uncoupling and enhances ROS-dependent cell migration via NF-kappaB activation in liver cells. *FEBS Lett.* 2014;588(1):175-83.
275. Valgimigli M, Valgimigli L, Trere D, Gaiani S, Pedulli GF, Gramantieri L, et al. Oxidative stress EPR measurement in human liver by radical-probe technique. Correlation with etiology, histology and cell proliferation. *Free Radic Res.* 2002;36(9):939-48.
276. Anstee QM, Reeves HL, Kotsiliti E, Govaere O, and Heikenwalder M. From NASH to HCC: current concepts and future challenges. *Nat Rev Gastroenterol Hepatol.* 2019;16(7):411-28.
277. Garcia-Ruiz C, and Fernandez-Checa JC. Mitochondrial Oxidative Stress and Antioxidants Balance in Fatty Liver Disease. *Hepatol Commun.* 2018;2(12):1425-39.
278. Tang Y, Cao G, Min X, Wang T, Sun S, Du X, et al. Cathepsin B inhibition ameliorates the non-alcoholic steatohepatitis through suppressing caspase-1 activation. *J Physiol Biochem.* 2018;74(4):503-10.
279. Ruan J, Zheng H, Rong X, Rong X, Zhang J, Fang W, et al. Over-expression of cathepsin B in hepatocellular carcinomas predicts poor prognosis of HCC patients. *Mol Cancer.* 2016;15:17.
280. Guo R, Yu Q, Liong EC, Fung ML, and Tipoe GL. Cathepsin-B dependent autophagy ameliorates steatoheaptitis in chronic exercise rats. *Histol Histopathol.* 2020:18204.

7. Declaration of contribution

Johannes Schwenck designed the studies and performed the *in vivo* experiments. He prepared the samples for *ex vivo* validation and supported the flow cytometry analysis as well as RNA extraction and gene expression analysis. Johannes Schwenck analyzed and interpreted the datasets of the *in vivo* and *ex vivo* experiments and wrote the manuscript for the publications. Furthermore, Johannes Schwenck wrote this cumulative thesis submitted as requirement to fulfill the degree “Doctor of Philosophy” (Ph.D.).

Manfred Kneilling supported the design of the experiments, the data interpretation of the *in vivo* and *ex vivo* experiments as well as the preparation of the manuscript for the publications.

Roman Mehling helped to perform the *in vivo* experiments and the preparation of the samples for *ex vivo* validation. Additionally, Roman Mehling worked on flow cytometry experiments and was involved in the data analysis.

Daniel Bukala performed RNA extraction and gene expression analysis, helped to conduct the *in vivo* experiments as well as prepared the samples for *ex vivo* validation.

Wolfgang Thaiss as well as Kerstin Fuchs and Christoph Grießinger helped to run the *in vivo* experiments as well as the preparation of the samples for *ex vivo* validation. Hasan Halit Öz, Julia Holstein and Philipp Knopf performed flow cytometry experiments and were involved in the data analysis. Active site labeling was performed by Andreas Maurer, Natalie Mucha und Dennis Haupt. Immunofluorescence microscopy was conducted and analyzed by Birgit Fehrenbacher. Histology was stained and analyzed by Leticia Quintanilla-

Martinez and Irene Gonzalez Menendez. Daniela Kramer performed RNA Extraction and Gene Expression Analysis.

Thomas Reinheckel provided cathepsin B-deficient and cathepsin Z-deficient mice, contributed technical expertise and critically edited the published manuscript. Harald Carlsen provided NF-κB-luciferase-reporter mice and contributed technical expertise. Michael Gütschow contributed the inhibitor 17 and contributed technical expertise. Klaus Schulze-Osthoff, Stephan Hailfinger, Kamran Ghoreschi, Martin Schaller, Martin Röcken, Hubert Kalbacher and Dominik Hartl contributed expertise in experimental design and data analysis.

Bernd Pichler supervised the projects, contributed expertise in experimental design and data analysis as well as critically edited the published manuscripts.

8. Acknowledgements

Here, I would like to thank Prof. Dr. Bernd Pichler and Dr. Manfred Kneilling as well as the members of the doctoral committee Prof. Dr. Christian la Fougere and Prof. Dr. Samuel Wagner for their excellent supervision and great support.

I would also like to thank the entire group of the Werner Siemens Imaging Center for the friendly atmosphere, great helpfulness, interesting discussions and good cooperation, in particular all colleagues, who have been involved in these long lasting projects included in this thesis. Furthermore, I would like to thank our collaboration partners from the University of Tübingen and beyond.

I would like to acknowledge the “PATE” program of the Medical Faculty, the “Junior Academy” as well as the PhD program “Experimental Medicine” for supporting me.

Moreover, I would like to thank my clinical colleagues in the Department of Nuclear Medicine and Clinical Molecular Imaging for there good cooperation and support to accomplish this scientific work besides clinical duties.

Finally, I would also like to thank my family and friends for their support during this time, especially those who proofread this work.